The link between the centrosome, TSC disease and epithelial differentiation

Laia Gómez Baldó

UNIVERSITAT DE BARCELONA

FACULTAT DE MEDICINA

DEPARTAMENT DE CIÈNCIES CLÍNIQUES

PROGRAMA DE DOCTORAT EN BIOMEDICINA

(Bieni 2005/2007)

THE LINK BETWEEN THE CENTROSOME, TSC DISEASE AND EPITHELIAL DIFFERENTIATION

ESTUDI DE LA CONNEXIÓ ENTRE EL CENTROSOMA, L'ESCLEROSI TUBEROSA I LA DIFERENCIACIÓ EPITELIAL

LAIA GÓMEZ BALDÓ

May, 2010

THE LINK BETWEEN THE CENTROSOME, TSC DISEASE AND EPITHELIAL DIFFERENTIATION

ESTUDI DE LA CONNEXIÓ ENTRE EL CENTROSOMA, L'ESCLEROSI TUBEROSA I LA DIFERENCIACIÓ EPITELIAL

Memòria presentada per **Laia Gómez Baldó** per optar al grau

de **Doctor per la Universitat de Barcelona**

Becada per la Fundació Privada Institut d'Investigació

Biomèdica de Bellvitge (IDIBELL)

Aquesta tesi doctoral ha estat realitzada sota la direcció del Dr. Miguel Angel Genestar Pujana al Laboratori de Recerca Translacional de l'Institut Català d'Oncologia.

L'Hospitalet de Llobregat, Maig de 2010

Dr. Miguel Angel Genestar Pujana
Director

Dr. Victor Raúl Moreno Aguado
Tutor

Laia Gómez Baldó
Doctoranda

Als meus pares, n'Alícia i en Lluís

A Rodrigo

Mentre escolto "*Wish you were here*" de Pink Floyd, faig memòria i me'n adono que ja han passat quatre anys i mig des que vaig emprendre aquest camí. Hi ha hagut molts moments en que he pensat que no s'acabaria mai, però, evidentment, m'equivocava. Reconec que no ha estat fàcil, però gràcies a la força que m'heu donat molts de vosaltres en els moments més durs ara puc estar escrivint aquestes línies. Per això, vull dedicar les primeres planes d'aquest treball que hem aconseguit entre tots a agrair-vos la comprensió, l'ajut, l'energia, el bon rotllo i les ensenyances que m'heu transmès al llarg d'aquests anys.

En primer lloc vull agrair al meu boss, en **Miguel Angel** (**MA**), que em donés la oportunitat de començar aquest projecte, no només pel que científicament hàgim aconseguit, sinó també per tot el que m'ha ensenyat. Gràcies per dedicar el teu temps en ajudar-me a fer els meus primers westerns, les primeres co-IPs (a la cambra freda, of course), els primers passes de cèl·lules,…Gràcies també per tot el que he arribat a aprendre en congressos i cursos, per donar-me la oportunitat de marxar als USA. I sobretot, gràcies MA per aquesta última etapa de redacció en que has tingut en compte cada línea, cada punt, sé que no ha estat fàcil corregir-me!

També voldria agrair al **Victor Moreno** que acceptés ser el meu tutor i que m'hagi deixat un lloc a la UBS per poder escriure aquesta tesi. Moltes gràcies Victor.

Gràcies als membres del nostre mini-grup, que m'heu hagut d'aguantar les manies, els nervis, el bon humor i el mal humor. A l'**Helena** i la **Griselda**, les meves companyes de poiata, reactius, cèl·lules, etc… Gràcies per tot el que m'heu ajudat i ensenyat aquests anys. Em quedo amb els bons moments, que n'hi ha hagut molts. A la **Núria**, que aquests últims mesos m'has escoltat, aconsellat, ajudat…Pels cafès a les escales (ahí también te incluyo a tí, **Rebeca**), per tots els dinars juntes, per fer-me sentir sempre acollida, per ser tan coherent i donar aquelles paraules de calma en el moment adequat. Moltes gràcies i espero que quan estiguis escrivint la tesi d'aquí un any i mig o dos (més o menys…) tinguis algú al teu costat que et doni el recolzament que m'has donat tu a mi. Gràcies també al **Jordi** que, encara que no hagim coincidit massa, sempre m'has donat un cop de mà si ho he necessitat. **Chris**, I'm not forgetting you ;) Thanks for your help during these years…you've taught me so many things!!! Many thanks for your transoceanic help during the last 6 months!! Wish you the best in Vancouver!!

A tota la gent del LRT1…ostres hi ha una llista tan llarga de persones a qui agrair grans gestos o petits detalls!!!

A l'**Ari**, probablement la primera que em va dir d'anar a dinar quan vaig començar al LRT1. Ai Ari, com t'he trobat a faltar tot aquest any!!! Tu ja saps que t'hauria de dedicar una plana sencera per agrair-te tot el que has fet per mi des que ens coneixem. Les nostres converses a la poiata, les converses a la màquina de cafè…entremig potser alguna PCR o algun WB ;) El cap de setmana a NY, dormint tots tres en el matalàs al terra…Sempre has estat al meu costat quan t'he necessitat…Gràcies!!!

I a l'altre banda de la poiata….la **Gemma**!!! Quantes vegades ens hem mirat pel foradet de les nostres poiates i ja ens hem entès!! I tots els cafès al moll explicant-nos les penes (i alguna alegria, va…). La setmana que ve et toca llegir la tesi i estic convençuda que ho faràs molt bé i que el que t'espera d'ara en endavant serà com tu ho desitgis.

No puc oblidar algú que ha estat essencial per mi, l'únic amic que em queda al lab (tu i jo ja ens entenem), el **Marc**. Primer em vas acollir a Madrid quan gairebé no ens coneixíem i després m'has robat les millors rialles amb el teu sarcasme. Sempre tan positiu (ironia), de bon humor (ironia, també), amb aquesta salut de ferro que t'han donat (que no et queixes mai, no pas!)…aquesta tesi no hagués estat el mateix sense tu, en serio, ens hem entès sempre molt bé, les teves bromes m'han alegrat els dies més grisos….MERCI Marc i molts èxits!!! I com no, l'etern company d'en Marc, l'**Ernest**, gràcies per ser tan bo, tan generós amb el teu temps, per dedicar-me un moment sempre que ho he necessitat. Ara que emprens un nou camí, et desitjo el millor per tu i la teva família. Ningú ho mereix més que tu.

A **Pancha**, que tantas horas me has dedicado!!! Hemos reído y llorado juntas, compartido música, conciertos, horas de poyata y ordenador…Amiga y confidente, me hubiera gustado tener la oportunidad de hacer muchas más cosas juntas…no descarto que lo hagamos en algún momento. Estemos donde estemos, esto no termina aquí. Gracias por apoyarme tanto y decir siempre lo que piensas de verdad!!

A **Regi**, cuántas mañanas hemos compartido en tu coche de camino al lab!!! Y no sólo eso, las cañitas por el barrio, las cenas en tu casa, alguna escapadita a la Torre Ponsa…gracias a tí también, **Miguel**!!! Los dos me habéis ayudado mucho con vuestros consejos desde otra perspectiva, en los buenos momentos y en los malos

estuvisteis siempre ahí. Gracias por ser tan amigos de vuestros amigos, sólo espero poder corresponderos como merecéis…por lo pronto, os debo unas bravas en el Tomás!

A tots els que ja han marxat del lab, per tot el que vam compartir. Al **Pepe Mari**, que sempre ha tingut un moment per mi…ja des d'abans de començar la tesi (te'n recordes quan estava al lab Z de l'IRO i venies a veure'ns???). A l'**Àlvaro**, per totes les bones estones a la màquina de cafè…no hem rigut ni res!!! A la **Neus** i la **Maria Martinez** (metge)…fidels seguidores d'aquella sèrie de TV; no sé què era millor, si veure la sèrie o comentar-la amb vosaltres al dia següent. A l'**Alena** i la **Sonia**, que sempre eren allà quan necessitava algo. A l'**Ester**!!!!!!!!!!!! Com et trobo a faltar, nena!!! Quantes vegades ens hem fotut el rotllo pels passadissos!!! Bé, i ara ho fem pel facebook quan ens trobem! A la **Wilmar**, la meva companya de la sala de becaris, la cacatua nº1 (jo sóc la nº2, que encara no tinc criatures). Ostres, com hem arribat a riure i quantes bones estones hem passat juntes (te'n recordes de la virulana?? Va quedar pendent que te'n portés!!). A la **Laura**, la Padu, que fa poc que no hi ets, però ja es nota. Merci per ser sempre tan oberta i sincera, per no tenir mai por de preguntar. Aquests últims mesos sempre m'has escoltat i m'has donat un cop de mà en el que he necessitat, moltes gràcies. A **Bea**, que me enseñaste a hacer los primeros westerns, no sé qué hubiera sido de esta tesis sin tu ayuda durante mi primer año (llegué a los 254 westers!!!!!). A **Vanesa**, por dedicarme la "Bomba Latina" (eso fue especial), por escucharme cuando tenía algo que decir, por compartir recetas, por ser tan buena persona y tener un corazón tan noble. Tenemos una comida pendiente, no me olvido. A tots vosaltres que a dia d'avui encara continuem en contacte, espero que no el perdem mai!!!

No puc deixar d'agrair a les meves companyes d'Escolab, la **Maria**, la **Marta** i la **Bego** que em donessin la oportunitat de formar part del team. La Marta, la cacatúa nº3 (si, si…no te'n lliures del títol), que em va deixar cobrir-la mentre ella cuidava d'en Jan. A la Bego, que em va ensenyar com fer les extraccions de sang i em va explicar tot el que necessitava saber per fer la pràctica. I aquest últim any, gràcies a les dues, a la **Maria** i a la **Marta**, pels bons moments que hem compartit fent les pràctiques, rifant qui faria l'última presentació o comentant lo bo o dolent que era el grup d'aquell dia. Gràcies també a la **Núria Sala** per fer-se càrrec de tot i permetre'm substituir a la Bego.

Del LRT1 encara hi ha molta gent que d'una forma o una altra m'han donat un cop de mà. Al **David**, que sempre m'has tractat de meravella i m'has ajudat sense dubtar-ho. A la **Mireia**, la meva companya de ball…tan dolça, merci per canviar-te

tan ràpid per no fer-me esperar, ets un sol. A la **Fati**, que sempre ha tingut un somriure per mi. A la **Clara**, la **Sara**, la **Mercè** (en especial, gràcies per agafar el relleu de representant de becaris), la **Gabi**, la **Cris**, la **Marta Jiménez**, l'**Alba**, l'**Edu** (un gran company de poiata…cuida de la Gris a partir d'ara, eh?), el **Raul**, la **Lara** i la **Marta**, l'**Helena**, la **Marta** (d'Angio) que sou la nova generació del lab, gràcies per compartir amb mi els últims mesos de tesi i "no morir en el intento"! A **Berta**, siempre de buen humor y con esa carcajada tan contagiosa!! A la **Mar**, que sempre té un moment de tranquil·litat per preguntar-te com van les coses. A la **Maria** (la Puigivila), gràcies per la teva alegria, per adonar-te'n quan estic malament i fer-me riure!!! Ets un 10!!!! A **Miguel**, que eres un trozo de pan, gracias por decirme las palabras adecuadas cuando lo necesité (seguro que tu no te acuerdas, pero yo sí); me encantó conocerte y te deseo lo mejor. A **Jordi** (un gentleman) y a **Juanjo** (el estilista del lab), que siempre habéis estado ahí para hacer unas risas y para resolverme problemillas, sobretodo estas últimas semanas (Jordi, tú cómo entregaste la tesis provisional, anillada o en canutillo?). A **Rafa**, que hace mucho que nos conocemos, pero poco que estás en el lab y ya me has ayudado tanto como has podido. Gracias por transmitirme ese espíritu científico que al final de la tesis cuesta tanto de encontrar!

Voldria dedicar unes ratlles a tots els IPs que m'han ajudat a començar, definir i acabar aquesta tesi. Gràcies **Marga** pels teus savis i desinteressats consells. Com no, he d'agrair enormement al **Francesc** per totes les vegades que m'ha tret les castanyes del foc (que en són unes quantes) a canvi de només uns pocs conguitos. A l'**Alberto**, que siempre has estado ahí para lo que he necesitado, al otro lado de la poyata, compartiendo risas y sin quejarte nunca del jaleo que podíamos estar haciendo Marc y yo!! A **Ander**, gracias por tu ayuda, buenos consejos y por tener siempre tan buen humor.

Gràcies a tots els membres de la UBB (o UBS??), el **Dani** (el meu proveïdor de culleretes), la **Rebeca**, el **Xavi** (merci per ajudar-me amb els P valors!!!!), el **Toni**, el **Ferran**, l'**Elisabet**, l'**Elisabet Luquin**, el **David** i la **Marta**, que m'heu acollit aquests mesos de redacció. Quiero agradecerte especialmente a ti, **Rebeca**, por el montonazo de consejos que me has dado, por ayudarme con tantas cositas de formato, de redacción, con la portada, por consolarme tras cada imprevisto burocrático, por compartir conmigo tus experiencias y hacerme sentir un poquito menos rara.

Gràcies a les meves nenes de l'IRO, que sempre heu estat al meu costat. A la **Vane**, que ens vam conèixer gràcies a aquell viatge que vas fer a l'Argentina i des

de llavors he pogut contar amb tu sempre que ho he necessitat. Hem passat moltes coses des de llavors i segur que continuaran passant, el que importa és que estiguem a prop per compartir-ho. Ja veuràs com trobarem el camí. A **Itzi**, por todas las horas que hemos pasado juntas en virus, por pasarme células, protocolos, por escucharme, por compartir conmigo desde los cursos de doctorado hasta la redacción de mi tesis. Siempre has estado a mi lado y yo espero poder corresponderte cuando te toque a ti (que espero sea pronto). Cuenta conmigo siempre! A **Mon**, que eres una grande!!! Siempre de buen rollo, con esa frase adecuada para el momento, lista para reír o para escuchar y aconsejar, gracias! A **Sandra** y **Jessica**, que me animasteis a hacer el doctorado cuando compartíamos laboratorio en el Z. Las mejores compañeras que tuve nunca. No sé si alguna vez había tenido la oportunidad de agradeceros el año que pasamos juntas en el IRO…lo hago ahora, GRACIAS a las dos!!! Y, por supuesto, a **Nadia**, que he tenido la suerte de tenerte cerca en el IRO y en el ICO…Eres un sol y te agradezco todas las risas, los buenos ratos y el escucharme siempre!!! I a la **Gemma Aiza**, per suposat, la meva veïna de Poblenou!!! Gràcies per tenir sempre un somriure llest i per seguir-me les bromes!! Nosaltres sempre compartirem barri!!!

A tot l'LRT2, la **Mireia Morell**, la **Mireia Menéndez**, la **Juani**, la **Marta Pineda**, la **Vane**, la **Mireia Gausachs** (del barri de tota la vida…), l'**Eva,** la **Sara,** la **Olga**, l'**Eva Montes**, l'**Anna**, a totes, moltes gràcies per tenir sempre un somriure preparat pels passadissos. Per suposat, donar les gràcies a la **Conxi**, que és qui em va presentar a l'MA i, per tant, gràcies a qui vaig començar aquesta tesi.

He de dedicar un espai especial a les meves nenes de Menorca, les millors amigues que ningú podria tenir, la **Duna**, la **Marta**, la **Mireia** i la **Sole**. Sempre fidels, sempre al meu costat, m'heu fet riure quan no en tenia ganes, m'heu escoltat quan més ho necessitava, m'heu distret…Som un equip, noies, i sóc molt conscient de la sort que tinc de tenir-vos a la meva vida. Gràcies.

Last, but not least, I would like to sincerely thank **Aris**, first for receiving me in Philly without any doubt and second for his inestimable help. You are not only an outstanding scientist but also a wonderful person. Meeting you and **Matilda** has been a great pleasure for me and I really hope never loosing the contact. From Philly, I also want to thank **Garrett**, **Eka**, **Rachel**, **Andres** and **Alberto** for being so nice to me from the very beginning, for leading me come into their lives and share wonderful moments together. I will never forget my first Baseball game in the US!!! Thanks guys, you're awesome!!!

A la **Stella**, que és com la germana que no he tingut mai. Gracias por el apoyo que me has dado estos meses, por creer tanto en mi, por hacerme sentir que lo que hago vale la pena. Te quiero. A la **Pauli**, la meva reina, gràcies per tots els cafès a casa teva, per escoltar-me i no jutjar mai, pels sopars al Paulatinamente. Y no puedo olvidarme de agradecer a **Cris** el ser tan buena amiga, tener tan buen corazón y estar siempre dispuesta a escuchar. Gracias Cristy por tu desinteresada ayuda en el último momento!!!

A mi familia de Argentina, que a pesar de estar a más de 14.000 km siempre me han dado el apoyo, la fuerza, el calor que he necesitado. Gracias **Susana** y **Tito** por ser tan amorosos conmigo, por quererme tanto y hacerme sentir una más entre ustedes. Gracias por ser tan nobles y apoyarme siempre. Les quiero.

Gràcies **Victor**, per les teves correccions i sugerències, per la teva ajuda amb el Word, els formats, pel teu suport incondicional…la teva contribució ha estat imprescindible! I sobretot, gràcies **Oncle Swing** per crear la banda sonora d'aquesta tesi; hores de bona música que m'han ajudat a concentrar-me quan ja no em quedaven ganes de res.

Voldria agrair especialment a la meva mare, l'**Alícia**, per tot el que m'ha ajudat i recolzat, no només al llarg d'aquests anys de tesi, sinó de sempre. Les dues sabem que si avui estic a punt de dipositar la tesi és gràcies a tu. Sé que no sóc fàcil, que aquests mesos han estat especialment delicats i et vull agrair la paciència que has tingut en tot moment i les forces que m'has donat quan ha fet falta. T'estimo.

Por último, pero no menos importante, quiero agradecer TODO a mi compañero, mi amigo, mi amor, a **Ro**. No imagino, ni por un segundo, lo que hubiera sido de mí sin ti. Gracias por escucharme, aconsejarme, apoyarme, quererme en mis peores momentos, gracias por creer en mí. Gracias por cuidarme cuando yo no lo he hecho, por tenerlo todo listo cuando llegaba a casa agotada, por tener tanta paciencia y no reprocharme nunca nada. Esta tesis es tan mía como tuya. Gracias por ser lo mejor que me ha pasado nunca.

Doncs fins aquí hem arribat. De fons continua sonant *"Wish you were here"*. Sempre ho ha fet i m'ha ajudat a agafar forces i donar-li tot el sentit del món a aquesta feina.

Gràcies a tots!!

Ever tried. Ever failed. No matter.
Try again. Fail again. Fail better.

Samuel Beckett
(1906-1989)

TABLE OF CONTENTS

Table of contents

TABLE OF CONTENTS ..... **I**

ACRONYMS ..... **IX**

SUMMARY **1**

INTRODUCTION **5**

1 The centrosome **7**

1.1. Overview 7

1.2. Centrosome organization 7

1.3. The centrosome cycle 8

1.4. Regulation of the centrosome cycle 10

1.5. The centrosome and cell division 11

1.6. Centrosomes and cell polarity 14

1.7. Centrosomes, aneuploidy and cancer 14

2 Transforming coiled-coil motif-containing proteins **16**

2.1. Overview 16

2.2. Intracellular localization of TACCs 18

2.3. TACC functional roles 20

2.4. TACCs and mitosis 21

2.5. TACCs and cancer 21

2.6. TACC3, pathology and mitosis 22

3 The Tuberous Sclerosis Complex **24**

3.1. Overview 24

3.2. Clinical and pathological features 24

3.3. TSC genetics 25

3.4. TSC gene products: hamartin and tuberin 26

3.5. Role of TSC1 and TSC2 in cell growth and proliferation 27

3.6. TSC and the cell cycle 28

3.7. Novel functions of TSC1 and TSC2: the centrosome and cell polarity 30

HYPOTHESIS..... 31

AIMS OF THE STUDY 35

MATERIALS AND METHODS..... 39

1 MATERIALS 41

1.1. Cell culture 41

1.2. Antibodies 42

1.3. Expression vectors 44

2 EXPERIMENTAL PROCEDURES..... 45

2.1. Yeast two-hybrid screens 45

- Mating screening protocol 46
- Transformation screening protocol 47

2.2. Expression profile analysis.....48

2.3. Phylogenetic analyses 48

2.4. Cell cycle synchronization with the double thymidine block protocol.....49

2.5. MT binding assay 49

2.6. Cytokinesis assay 50

2.7. Cell fractionation analysis.....50

2.8. Cell viability/proliferation assay.....51

2.9. Three-dimensional culture of MCF10A cells on reconstituted basement membranes 51

2.10. Co-affinity purification assays 52

2.11. Co-immunoprecipitation assays.....52

2.12. Western blotting 52

2.13. Immunofluorescence 53

- Immunofluorescence staining of MCF10A cells cultured in rBM.....53

2.14. shRNA design and viral preparation 54

RESULTS **57**

1 A high-confidence TACC3 interactome network linked to centrosome biology **59**

2 TACC3 and TSC2 localize to the nuclear envelope and their depletion causes morphological alterations of this structure **69**

3 pS939-TSC2 localizes to cytokinetic structures in a TACC3-dependent manner **74**

4 TACC3 or TSC2 deficiency results in cytokinetic delay and increased appearance of binucleated cells **80**

5 *TSC2* acts epistatically to *TACC3* in the control of cell viability **86**

6 Depletion of TACC3 or TSC2 results in abnormal cellular organization and loss of cell polarity **89**

DISCUSSION **95**

CONCLUSIONS **107**

RESUM EN CATALÀ **111**

BIBLIOGRAPHY **131**

PUBLICATIONS **165**

List of figures

Figure 1: The centrosome structure 8

Figure 2: The centrosome cycle 9

Figure 3: The centrosome and mitosis 13

Figure 4: The TACC family of proteins 17

Figure 5: Model for TACC protein function at the spindle poles 19

Figure 6: Domains and motifs of TSC1 and TSC2 26

Figure 7: TSC/mTOR signaling pathway 29

Figure 8: Gateway destination vectors 44

Figure 9: Y2H Gateway vectors 47

Figure 10: Vectors used for lentiviral preparation 56

Figure 11: Y2H results for TACC3-TACC homo and heterodimers 59

Figure 12: A high-confidence TACC3 interactome network 60

Figure 13: Phylogenetic tree representing the evolutionary relationships among human TACCs and related proteins 62

Figure 14: Phylogenetic analysis of TACCs within coiled-coil motif-containing proteins (large tree) 63

Figure 15: Validation of TACC3 interactions by co-APs 65

Figure 16: Validation of TACC3 interactions by co-IP 66

Figure 17: Validation of TACC3-TSC2 interaction by co-IP 67

Figure 18: TSC2 N-term region mediates TACC3 interaction 68

Figure 19: MT association of TSC1 and TSC2 69

Figure 20: Nuclear envelope localization of TSC2/Tsc2 70

Figure 21: Nuclear envelope localization of TACC3 70

Figure 22: Tacc3 and Tsc2, but not Tsc1, co-purify with the nuclear fraction 71

Figure 23: Morphological alterations of the nuclear envelope in Tacc3- and Tsc2-deficient MEFs 72

Figure 24: Subcellular localization of TSC2 during cell division 74

Figure 25: Subcellular localization of total- and pS558-TACC3 during cell division.75
Figure 26: Subcellular localization of TACC3 and TSC2 during mitosis and cytokinesis.....76
Figure 27: TACC3-TSC2 interaction through the cell cycle.....77
Figure 28: TACC3-dependent subcellular localization of pS939-TSC2 during cell division 78
Figure 29: Localization of pS2448-mTOR during cell division is not affected in TACC3-depleted HeLa cells 79
Figure 30: Tacc3- and Tsc2-deficient MEFs show abnormal cytokinesis compared to controls.....80
Figure 31: Tacc3-deficient and Tsc2-deficient MEFs present higher percentages of binucleated cells relative to wild-type counterparts 81
Figure 32: Tsc2-deficiency causes delay in cytokinesis progression 82
Figure 33: Tsc1-deficiency causes delay in cytokinesis progression 83
Figure 34: Tsc1-deficient MEFs present high percentage of binucleated cells but not aberrant cytokinesis.....84
Figure 35: Association of M/G1 genes with Eker status.....85
Figure 36: *TACC3-TSC2* epistatic relationship.....86
Figure 37: *TACC3-TSC2* convergence to the early mitotic checkpoint mediated by CHFR 87
Figure 38: mTOR/TSC mediated regulation 88
Figure 39: Depletion of TACC3 and TSC2, but not TSC1, impair apicobasal polarization.....89
Figure 40: Depletion of TACC3 and TSC2, but not TSC1, affects apicobasal polarity 90
Figure 41: Simultaneous depletion of TACC3/TSC2 and TACC3/TSC1 impairs apicobasal polarization 91
Figure 42: Simultaneous depletion of TACC3/TSC2 and TACC3/TSC1 affects apicobasal polarity.....92

Figure 43: Model for TACC3-TSC2 associations in cell division 103

List of tables

Table 1: List of primary antibodies.....43

Table 2: Target sequences used to down-regulate *TACC3*, *TSC2* and *TSC1* expressions 55

Table 3: Over-represented GO biological process terms in the TACC3 interactome 64

ACRONYMS

3-AT	3-amino-1,2,4-triazole
3D	Three-dimensional
A	Ampere
aa	Amino acid
ab	Antibody
AD	Activation domain
AKT	RAC-alpha serine/threonine-protein kinase
APC/C	Anaphase promoting complex/cyclosome
ARHGEF2/GEF-H1	RHO/RAC guanine nucleotide exchange factor 2
AURKA	Aurora kinase A
AURKB	Aurora kinase B
bp	Base pair
BSA	Bovine serum albumin
BT474	Human breast tumor cell line
BUB1B	Budding uninhibited by benzimidazoles 1 homolog beta (yeast)
CCNA	Cyclin A
CCNB1	Cyclin B1
CDC20	Cell division cycle 20 homolog (*S. cerevisae*)
CDH1	Cadherin 1, type 1, E-cadherin (epithelial)
CDK	Cyclin-dependent kinase
cDNA	Complementary deoxyribonucleic acid
CEP164	Centrosomal protein 164 kDa
CHFR	Checkpoint with forkhead and ring finger domain protein
ch-TOG	Colonic and hepatic tumor overexpressed protein
CIN	Chromosomal instability
C-NAP1	CEP250, centrosomal protein 250 kDa
CO_2	Carbon dioxide
Co-AP	Co-affinity purification
Co-IP	Co-immunoprecipitation
CP110	Centrosomal protein 110 kDa
CPEB1	Cytoplasmic polyadenylation element binding protein
CROCC	Ciliary rootlet coiled-coil, rootletin
CS	Cowden syndrome
C-term	Carboxy-terminus
DAPI	4',6-diamidino-2-phenylindole
DBD	DNA binding domain
DMSO	Dimethyl sulfoxide
DNA	Deoxyribonucleic acid

dNTP	Deoxyribonulceotide triphosphate
DOX	Doxycycline
DTT	Dithiothreitol
ECL	Enhanced chemiluminescence
EDTA	Ethylene-diamine-tetracetic acid
ELT3	Eker rat leiomyoma tumor cell line
ERM	Ezrin-radixin-moesin
FBS	Fetal bovine serum
FDR	False discovery rate
FGFR	Fibroblast growth factor receptor
g	Gram
G418	Geneticin
GAP	GTPase activating protein
gcRMA	Gene chip multi-array average
GDP	Guanosine-5'-diphosphate
GO	Gene ontology
GSEA	Gene set enrichment analysis
GST	Glutathione S-transferase
GTP	Guanosine-5'-triphosphate
h	Hour
HBD	Hamartin binding domain
HCl	Hydrochloric acid
HEF1	Enhancer of filamentation 1
hEGF	Human epidermal growth factor
HEK293	Human embryonic kidney cell line
HeLa	Human epithelial cervical cancer cell line
HEPES	4-(2-hydroxyethyl)-1-piperazinethanesulfonic acid
HERC1	HECT domain and RCC1-like domain-containing protein 1
HIS	Histidine
HIV	Human immunodeficiency virus
HME/TERT	Telomerase-immortalized human mammary epithelial cells
HMMR	Hyaluronan-mediated motility receptor
HRP	Horseradish peroxidase
IgG	Immunoglobulin
kb	Kilo base
KCl	Potassium chloride
kDa	Kilo Dalton
L	Liter

LAM	Lymphangioleiomyomatosis
LATS2	Large tumor suppressor, homolog 2 (*Drosophila*)
LEU	Leucine
LiAc	Lithium acetate
LMNA	Lamin A
LOH	Loss of heterozygosity
LZTS2/LAPSER1	Leucine zipper, putative tumor suppressor 2
m	Meter
M	Molar
m	Milli
MAD2	Mitotic arrest deficient 2-like protein 1
MCF7	Human breast adenocarcinoma cell line
MEFs	Mouse embryonic fibroblasts
MEGM	Mammary epithelial growth media
min	Minute
ML	Maximum likelihood
mRNA	Messenger ribonucleic acid
Msps	Mini spindles
MT	Microtubule
MTOC	Microtubule organizing center
mTOR	Mammalian target of rapamycin
MTT	3-(4,5-dimethylthiazol-2-yl)-2,5-diphenyl tetrazolium bromide
n	Nano
NaCl	Sodium chloride
NaF	Sodium fluoride
NaOH	Sodium hydroxide
NDEL1	Nuclear element distribution-like 1
NEB	Nuclear envelope breakdown
NEK2	NIMA (never in mitosis a)-related kinase 2
NIH3T3	Mouse embryonic fibroblast cell line
NLS	Nuclear localization signal
N-term	Amino terminus
ºC	Degree Celsius
OD	Optical density
OMIM	Online Mendelian inheritance in man
ORF	Open reading frame
P70S6K	Ribosomal protein S6 kinase, 70 kDa, polypeptide 1
PAGE	Polyacrylamide gel electrophoresis

PATJ	PALS1-associated tight junction protein
PBS	Phosphate buffered saline
PCC	Pearson correlation coefficient
PCM	Pericentriolar material
PCR	Polymerase chain reaction
PEG	Polyethylene glycol
PI3K	Phosphoinositide-3-kinase
PIP2	Phosphatidyl-inositol (4,5) biphosphate
PIP3	Phosphatidyl-inositol (3,4,5) triphosphate
PJS	Peutz-Jegher syndrome
PKD1	Polycystic kidney disease 1
PLK1	Polo-like kinase 1
PP4	Protein phosphatase 4
PSI-BLAST	Position-specific iterated BLAST
PVDF	Polyvinylidene fluoride
RAPTOR	Regulatory-associated protein of mTOR, complex 1
rBM	Reconstituted basement membrane
RHEB	RAS homolog enriched in brain
RHOA	Ras homolog gene family, member A
RICTOR	RAPTOR independent companion of mTOR, complex 2
RNA	Ribonucleic acid
rpm	Revolutions per minute
RPS6	Ribosomal protein S6
RT-PCR	Reverse transcriptase polymerase chain reaction
SAC	Spindle assembly checkpoint
SAF	Spindle assembly factor
SDS	Sodium dodecyl sulfate
SEN	Subependymal nodules
Ser	Serine
shRNA	Short hairpin RNA
TBS	Tris buffered saline
TPX2	Targeting protein for xklp2 homolog (*Xenopus laevis*)
Tris	Tris(hydroxymethyl)aminomethane
TRP	Tryptophan
TSC	Tuberous Sclerosis Complex
TSC1	Hamartin
TSC2	Tuberin
TUBA	α-tubulin

V	Volt
WCE	Whole cell extract
WHS	Wolf-Hirschhorn syndrome
Wild type	Wt
x g	Centrifugal force
XMAP215	Microtubule-associated protein 215 kDa (*Xenopus laevis*)
Y2H	Yeast two-hybrid
YPD	Yeast peptone dextrose
ZO-1	Tight junction protein zona occludens 1
γ-TURC	γ-tubulin ring complex
µ	Micro

SUMMARY

Studies of the role of tuberous sclerosis complex (TSC) proteins (TSC1/TSC2) in pathology have focused mainly on their capacity to regulate translation and cell growth, but their relation to alterations of cellular structures and the cell cycle is not yet fully understood. The transforming acidic coiled-coil (TACC) domain-containing proteins are central players in structures and processes involving the microtubule network. Here, TACC3 interactome mapping identified TSC2 and 15 other proteins, including TACC homo and heterodimers, and two evolutionary conserved interactors (ch-TOG/CKAP5 and FAM161B). TACC3 and TSC2 co-localize and co-purify with components of the nuclear envelope, and their deficiency causes morphological alterations of this structure. During cell division, TACC3 is necessary for the proper localization of phospho-Ser939 TSC2 at the spindle poles and cytokinetic bridges. Consistently, abscission alterations and increased frequency of binucleated cells were observed in Tacc3- and Tsc2-deficent cells relative to controls. In regulating cell division, *TSC2* acts epistatically to *TACC3* and, in addition to canonical TSC/mTOR signaling and cytokinetic associations, converges to the early mitotic checkpoint mediated by CHFR. Our findings link TACC3 to novel structural and cell division functions of TSC2, which may provide additional explanations for the clinical and pathological manifestations of lymphangioleiomyomatosis disease and TSC syndrome, including the greater clinical severity associated with *TSC2* germline mutations relative to *TSC1*.

INTRODUCTION

1 The centrosome

1.1. Overview

The term "centrosome" was coined by Theodor Boveri almost one century ago as a *"single extremely minute body, or more commonly a pair of bodies, staining intensely with haematoxylin (…) and surrounded by a cytoplasmic radiating aster"* (Boveri, 1914). In addition, because the poles that define the essential bipolar nature of the mitotic spindle contain a centrosome, Boveri described this organelle as the *"special organ of cell division"*. Since these first observations, fundamental questions have yet to be answered regarding the regulation of the centrosome, its role in cell biology and its alteration in disease.

The centrosome is the major microtubule organizing center (MTOC) in most animal cells. During interphase it influences microtubule (MT)-dependent processes, including organelle transport, cell shape, polarity and motility (reviewed in (Bettencourt-Dias and Glover, 2007; Nigg and Raff, 2009; Sankaran and Parvin, 2006)). Furthermore, centrosomes play a critical role in cell division, where they control mitotic spindle bipolarity, spindle positioning and cytokinesis (reviewed in (Meraldi and Nigg, 2002)). Aberrations in centrosome number, structure or function can interfere with bipolar spindle formation and, therefore, equal segregation of genomic material in daughter cells, leading to chromosome instability (CIN). In this context, centrosome duplication is tightly regulated throughout the cell cycle (Meraldi and Nigg, 2002).

1.2. Centrosome organization

The centrosome is a tiny (1-2 μm of diameter) and cytoplasmic centrally-positioned cellular organelle (Wilson, 1925). Structurally, it is highly conserved among higher eukaryotes and consists of two cylindrical centrioles embedded in an electron dense mesh called the pericentriolar material (PCM) (**Figure 1**) (reviewed in (Bettencourt-Dias and Glover, 2007)).

The PCM provides a scaffold for proteins that are important for regulating centrosome duplication and function, containing the basic unit for MT nucleation, the γ-tubulin ring complex (γ-TURC) (Moritz et al., 1995). Embedded within the surrounding PCM, the two centrioles are composed of a symmetrical barrel-shaped array of nine triplets of MTs. The two centrioles within a centrosome are positioned in an orthogonal arrangement with respect to each other and differ in appearance: one centriole has two sets of nine appendages at the end distal to its partner and is

called the mature centriole (also called the mother or maternal centriole), while the other lacks these structures (Vorobjev and Chentsov Yu, 1982).

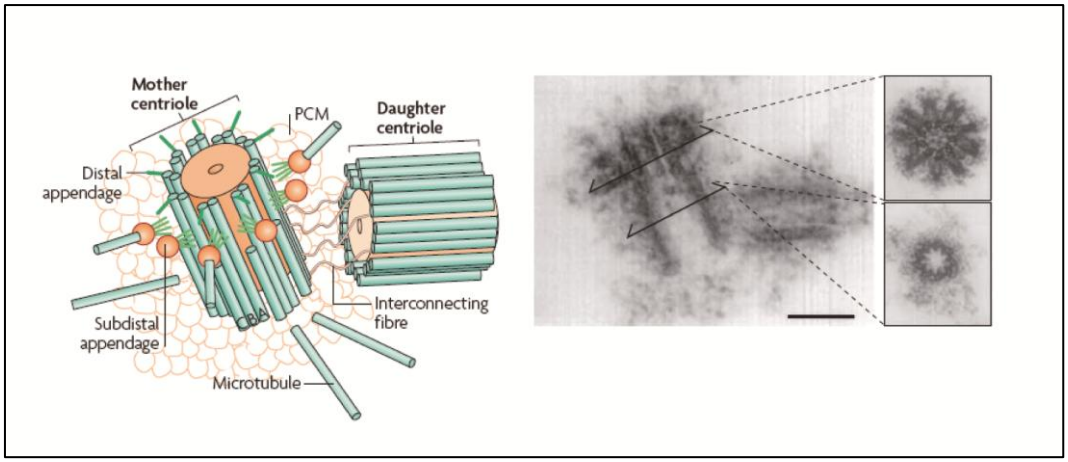

Figure 1: The centrosome structure

Schematic view of centrosome parts (left panel). Electron micrograph of the centrosome. The top inset indicates a cross-section of subdistal appendages; the bottom inset indicates a cross-section of the proximal part of the centriole (right panel). Scale bar represents 0.2 μm. Adapted from (Bettencourt-Dias and Glover, 2007).

1.3. The centrosome cycle

In addition to their role as the MTOC in interphase and mitotic cells, centrosomes are also closely related to cell cycle progression (Hinchcliffe et al., 2001; Khodjakov and Rieder, 2001). Centrosome duplication begins at the G1-S phase of the cell cycle and is strictly coordinated with DNA replication, mitosis and cell division (Sluder and Hinchcliffe, 2000) (**Figure 2**). Five consecutive steps lead to centrosome division: 1st/ centriole disorientation, where centrioles in a centrosome lose their orthogonal configuration; 2nd/ nucleation of the daughter centrioles; 3rd/ elongation of the procentrioles; 4th/ centrosome maturation; and 5th/ separation of centrosomes (reviewed in (Lukasiewicz and Lingle, 2009)) (for a schematic representation see **Figure 2**).

The physiological significance of centrosome disorientation remains unclear. Although this step has commonly been considered a pre-requisite for centrosome duplication (Freed et al., 1999; Lacey et al., 1999), it has also been observed that by the end of M phase the two centrioles separate from each other, and this event also seems to be prerequisite for proper cytokinesis completion (Piel et al., 2000; Piel et al., 2001).

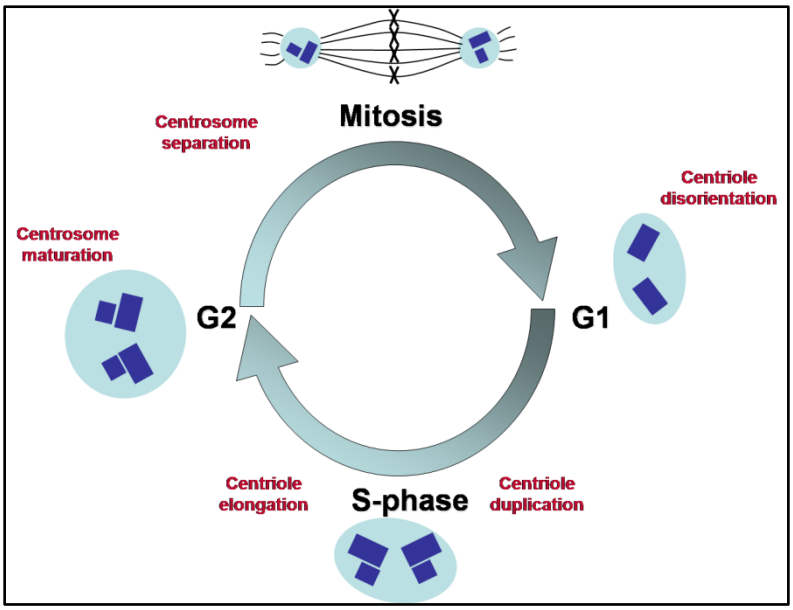

Figure 2: The centrosome cycle

Schematic representation of centrosome duplication coupled to cell cycle phases. Centrioles are shown in dark blue and PCM in light blue.

Centrosome duplication is a semi-conservative process that takes place at the beginning of or during S phase through the appearance of procentrioles growing at right angles in a region close to the proximal end of each parental centriole (Kochanski and Borisy, 1990). Next, elongation of the procentrioles occurs throughout S and G2 phases, so that in late G2 the centrosome is composed of two pairs of centrioles.

Centrosome maturation begins at G2/M phases and is characterized by a dramatic increase in centrosome size due to the recruitment of several proteins, in particular of the γ-TURC (Zheng et al., 1995). During this process, the amount of γ-tubulin at vertebrate centrosomes increases approximately three- to five-fold (Khodjakov and Rieder, 1999), accompanying a striking augmentation of MT-nucleating activity at the centrosome (De Brabander, 1982; Gorgidze and Vorobjev, 1995; Piel et al., 2000). Simultaneously, centrosome separation begins in G2 phase so that by prophase of mitosis the centrosomes can migrate to opposite sides of the nucleus, where they will form the bipolar mitotic spindle (Ault and Rieder, 1994). Once the chromosomes have been equally segregated, the cell undergoes cytokinesis yielding two daughter cells, each with one centrosome containing two centrioles. At the end of mitosis and beginning of G1 phase, the centrosome cycle begins again with centriole disorientation (Lukasiewicz and Lingle, 2009).

1.4. Regulation of the centrosome cycle

Centrosome duplication occurs once per cell cycle and is subject to strict control within cells. Several studies have identified both phosphorylation and proteolysis as major biochemical mechanisms for the regulation of the centrosome cycle (reviewed in (Fry et al., 2000; Hansen et al., 2002; Meraldi and Nigg, 2002)). For the correct execution of cell division, centrosome duplication must be coordinated with other cell cycle events. In this scenario, a key player is the cyclin-dependent kinase 2 (CDK2), which regulates DNA replication and centrosome duplication (Hinchcliffe et al., 1999; Lacey et al., 1999; Matsumoto et al., 1999; Meraldi et al., 1999). Indeed, recent work shows that centrosomal localization and activation of CDK2 is required for both replication events (Ferguson and Maller, 2010).

Phosphorylation activity increases substantially at the centrosome during the maturation step (reviewed in (Rusan and Rogers, 2009)). A major player in maturation appears to be aurora kinase A (AURKA), which regulates the localization, levels and/or biochemical modification of several centrosomal proteins, including enhancer of filamentation 1 (HEF1) (Pugacheva and Golemis, 2005), large tumor suppressor, homolog 2 (*D. melanogaster*) (LATS2) (Toji et al., 2004), polo-like kinase 1 (PLK1) (Lane and Nigg, 1996) and targeting protein for *Xenopus* kinesin-like protein 2 (TPX2) (De Luca et al., 2006). HEF1, a protein initially defined as a component of cell attachment machinery (Bouton et al., 2001), plays an additional role in cell division through the interaction with AURKA and regulation of centrosome cohesion and amplification (Pugacheva and Golemis, 2005). The tumor suppressor LATS2 requires AURKA phosphorylation for its centrosomal localization, where it may regulate cell proliferation (Toji et al., 2004). Regarding PLK1, AURKA phosphorylates this kinase at mitotic entry, suggesting that they both function in the same centrosome maturation pathway (Macurek et al., 2008; Seki et al., 2008a; Seki et al., 2008b). Interestingly, besides the known role of TPX2 in MT organization, TPX2 seems to be involved in centrosome maturation, probably in a coordinated manner with AURKA and PLK1 (De Luca et al., 2006).

Next, centrosome separation occurs early in mitosis with a major role assigned to the NIMA (never in mitosis a)-related kinase 2 (NEK2) (Fry et al., 1998). Throughout most of the cell cycle, the proximal ends of the original centrioles are connected in part by the centriole-associated coiled-coil protein C-NAP1 (also known as CEP250) and the ciliary rootlet coiled-coil protein CROCC (also known as rootletin) (Fry et al., 1998; Mayor et al., 2000). C-NAP1 and CROCC maintain centriole cohesion until they are phosphorylated by NEK2, leading to displacement of these proteins and subsequent centrosome separation (Bahe et al.,

2005; Fry et al., 1998). AURKA and PLK1 have also been associated with this step (reviewed in (Lukasiewicz and Lingle, 2009)). Studies in *D. melanogaster* showed that *AurA* mutant embryos were unable to form bipolar spindles, leading to tetraploid cells as a result of incomplete chromatin separation in anaphase (Glover et al., 1995). Similarly, human cells injected with antibodies directed against PLK1 form monopolar spindles containing two small unseparated centrosomes (Lane and Nigg, 1996).

While diverse kinase activities are key in regulating the centrosome cycle, ubiquitin-dependent proteolysis also plays an important role (reviewed in (Hansen et al., 2002)). Components of the E3 ubiquitin ligase complexes SCF (SKIP, Cullin and F-box) and anaphase promoting complex/cyclosome (APC/C) localize to the centrosome throughout the cell cycle in mammalian cells (Freed et al., 1999; Gstaiger et al., 1999; Wigley et al., 1999) and were shown to regulate the G1/S transition and entry into mitosis, respectively (Sankaran and Parvin, 2006). Recently, it has been reported that APC/C is responsible for degradation of certain spindle assembly factors (SAFs), including RHAMM/*HMMR*, providing a molecular basis for APC/C regulation of spindle assembly (Song and Rape, 2010). Furthermore, other studies have demonstrated that proteasome inhibition leads to accumulation of several centrosomal proteins at the PCM (Didier et al., 2008; Zhao et al., 2003) and spindle pole fragmentation during mitosis (Ehrhardt and Sluder, 2005).

1.5. The centrosome and cell division

As described above, at the transition of G2/M phases the two centrosomes move to opposite poles of the cell and form the mitotic spindle (**Figure 3**). The assembly of this MT-comprised structure is initiated during the first mitosis sub-phase, the prophase. Next, in prometaphase, nuclear envelope breakdown (NEB) occurs, which is required for spatial separation of the duplicated chromosome sets (Zhai et al., 1996). The MT strands of the mitotic spindle consist of α- and β-tubulin dimers which are nucleated at the centrosome (minus-end) and depolymerized at their tips (plus-end) (Erickson and Stoffler, 1996; Fygenson et al., 1994; Mitchison and Kirschner, 1984a, b; Weisenberg et al., 1968; Weisenberg et al., 1976). The dynamic interplay is crucial in order to achieve the proper bipolar attachment of the MT arms to the chromosomes (Nicklas and Ward, 1994).

MT contact with the condensed DNA occurs at the kinetochores, protein structures at the centromeres of chromosomes. Eventually, in metaphase, all

chromosomes are attached to the spindle MTs in a bipolar fashion and converge at the midzone. Correct chromosome capture and alignment are crucial, since alterations in these processes may lead to aneuploidy (Doxsey, 2002; Nigg, 2002, 2006; Sluder, 2005). To ensure an accurate segregation of chromosomes, the mitotic checkpoint (also known as the spindle checkpoint) delays sister chromatid separation until all kinetochores are bound to the spindle. The checkpoint is activated by sensing kinetochores that are not attached to MTs or lack of tension across attached kinetochores (McIntosh, 1991). Recruitment of the components of the mitotic checkpoint, which include the budding uninhibited by benzimidazoles 1 homolog beta (yeast) (BUB1B) and the mitotic arrest deficient 2-like protein 1 (MAD2), is essential in delaying mitotic progression by inhibiting the activity of the cell division cycle 20 homolog (*S. cerevisae*) (CDC20), which in turn is required for activation of the APC/C (Mao et al., 2003; Sudakin et al., 2001; Wassmann et al., 2003). When all kinetochores are completely attached to the spindle MTs, mitotic checkpoint signals are relaxed and CDC20 activates the APC/C E3 ubiquitin ligase activity, leading to sister chromatid separation (Hwang et al., 1998). This movement hallmarks the onset of the anaphase, which is followed by the telophase, when the chromatids reach their respective spindle poles and begin to decondense. A new nuclear envelope forms around the DNA, while the beginning of cytokinesis is recognized by the progression of cell division with the development of a constriction (cleavage furrow) around the midzone.

The process of cytokinesis can be divided into four stages: cleavage furrow initiation, cleavage furrow ingression, midbody formation and abscission (reviewed in (Li et al., 2010)). Each stage is dependent on the proper execution of the prior stage, thus interference with any stage may result in cytokinesis failure. The first stage specifies the cleavage plane by recruiting a central regulator of cytokinesis, the ras homolog gene family, member A (RHOA), to the site of cleavage (Bement et al., 2005; Drechsel et al., 1997; Jantsch-Plunger et al., 2000; Kamijo et al., 2006; Kishi et al., 1993; Nishimura and Yonemura, 2006; Yonemura et al., 2004; Yoshizaki et al., 2003; Yuce et al., 2005). If this step is perturbed, cytokinesis will not initiate properly (Guidotti et al., 2003; Kudryavtsev et al., 1993; Margall-Ducos et al., 2007; Toyoda et al., 2005). In the second stage of cytokinesis, the cleavage furrow ingresses through formation of an actomyosin ring and a myosin-dependent motor activity (reviewed in (D'Avino, 2009; Matsumura, 2005)). Failure at this step may prevent furrow initiation or lead to partial ingression of the furrow followed by regression (Gunsalus et al., 1995; Haviv et al., 2008; Straight et al., 2003). The third stage of cytokinesis is characterized by formation of the midbody and

stabilization of the cytokinetic furrow (reviewed in (Margolis and Andreassen, 1993)). This stage requires proper function of proteins located in the central spindle (e.g. KIF23 (Matuliene and Kuriyama, 2002, 2004), AURKB (Terada et al., 1998) or LAPSER1 (Sudo and Maru, 2007)) and failure at this point will lead to defective cytokinesis, polyploidy and increased genome instability (Delaval et al., 2004; Sudo and Maru, 2007; Zhu et al., 2005). The final stage in cytokinesis, abscission, is the step in which cytoplasmic contents are finally separated from one another. This event requires the presence of a functional midbody, but also additional proteins involved in vesicle trafficking and fusion (reviewed in (Li et al., 2010)). Moreover, the centrosomal protein CEP55 is essential for this step and its absence leads to midbody formation defects (Zhao et al., 2006).

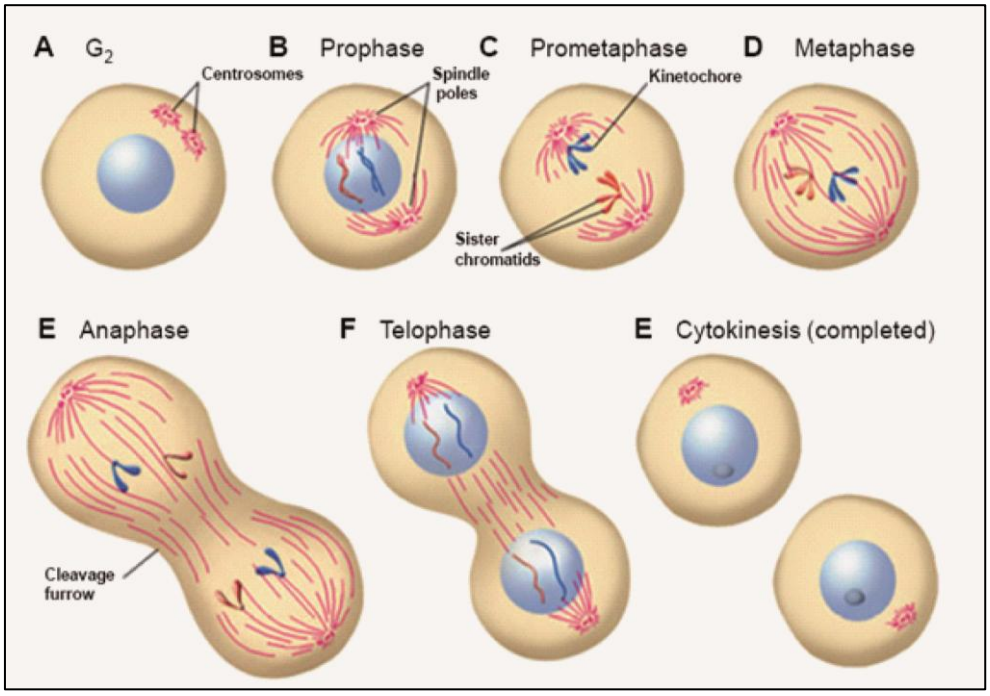

Figure 3: The centrosome and mitosis

The centrosome is duplicated during S/G2 phases (**A**) and, subsequently, mitotic spindle poles take positions on the opposite sides of the nucleus (**B**). Nuclear envelope breakdown takes place in prophase and the mitotic spindle is assembled at the (pro)metaphase (**C-D**). Anaphase is initiated with cyclin B1 (CCNB1), enabling chromosome segregation to begin (**E**). Nuclear envelopes of daughter cells are re-assembled during the telophase (**F**) and cell division is completed with cytokinesis (**G**). Adapted from (Lodish, 1999).

1.6. Centrosomes and cell polarity

For many cell types, including epithelial cells, the position of the centrosome relative to the nucleus defines a structural "cell axis" (Wilson, 1925) that determines the functional polarity of the cell (Buendia et al., 1990). It was initially proposed that polarity is maintained, in part, by the organization of MT arrays originating from the centrosome and by directional vesicular trafficking that proceeds along these MTs (Rindler et al., 1987). Further studies in *C. elegans* embryos assessed the contribution of the centrosome to polarity establishment by ensuring proper positioning of the organelle close to the cortex and by increasing the assembly of pericentriolar material (Cowan and Hyman, 2004; Cuenca et al., 2003; Goldstein and Hird, 1996; O'Connell et al., 2000; Sadler and Shakes, 2000; Wallenfang and Seydoux, 2000). Therefore, an abnormal number of centrosomes may adversely affect maintenance of cell polarity in interphase cells (Lingle et al., 1998).

More recently, centrosome localization has been shown to be necessary for determining neuronal polarity (de Anda et al., 2005). In addition, centrosome repositioning is essential for migration in neuronal cells (Bellion et al., 2005; Tsai and Gleeson, 2005). A model for neuronal migration has been suggested in which the nucleus closely follows the centrosome due to their tight association by MTs (Tsai and Gleeson, 2005). Here, it is worth noting that many human neurological diseases have been either directly or indirectly linked to disordered neuronal migration (Tsai and Gleeson, 2005).

1.7. Centrosomes, aneuploidy and cancer

The correct execution of centrosome duplication, maturation and separation underlies mitotic bipolar spindle formation and, as a result, faithful chromosome segregation. Consequently, deregulation of centrosome function can impair the accurate inheritance of genetic material (reviewed in (Zyss and Gergely, 2009)). Theodor Boveri proposed that cancer commonly arises through aneuploidy linked to abnormal mitoses and postulated the underlying cause of this phenotype to be aberrant centrosomes (Boveri, 1914). This idea has recently attracted renewed interest and several studies report frequent centrosome abnormalities in cancer cells, including an increase in number and volume, supernumerary centrioles, accumulation of excess pericentriolar material and aberrant phosphorylation of centrosomal proteins (Lingle et al., 2002; Lingle et al., 1998; Lingle and Salisbury, 1999; Pihan et al., 1998).

The main centrosome aberrations observed in pathological conditions are amplification (i.e. more than two centrosomes in a cell) and hyperplasia (i.e. centrosomes that appear significantly larger than normal). Centrosome amplification can result from (i) uncoupling of the centrosome duplication, (ii) fragmentation, (iii) failure of cytokinesis, or (iv) aberrant expression of certain centrosomal proteins (e.g. AURKA (Meraldi et al., 2002) or SCF (Nakayama et al., 2000)) (reviewed in (Sankaran and Parvin, 2006)). Several studies have suggested that centrosome amplification may drive aneuploidy by increasing the frequency of abnormal mitosis that leads to chromosome missegregation (Boveri, 1914; Lingle et al., 2002; Lingle et al., 1998; Pihan et al., 2001; Zhou et al., 1998). Accordingly, centrosome amplification is a common feature of both hematological cancer and solid tumor cells (Chng et al., 2006; Lingle et al., 1998; Lingle and Salisbury, 1999). Moreover, precancerous and preinvasive neoplastic lesions can exhibit centrosome amplification, which suggests that amplification may be a causative event of carcinogenesis in some conditions (Chng et al., 2006; Pihan et al., 2003).

Although it has been difficult to establish a causal relationship between centrosome abnormalities and cancer, deregulation of several oncogenes and tumor suppressor genes is well known to affect the number of centrosomes (reviewed in (Fukasawa, 2007)) and to promote tumorigenesis in model organisms (Babu et al., 2003; Baker et al., 2004; Sotillo et al.) This observation includes components of diverse signaling pathways or biological processes; regulators of centrosome biology are implicated in the recognition of DNA damage (e.g. ATR (Brown and Costanzo, 2009), BRCA1 (Xu et al., 1999), BRCA2 (Tutt et al., 1999), GADD45 (Hollander et al., 1999), MDM2 (Carroll et al., 1999), p21 (Mantel et al., 1999) and p53 (Fukasawa et al., 1996)), ubiquitin-dependent protein degradation (e.g. SKP2 (Gstaiger et al., 1999) and TSG101 (Xie et al., 1998)) and mitotic progression (e.g. AURKA (Meraldi et al., 2002) and BIRC5 (Li et al., 1999)) (reviewed in (Meraldi and Nigg, 2002)). In addition, aneuploidy caused by deregulation of essential components of the mitotic checkpoint (MAD2, BUB3, or BUB1B) has been implicated in tumorigenesis (Babu et al., 2003; Baker et al., 2004; Michel et al., 2001; Sotillo et al., 2010). Together, these observations highlight the convergence of diverse pathways or processes on the proper regulation of centrosome biology and, when perturbed, its wide-spread link to disease and pathology.

2 Transforming coiled-coil motif-containing proteins

2.1. *Overview*

Proteomic analysis of human centrosomes revealed that a relatively high percentage of proteins in this organelle (~75%) contain one or several coiled-coil motifs (Andersen et al., 2003). This motif type is an evolutionarily conserved structure tailored to mediate protein-protein interactions (Salisbury, 2003). Thus, several coiled-coil-containing proteins are known to act as anchors for other essential centrosome components and/or for key regulators of centrosome function (Salisbury et al., 2004). In recent years, proteins with a conserved transforming acidic coiled-coil (TACC) domain have emerged as important players in centrosome biology, initially described in *D. melanogaster* as necessary for centrosome activity and MT assembly during cell division (Gergely et al., 2000b). The TACC domain covers ~200 amino acids (aa) at the corresponding carboxyl terminus (C-term) (Gergely, 2002) and is necessary for protein localization to the centrosome and spindle apparatus (Gergely, 2002).

TACC proteins have been described in different organisms, ranging from yeasts to mammals. A single TACC member has been described in *C. elegans* (TAC-1) (Bellanger and Gonczy, 2003; Le Bot et al., 2003; Srayko et al., 2003), *D. melanogaster* (D-TACC) (Gergely et al., 2000b), *X. laevis* (maskin or tacc3) (Stebbins-Boaz et al., 1999), and *S. pombe* (alp7) (Sato et al., 2004) proteomes. In mammals, the TACC family consists of at least three members: TACC1 (Still et al., 1999a), TACC2 (Chen et al., 2000; Pu et al., 2001) and TACC3 (McKeveney et al., 2001; Sadek et al., 2000; Still et al., 1999b) (see **Figure 4** for description). Two additional candidates have been proposed: TACC4 in *O. cuniculus* (Steadman et al., 2002) and RHAMM (*HMMR* gene) in humans (Maxwell et al., 2003). Evidence used to support the claim that RHAMM may be a fourth human TACC family member, although evolutionarily distant (Still et al., 2004), includes the conserved genomic organization of the corresponding loci, the prediction of coiled-coil-containing domain and RHAMM localization and regulation at the centrosome (Maxwell et al., 2003).

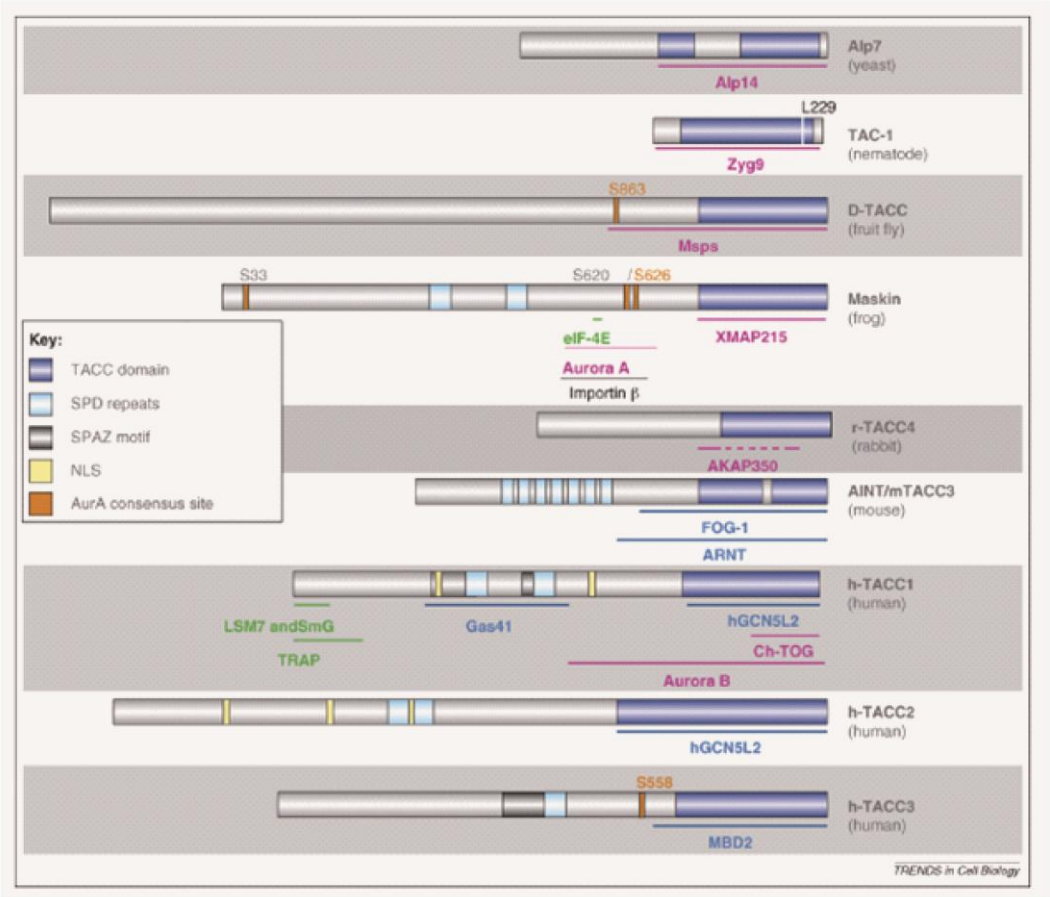

Figure 4: The TACC family of proteins

Structural organization and regions of interaction with binding partners of TACCs. The blue box represents the conserved TACC domain. Some members have highly acidic, imperfect repeats of 33 aa (pale-blue boxes) or a serine-proline Azu-1 motif (dark-grey boxes). Yellow lines indicate the position of nuclear localization signals (NLSs), and the conserved consensus sequences for AURKA phosphorylation are shown as orange bars. Adapted from (Peset and Vernos, 2008).

2.2. *Intracellular localization of TACCs*

It has been ten years since Gergely and colleagues identified D-TACC as a protein concentrated at centrosomes that is essential for normal spindle formation (Gergely et al., 2000b). This group also described the intracellular localization of human TACCs: TACC1 was found to be weakly concentrated at the centrosomes and mitotic spindles, while TACC2 and TACC3 showed a contrasting pattern (Gergely et al., 2000a); in particular, TACC3 was found to be strongly concentrated in a diffuse region surrounding the centrosomes and showed the strongest association with the mitotic spindle apparatus (Gergely et al., 2000a). However, localization of TACC orthologs is not restricted to the centrosome, and most of them also associate with MTs during interphase and cell division to varying extents; tacc3 and TAC-1 localize all along spindle MTs, while D-TACC associates with both spindle and astral MTs (Bellanger and Gonczy, 2003; Gergely et al., 2000b; Giet et al., 2002; O'Brien et al., 2005; Peset et al., 2005). In addition, TACC1 and TACC3 were also located in the nucleus of interphase HeLa cells, with TACC3 being slightly concentrated (Gergely et al., 2000a).

Consistent with a key role in centrosome biology, localization of TACCs to centrosomes is dependent on phosphorylation by AURKA in human cells and by its orthologs in *C. elegans*, *D. melanogaster* and *X. laevis* (Barros et al., 2005; Giet et al., 2002; Kinoshita et al., 2005; Peset et al., 2005). Moreover, it has been proposed that this modification is required to regulate spindle dynamics and organization (Barros et al., 2005; Giet et al., 2002; Kinoshita et al., 2005; LeRoy et al., 2007; Peset et al., 2005). These studies have specifically identified the conserved residues Ser626 of tacc3 and Ser863 of D-TACC as the site phosphorylated by AURKA (Barros et al., 2005; Kinoshita et al., 2005). Importantly, this serine is conserved in human TACC3 (Ser558) and requires phosphorylation by AURKA for proper centrosomal and mitotic spindle localization (LeRoy et al., 2007). Recently, quantification of phosphorylated TACC3 localization to mitotic spindle has been used as a novel pharmacodynamic approach for measuring AURKA activity (LeRoy et al., 2007), which is frequently overexpressed in human cancers (Bischoff et al., 1998; Miyoshi et al., 2001; Sen et al., 1997; Sen et al., 2002; Tanaka et al., 1999; Zhou et al., 1998).

At the mitotic spindle, TACCs interact through their coiled-coil domain with the MT-stabilizing and evolutionarily highly conserved family of proteins Msps/xmap215/ch-TOG (Cullen and Ohkura, 2001; Lee et al., 2001). Ch-TOG orthologs play an important role in centrosome integrity, centrosome-dependent assembly of MTs during mitosis, and spindle stability (Gergely et al., 2003;

Kinoshita et al., 2002; O'Brien et al., 2005; Peset et al., 2005). Proof of these observations came from assays in which depletion of TACC3 or D-TACC led to mislocalization of ch-TOG orthologs from centrosomes, abnormally short and partially destabilized spindle centrosomal MTs, and defects in chromosome congression (Gergely et al., 2003; O'Brien et al., 2005). Indeed, experiments performed in different model organisms support the idea that TACCs are required for the efficient recruitment of ch-TOG to the centrosome (Bellanger and Gonczy, 2003; Cullen and Ohkura, 2001; Kinoshita et al., 2005; Le Bot et al., 2003; Lee et al., 2001; Sato et al., 2004; Srayko et al., 2003). Moreover, some studies hypothesize that TACCs may promote a conformational change in ch-TOG that renders the molecule more efficient for MT binding and stabilization (Kinoshita et al., 2005; Peset et al., 2005). However, it remains unclear how the TACC-ch-TOG complex stabilizes MTs, with alternative models proposed (**Figure 5**) (reviewed in (Brittle and Ohkura, 2005)).

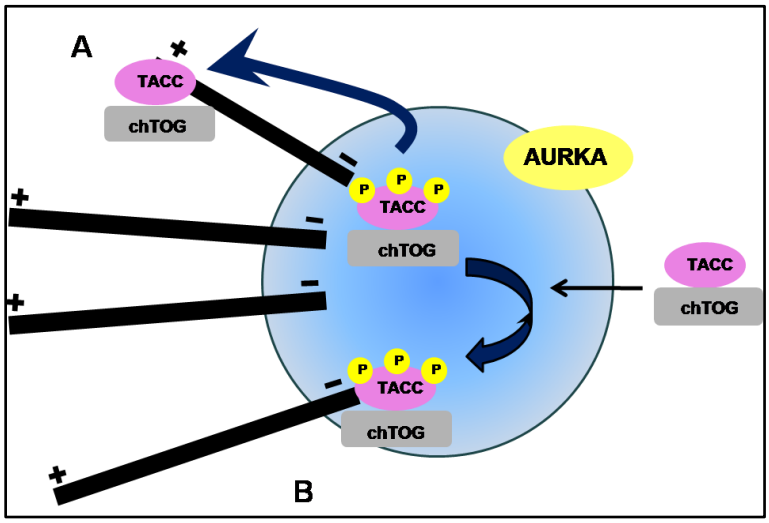

Figure 5: Model for TACC protein function at the spindle poles

Black lines represent MTs with minus ends focused at the centrosome (blue) and plus ends extending away. (**A**) AURKA phosphorylates TACCs and recruits their interacting partner ch-TOG to the centrosome. (**B**) Phospho-TACC/ch-TOG is retained at the centrosome and stabilizes the attachment of the minus ends of MTs to the centrosome. Adapted from (Brittle and Ohkura, 2005).

2.3. *TACC functional roles*

Deregulation of the TACC proteins has been commonly associated with defects in MT stability and/or organization. TAC-1-depleted embryos showed defects in pronuclear migration, shorter spindles and defective spindle elongation in anaphase (Bellanger and Gonczy, 2003; Le Bot et al., 2003). These studies also revealed shorter astral MTs and, as a result, spindle-positioning defects in TAC-1-depleted embryos (Bellanger and Gonczy, 2003; Le Bot et al., 2003). Interestingly, MT assembly in the cytoplasm was not affected, suggesting that TAC-1 function is only critical at the centrosome (Srayko et al., 2003). Moreover, depletion of D-TACC caused female sterility with defective pronuclear fusion, nuclear migration, and chromosome segregation (Gergely et al., 2000b). Thus, the corresponding embryos showed abnormally short centrosomal MTs at all stages of the cell cycle (Gergely et al., 2000b). Consistently, tacc3 was also shown to play an essential role in MT growth and stability during M-phase (O'Brien et al., 2005). Assembly of spindles in tacc3-depleted egg extracts showed reduced size and MT content, and centrosomes nucleated fewer and shorter MTs (Kinoshita et al., 2005; O'Brien et al., 2005; Peset et al., 2005). Finally, mammalian TACCs were also found to play principal role in stabilizing MTs and to be important structural components of the mitotic spindle apparatus (Conte et al., 2003; Gergely et al., 2003; Gergely et al., 2000a; Schneider et al., 2007a; Yao et al., 2007).

In addition to the main functions of TACCs in centrosome biology, including MT dynamics and organization, evolutionary studies have suggested that they may have additional roles in protein translation, mRNA processing and transcription (reviewed in (Still et al., 2004)). Studies in *X. laevis* reporting the involvement of tacc3 in translational regulation during oocyte development supported this idea (Groisman et al., 2000). Specifically, these observations revealed the interaction between tacc3 and the cytoplasmic polyadenylation element binding protein (cpeb1) at the centrosomes and mitotic spindles, where they work together in controlling local cyclin B1 mRNA translation (Groisman et al., 2000). In this context, it should be noted that other studies revealed that different classes of mRNAs are associated with mitotic spindle (Blower et al., 2007; Blower et al., 2005). Moreover, several physical interactors of TACC orthologs are known regulators of gene transcription. Indeed, Tacc3 was shown to affect localization of the aryl hydrocarbon receptor nuclear translocator (Arnt), a transcription factor involved in xenobiotic and hypoxic response (Sadek et al., 2000), as a mechanism of inactivation of its transcriptional function. TACC3 was also found to influence the subcellular localization of friend of GATA-1 (FOG-1) by sequestration to the

centrosome, impairing its interaction with the erythroid transcription factor (GATA-1), thus inhibiting its cooperation in the transcriptional regulation of GATA-1 target genes (Garriga-Canut and Orkin, 2004).

2.4. *TACCs and mitosis*

As described above, a main function of TACCs probably takes place during mitosis. TACC1 may be necessary for progression through the late stages of M phase (Delaval et al., 2004). Thus, TACC1 localizes diffusely to the midzone spindle in anaphase and concentrates sharply at the midbody (Delaval et al., 2004), colocalizing with a major regulator of cytokinesis, aurora kinase B (AURKB) (Tatsuka et al., 1998; Terada et al., 1998). Inhibition of AURKB leads to abnormal cell division and multinucleated cells, correlating with mislocalization of TACC1 at the midbody (Delaval et al., 2004). While little is known about the role of TACC2 in these processes, TACC3 was also shown to play an essential role in mitosis progression, including chromosomal alignment and separation, and cytokinesis (Gergely, 2002; Schneider et al., 2007a; Yao et al., 2007). Together, these data highlight a principal role of TACCs in cell division control through participation in different phases of this process.

2.5. *TACCs and cancer*

The three human genes encoding for TACC proteins map to chromosomal regions shown to be re-arranged in certain cancers (Adnane et al., 1991; Still et al., 1999a; Still et al., 1999b). *TACC1*, located in chromosome 8p11, was originally found to be overexpressed in breast cancer (Still et al., 1999b), while other studies report reduced expression in ovarian and breast tumor samples (Conte et al., 2003; Lauffart et al., 2003). The *TACC2* splice variant *AZU-1*, located in chromosome 10q26, was first isolated in a screen for tumor suppressor genes in human breast cancer (Chen et al., 2000), but the absence of a tumor phenotype in *Tacc2*-knockout mice in more recent research did not support this idea (Schuendeln et al., 2004). TACC3 has been also linked to cancer in several reports (Chen et al., 2000; Lauffart et al., 2005; Still et al., 1999b; Ulisse et al., 2007). Together with *TACC1*, downregulation of *TACC3* has been associated with ovarian tumorigenesis (Lauffart et al., 2005). Thyroid cancer tissues also present alteration of *TACC3* expression (Ulisse et al., 2007). In contrast, *TACC3* has been shown to be overexpressed in small cell lung cancer (Jung et al., 2006). Recently, common genetic variation at the *TACC3* locus has been associated with risk of urinary bladder cancer (with

TACC3 and/or *FGFR3* being the putative candidate genes) (Kiemeney et al., 2010), and breast cancer (Olson et al., 2010). Together, these observations suggest a link between TACCs deregulation and cancer susceptibility and/or progression, through alterations of proper cell division and/or polarity.

2.6. *TACC3, pathology and mitosis*

The third member of the mammalian TACC family, TACC3, was identified by Still and colleagues using a homology-based approach (Still et al., 1999b). *TACC3* localizes to chromosome 4p16, a region frequently rearranged in certain cancer types (Still et al., 1999b) and also affected by germline partial chromosome deletions that cause Wolf-Hirschhorn syndrome (WHS) (disease identifiers Orphanet 280 and OMIM 194190) (Zollino et al., 2003). WHS is characterized by mental retardation, microcephaly, seizures, poor muscle tone, cleft lip and/or cleft palate and, occasionally, renal pathology such as hypoplastic and cystic dysplastic kidneys (Verbrugge et al., 2009). Notably, *TACC3* was shown to be included in a second critical genomic region for WHS (i.e. WHSCR-2) (Zollino et al., 2003).

In mice, *Tacc3* shows expression during embryonic development, presenting a transient increase at day 15, which correlates with a possible role during development (Still et al., 1999b). The absence of Tacc3 results in mid-to-late embryonic lethality probably caused by widespread apoptotic cell death linked to CIN (Piekorz et al., 2002). Lethality was overcome by crossing mice with a *Tp53*-null model, suggesting a link with the S-G2/M transition (Piekorz et al., 2002). In normal cells, the tumor suppressor p53 senses cytokinetic failure and undergoes cell cycle arrest and/or death (Carter, 1967; Hirano and Kurimura, 1974; Uetake and Sluder, 2004; Wright and Hayflick, 1972). However, in the absence of p53, cells continue cycling and become large multinucleated polyploidy cells (Andreassen et al., 2001; Lanni and Jacks, 1998; Minn et al., 1996). Importantly, early studies reported that p53-deficient mice show a high frequency of centrosome amplification (Fukasawa et al., 1996; Fukasawa et al., 1997). Further studies focusing on TACCs have shown that lack of Tacc3 causes failure of chromosome separation at anaphase and, therefore, failure of cytokinesis (Yao et al., 2007). Consistently, in the absence of Tacc3, NIH3T3 fibroblasts show cell cycle arrest at G2/M phase (Schneider et al., 2007a). Moreover, depletion of TACC3 in HeLa cells caused prolonged activation of the spindle assembly checkpoint (SAC) accompanied by polyploidization, supernumerary centrosomes and increased cell death (Schneider et al., 2007a).

Consistent with its role in cell division, expression of TACC3 has been found exclusively in proliferating tissues (Sadek et al., 2003), with higher levels observed during the S/G_2/M phases (Piekorz et al., 2002). It has recently been reported that TACC3 levels are accurately regulated during cell cycle progression via proteasome-mediated degradation (Jeng et al., 2009). This regulation would depend on a physical interaction with FZR1/CDH1, an activator of the APC/C (Nakayama and Nakayama, 2006; Visintin et al., 1997).

3 The Tuberous Sclerosis Complex

3.1. *Overview*

TSC is a genetic disorder with an autosomal dominant pattern of inheritance, variable penetrance, and a total population prevalence of 1-9/100,000 (disease identifiers Orphanet 805 and OMIM 191100/191092). TSC is caused by loss-of-function mutations in the tumor suppressor genes *TSC1* or *TSC2* (European Chromosome 16 Tuberous Sclerosis Consortium, 1993; van Slegtenhorst et al., 1997) and characterized by the presence of hamartomas, which consist of benign dysplastic and disorganized overgrowth within many organs (reviewed in (Crino et al., 2006; Kwiatkowski, 2003b; Pan et al., 2004)). In addition, TSC patients often present renal pathology, including angiomyolipomas and renal cysts; in particular, those patients with genomic deletions affecting *TSC2* and the adjacent *PKD1* gene on chromosome 16p13 develop severe, infantile polycystic kidney disease (disease identifiers Orphanet 731 and OMIM 263200) (Brook-Carter et al., 1994; Harris et al., 1995). Finally, *TSC1/TSC2* mutations have also been associated with sporadic pulmonary lymphangioleiomyomatosis (LAM) (disease identifiers Orphanet 538 and OMIM 606690) (reviewed in (Crino et al., 2006)), a rare disease affecting only women, characterized by abnormal smooth muscle cell proliferation in the lung parenchyma and cystic degeneration (Crino et al., 2006; Ryu et al., 2006).

3.2. *Clinical and pathological features*

The most common clinical manifestation of TSC is seizures in infancy or early childhood (Napolioni and Curatolo, 2008). In addition, population-based studies have estimated that around 80% of children with TSC present epilepsy and a prevalence of mental retardation of 44% (Joinson et al., 2003). Moreover, behavioral problems are common in TSC, particularly autism, autistic spectrum disorders, attention deficit, hyperactivity disorder, and sleep disturbance in children (Gillberg et al., 1994).

Consistent with the main clinical manifestations, the most frequent pathological lesions in TSC patients are tubers in the cerebral cortex and subependymal nodules (SEN) along the walls of the lateral ventricles (Gomez, 1999). Histologically, tubers consist of disorganized areas of cortex lacking the normal laminated architecture, and dysmorphic neurons with abnormal dendritic arborization (Caviness and Takahashi, 1991; Huttenlocher and Heydemann, 1984; Huttenlocher and Wollmann, 1991). Individuals with mental retardation tend to

present a relatively higher number of tubers (Curatolo et al., 2001; Shepherd et al., 1995), and it has been suggested that autism spectrum disorder is particularly associated with tubers in the temporal lobes (Bolton et al., 2002).

In addition to neural pathology, renal angiomyolipomas, which consist of benign neoplasms composed of fat, vascular, and smooth muscle elements, are found in ~80% of TSC patients (O'Callaghan et al., 2004). Renal cysts are also very common in TSC, occurring in 20% of children and as many as 50% of adults (Casper et al., 2002). Other frequent manifestations of TSC are cardiac rhabdomyomas, detected in ~60% of TSC patients and often the first clinical sign (Watson, 1991). In addition, nearly all patients exhibit skin signs, including hypomelanotic macules and forehead fibrous plaques (early expression), facial angiofibromas and ungula fibromas (later development), and shagreen patches (present by puberty) (Gomez, 1999).

In addition to the main clinical characteristics described above, 40-50% of women with TSC present LAM (Costello et al., 2000; Franz et al., 2001; Taveira-DaSilva et al.). Clinically, LAM is a progressive disorder of the lung, causing dyspnea, spontaneous pneumothorax (often multiple), hemoptysis, cough, chylothorax and chest pain, eventually leading to progressive respiratory failure and death. Histopathologically, LAM causes diffuse cystic destruction of the tissues of the lung by abnormal spindle-shaped, closely-packed smooth muscle cells (Chorianopoulos and Stratakos, 2008).

3.3. *TSC genetics*

Two thirds of TSC cases are "sporadic" (i.e. no related individuals are affected), and mutations in *TSC2* contribute more frequently to these cases (odds ratio 6:1 with respect to *TSC1* mutations) (Dabora et al., 2001). According to the two-hit model for tumor suppressor genes (Knudson, 1971), familial cases are present with a dominant pattern of inheritance, being autosomal in both *TSC1* and *TSC2* (chromosome 9q34 and 16p13, respectively (European Chromosome 16 Tuberous Sclerosis Consortium, 1993; van Slegtenhorst et al., 1997)). Mutations in *TSC1* usually appear with a milder clinical and pathological phenotype than *TSC2,* with multiple clinical aspects related to brain, kidney, dermatologic and retinal involvement (Dabora et al., 2001). While inactivation of *TSC1/TSC2* can occur through different mutational mechanisms, partial genomic deletions at chromosome 16p13 can affect both *TSC2* and *PKD1* genes and cause severe infantile polycystic kidney disease (Brook-Carter et al., 1994; Harris et al., 1995).

3.4. *TSC gene products: hamartin and tuberin*

The *TSC1* gene encodes for hamartin, a hydrophilic protein of 130 kDa with a putative coiled-coil motif near the C-term (van Slegtenhorst et al., 1997) (**Figure 6**). The *TSC1* gene product is ubiquitously expressed and has been shown to bind to the ezrin/radixin/moesin (ERM) family of actin-binding proteins (Goncharova et al., 2004; Lamb et al., 2000), which form crosslinks between cortical actin filaments and the plasma membrane. Moreover, TSC1 also regulates RHO activity through the RHO-activating domain within its amino terminus (N-term) (Lamb et al., 2000).

The *TSC2* gene encodes for tuberin, a 198 kDa protein that contains a region with homology to GTPase-activating proteins (GAP) (European Chromosome 16 Tuberous Sclerosis Consortium, 1993; Maheshwar et al., 1997). *TSC2* also contains a calmodulin-binding domain, an oestrogen-receptor-α-binding domain (York et al., 2005) and two coiled-coil motifs at aa positions 346-371 and 1008-1021 (van Slegtenhorst et al., 1998), the first being responsible for the interaction with TSC1 (**Figure 6**).

TSC1 and TSC2 associate physically *in vitro* and *in vivo* through their coiled-coil domains forming a heterodimer (Plank et al., 1998; van Slegtenhorst et al., 1998). In this complex, TSC1 plays a stabilizing role by inhibiting proteasome-mediated degradation of TSC2 (Chong-Kopera et al., 2006).

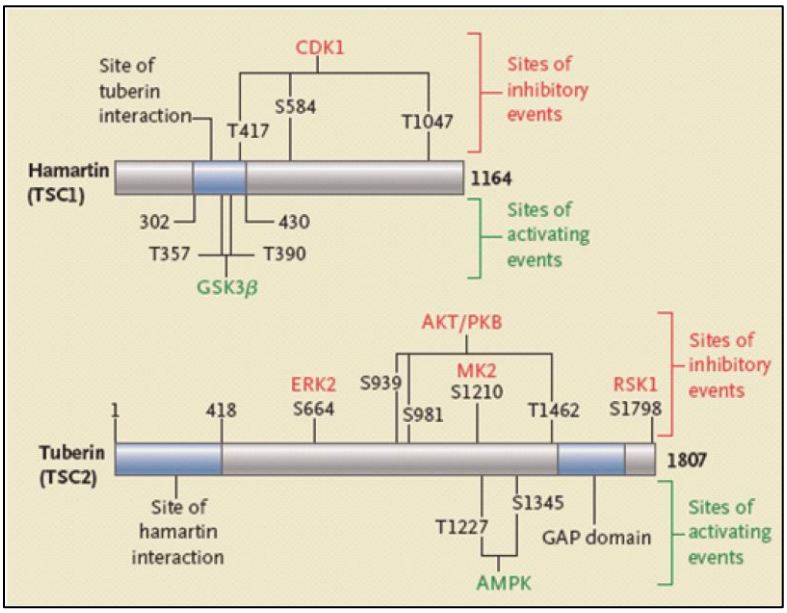

Figure 6: Domains and motifs of TSC1 and TSC2

The figure shows a representation of TSC1 and TSC2 with the regulatory phosphorylation sites and respective kinases responsible for their phosphorylation. Adapted from (Crino et al., 2006).

3.5. *Role of* TSC1 *and* TSC2 *in cell growth and proliferation*

The first evidence of a key role of TSC1 and TSC2 in the regulation of cell growth and size came from studies in *D. melanogaster*, which showed that deletions in *D-TSC1* and *D-TSC2* (gigas) increased cell and organ size (Gao and Pan, 2001; Potter et al., 2001; Tapon et al., 2001). Subsequently, many studies in different cellular and organism models have delineated the participation of TSC1 and TSC2 in the PI3K-AKT-mammalian target of rapamycin (mTOR) pathway of nutrient signaling and cell growth regulation (Dan et al., 2002; Kwiatkowski, 2003b; Kwiatkowski and Manning, 2005; Manning and Cantley, 2003; Pan et al., 2004). TSC2, through its GAP domain, enhances the GTPase activity of RAS homolog enriched in brain (RHEB), which, in turn, is a positive regulator of the rapamycin-sensitive kinase complex mTOR/RAPTOR termed mTORC1 (Castro et al., 2003; Garami et al., 2003; Inoki et al., 2003a; Kwiatkowski, 2003a; Manning and Cantley, 2003; Saucedo et al., 2003; Tee et al., 2003; Zhang et al., 2003). AKT1 phosphorylation decreases the GAP activity of TSC2, with consequent release of RHEB inhibition and increase in mTORC1 activity (Dan et al., 2002; Manning et al., 2002). In turn, mTORC1 positively regulates multiple processes, including CAP-dependent mRNA translation via p70S6K/S6 and 4E-BP1/eIF4E, ribosome biogenesis, autophagy, angiogenesis and apoptosis (Lazaris-Karatzas et al., 1990; Raught et al., 2004; Richardson et al., 2004; Wendel et al., 2004). In response to growth factors, amino acids and nutrients, mTORC1 functions by phosphorylating two effector molecules, p70S6K and 4E-BP1, to increase cell growth and proliferation (Hara et al., 1998; Inoki et al., 2003b; Kim et al., 2002). Specifically, phosphorylation of RPS6 causes increased ribosome biogenesis, and phosphorylation of 4E-BP1 permits messenger RNA (mRNA) translation (Gingras et al., 1999; Hannan et al., 2003) (**Figure 7**).

As described above, the major link between the TSC1-TSC2 heterodimer and mTORC1 is RHEB, a specific GTPase that acts downstream of TSC2 as shown in **Figure 7** (Inoki et al., 2003a; Saucedo et al., 2003; Stocker et al., 2003; Zhang et al., 2003). RHEB, like other RAS family members, cycles between an active GTP-bound state and an inactive GDP-bound state (Bourne et al., 1991). TSC2, via its GAP domain, stimulates the intrinsic GTPase activity of RHEB and thus the conversion of RHEB-GTP to RHEB-GDP, thereby inactivating RHEB. Loss of TSC2 function leads to enhanced RHEB-GTP signaling and mTOR activation (Castro et al., 2003; Garami et al., 2003; Inoki et al., 2003a; Tee et al., 2003). Mutations in the GAP domain of TSC2 lead to low GAP activity with respect to RHEB (Nellist et al., 2005), suggesting that the GAP activity of TSC2 is essential for its physiologic

function. Importantly, the functional characterization of TSC proteins as an intrinsic suppressor of rapamycin-sensitive mTOR signaling pathway suggested a possible therapeutic value of rapamycin (also named sirolimus) in the treatment of TSC disease (Bissler et al., 2008; Goncharova et al., 2006; Kenerson et al., 2005). MTOR also forms a second, rapamycin-insensitive complex (except long-term treatments and cell-type specific) when bound to RICTOR, termed mTORC2 (Jacinto et al., 2004; Sarbassov et al., 2004). MTORC2 positively regulates the actin cytoskeleton and influences apoptosis through critical phosphorylation of Ser473 in AKT1 and through PKC1/RHO activities (Jacinto et al., 2004; Peterson et al., 2009; Sarbassov et al., 2004; Sarbassov et al., 2005). Notably, the TSC1-TSC2 heterodimer activates mTORC2 in a RHEB-independent manner, and this function appears to be necessary for phosphorylation and, therefore, activation of AKT1 (Huang et al., 2008; Yang et al., 2006). However, in contrast to mTORC1, relatively little is known about the functions of mTORC2.

3.6. *TSC and the cell cycle*

A wide variety of molecular functions and biological processes have been linked to TSC1 and TSC2 (reviewed in (Napolioni and Curatolo, 2008)). Disruption of their heterodimer allows activation of mTOR and its downstream targets, leading to increased translation of a specific subset of mRNAs, many of which are involved in the cell cycle (Aicher et al., 2001; Goncharova et al., 2002; Manning et al., 2002). Loss of TSC2 affects the cell cycle, shortening G1 and causing cells in G0 to re-enter the cell cycle (Soucek et al., 1997; Soucek et al., 1998). Consistently, overexpression of TSC2 triggers an increase in the number of G1 cells in rat fibroblasts, human neuroblastoma cells and TSC2-depleted cells (Miloloza et al., 2002; Soucek et al., 1997; Soucek et al., 1998). Moreover, depletion of TSC2 in mouse embryonic fibroblasts (MEFs) causes a decrease of the Cdk inhibitor p27, leading to uncontrolled cellular proliferation (Soucek et al., 1998). In addition to its roles at G1/G0 phases, TSC1 is regulated at G2/M through phosphorylation by CDK1, including a residue within the TSC2-interacting domain (**Figure 6**) (Astrinidis et al., 2003). This modification appeared to be necessary for the activity of the TSC1-TSC2 complex during mitosis, and a mutant form that cannot be phosphorylated by CDK1 was shown to increase the inhibition of p70S6K (Astrinidis et al., 2003).

In keeping with a possible role of the TSC1-TSC2 complex in the cell cycle, TSC1 interacts with PLK1 in a phosphorylation-dependent manner, and both co-

localize at the centrosome (Astrinidis et al., 2006). The interaction is TSC1-dependent, with all three proteins present in the complex. Importantly, *Tsc1*-null mice show centrosome amplification compared to wild-type (wt), a phenotype that is rescued by rapamycin treatment (Astrinidis et al., 2006). Together, these observations suggest that TSC1 may play a role in centrosome biology and/or mitotic progression (Astrinidis et al., 2006). Similarly, Tsc2-deficient Eker rat cells have an abnormal, increased number of centrosomes (Gui et al., 2007).

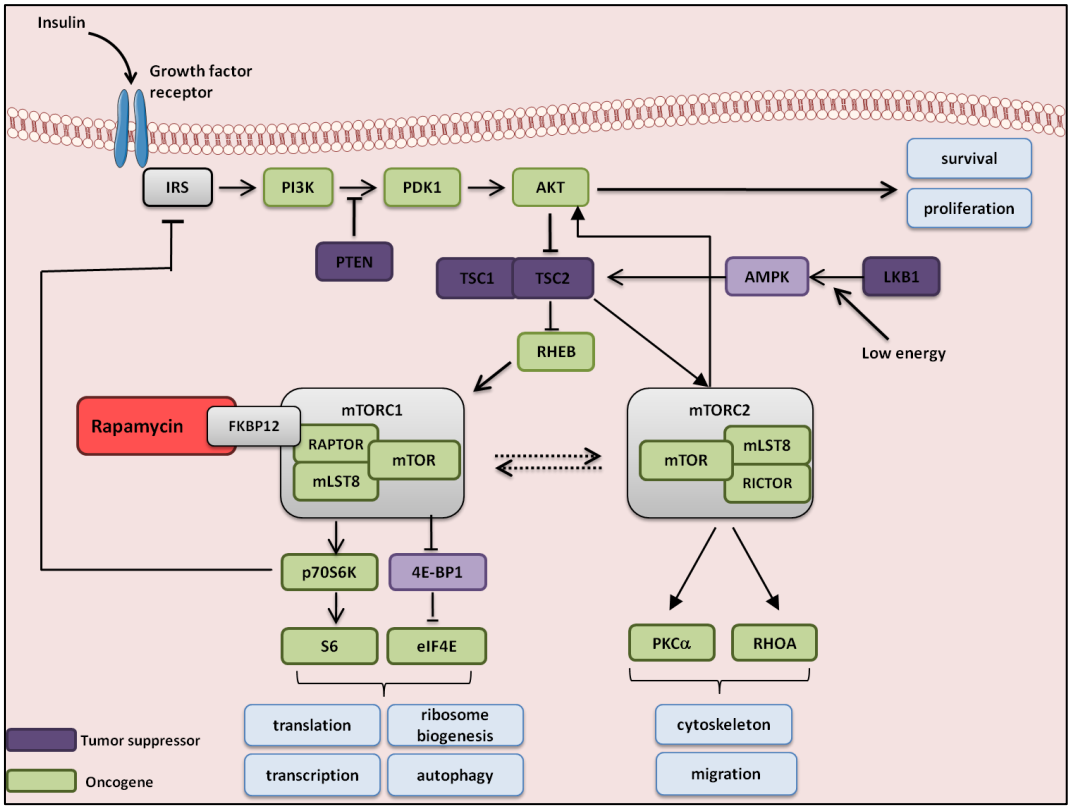

Figure 7: TSC/mTOR signaling pathway

PI3K is activated by growth factor receptors. These interactions recruit PI3K to its substrate phosphatidyl-inositol (4,5) biphosphate (PIP2), allowing generation of phosphatidyl-inositol (3,4,5) triphosphate (PIP3). AKT1 and PDK1 are recruited to the plasma membrane through association with PIP3. AKT1 is then activated through phosphorylation on Thr308 by PDK1 and Ser473 by mTORC2. Subsequently, active AKT1 can phosphorylate many downstream targets, including TSC2. Phosphorylation of TSC2 impairs the ability of the TSC1-TSC2 complex to act as a GAP towards the small GTPase RHEB. A negative-feedback loop exists in which mTORC1 and p70S6K phosphorylate IRS1 and block signaling to PI3K. Growth factors also increase mTORC2 activity through unknown mechanism. In addition, through a mechanism distinct from its regulation of RHEB and mTORC1, the TSC1-TSC2 complex can bind to mTORC2 and may be required for mTORC2 activation.

3.7. *Novel functions of* TSC1 *and* TSC2*: the centrosome and cell polarity*

Neuronal defects in TSC patients have been hypothesized to be caused, at least in part, by abnormal neuronal positioning and/or migration (Crino and Henske, 1999; Gutmann et al., 2000; Sparagana and Roach, 2000; Vinters et al., 1999). Notably, a recent report in mice models demonstrated a role of TSC1 and TSC2 in neuronal polarity, suggesting a coordinated role of the TSC1-TSC2 heterodimer in regulating polarization/growth in neurons (Choi et al., 2008). In addition, TACCs have recently been shown to be critical in the interkinetic nuclear migration necessary for maintaining the neural progenitor pool (Xie et al., 2007). On the other hand, renal cystic diseases are associated with the absence or dysfunction of the primary cilium and therefore loss of polarity and proper tissue architecture (Nauli et al., 2003; Yoder et al., 2002a; Yoder et al., 2002b).

Having possible pathological links between TSC and dysfunction of cell divison and polarity, new roles for TSC1 and TSC2 in the biology of centrosomes and the basal body of cilia have been recently described (Astrinidis et al., 2006; Bonnet et al., 2009; Hartman et al., 2009). Recent publications describe the role of the TSC1-TSC2 heterodimer in primary cilium formation and cell polarity (Bonnet et al., 2009; Hartman et al., 2009). TSC1 has been localized to the basal body of the primary cilium (Hartman et al., 2009) and TSC2 interacts with PKD1 (Shillingford et al., 2006), which has been localized to the primary cilium (Yoder et al., 2002a). Depletion of Tsc1 or Tsc2 in MEFs results in enhanced cilia development (Hartman et al., 2009) and further studies in this context not only show the involvement of these proteins in the regulation of cilium formation but also suggest that TSC1 and TSC2, together with PKD1, play a key role in maintaining cell polarity in pre-cystic renal and hepatic cells (Bonnet et al., 2009). Together, these findings open new research lines that may provide better understanding of the molecular mechanisms leading to TSC pathogenesis.

HYPOTHESIS

Hypothesis

Proper centrosome number, function and structural integrity are critical for most cellular properties, including motility, adhesion and polarity in interphase and division through mitosis and cytokinesis (reviewed in (Bettencourt-Dias and Glover, 2007)). It is well established that centrosome alterations are common in many types of neoplasias (reviewed in (Nigg, 2002)) and some neurological diseases (reviewed in (Badano et al., 2005)) and that they correlate with loss of cell polarity in different cellular models (reviewed in (Sankaran and Parvin, 2006)). Various studies have demonstrated a key role of TACC proteins in centrosome function and MT assembly during cell division (reviewed in (Peset and Vernos, 2008)). Three human genes encoding TACC proteins have been described whose expression is commonly altered in cancer cells but which show no clear specificities beyond their cellular and developmental localization (Gergely et al., 2000a) or their interactions with proteins involved in gene expression regulation (Angrisano et al., 2006; Gangisetty et al., 2004; Garriga-Canut and Orkin, 2004; Lauffart et al., 2002; Sadek et al., 2000; Still et al., 2004). To date, no other associations have been identified that may elucidate the role of TACCs in cellular structures or in processes related to human disease. To gain fundamental insight into these questions, we mapped the TACC3 interactome (i.e. TACC3 protein physical interactions). The results of this analysis revealed a physical interaction with TSC2, possibly involved in maintaining nuclear envelope structure and controlling different phases of cell division.

AIMS OF THE STUDY

Aims of the study

The main aims of the study that constitute this PhD dissertation were:

Aim #1: To study the functional specificities and genetic and molecular associations of human *TACC* genes and their products with regard to centrosome biology.

Aim #2: To evaluate the potential role of the novel genetic and/or proteomic associations identified in Aim #1 in human disease.

MATERIALS AND METHODS

1 MATERIALS

1.1. *Cell culture*

HeLa, MCF7 and HEK293 cells were cultured in Dulbecco's Modified Eagle's Medium (DMEM) supplemented with 10% fetal bovine serum (FBS), 2 mM L-glutamine and 2 mM sodium pyruvate. BT474 cells were cultured in DMEM F12 supplemented with 10% FBS, 2 mM L-glutamine and 2 mM sodium pyruvate. HME/TERT (telomerase-immortalized human mammary epithelial cells) were cultured in Mammary Epithelial Growth Medium (MEGM) supplemented with 10% fetal bovine serum and SingleQuots® (human epidermal growth factor (hEGF), insulin, hydrocortisone and gentamicin/amphotericin-B). MCF10A cells were cultured in HuMEC media (Invitrogen) containing 1/3 recommended hEGF. *Tsc2*$^{+/+}$ *Tp53*$^{-/-}$ and *Tsc2*$^{-/-}$ *Tp53*$^{-/-}$ MEFs (the gift of Dr. Elizabeth P. Henske, Fox Chase Center, Philadelphia, USA) were cultured in DMEM, 10% FBS, 2 mM L-glutamine and 100 μM non-essential amino acids. In this case, plates were pre-treated with collagen R (solution 2 mg/ml in 0.1% acetic acide). *Tacc3*$^{+/-}$, *Tacc3*$^{-/-}$ and wt MEFs were cultured in DMEM, 10% FBS and 2 mM L-glutamine. TSC2-deficient ELT3 cells (the gift of Dr. Elizabeth P. Henske, Fox Chase Center, Philadelphia, PA), derived from a uterine leiomyoma of Eker rats (Howe et al., 1995), were cultured in DMEM F12 supplemented with 15% FBS, 2 mM L-glutamine and 2 mM sodium pyruvate. *Tsc1*$^{-/-}$ MEFs were retrovirally reconstituted with human *TSC1*/pMSCVneo as previously described (Astrinidis et al., 2002). Stable clones were selected over two weeks by addition of 500 μg/ml G418 in the growth medium. All cell cultures were grown at 37ºC in a humidified 5% CO_2 atmosphere. Where indicated, HEK293 cells were arrested in G_2/M using 5 μg/ml nocodazole (Sigma-Aldrich) or vehicle control dimethyl sulfoxide ((DMSO), Sigma-Aldrich) for 12-24 hours (h). For rapamycin treatment, cells were grown in media with 20 nM rapamycin for 15 h. Double thymidine blocked-based assays are detailed in further sections.

1.2. *Antibodies*

Immunofluorescence studies were performed with anti-AURKA (IAK1 Catalog #610939, BD Biosciences) anti-AURKB (AIM-1 clone 6, BD Biosciences), anti-α6-integrin (clone GoH3, BD Biosciences), anti-pS2448-mTOR (Catalog #2971, Cell Signaling Technology), anti-NUP62 (clone 53, BD Biosciences), anti-TACC3 (H-300, Santa Cruz Biotechnologies), anti-TSC1 (clone 5C8A12, Zymed, Invitrogen), anti-TSC2 (clone 3G9D9, Zymed, Invitrogen), anti-pS939-TSC2 (Catalog #3615, Cell Signaling Technology), anti-TUBG1 (clone GTU-88, Sigma-Aldrich) and anti-ZO-1 (catalog #61-7300, Zymed, Invitrogen). The phosphorylation-specific polyclonal antibody against pS558-TACC3 was purchased from New England Peptide. Unpurified and purified sera were tested for specificity relative to a defined TACC3 antibody (H-300 Santa Cruz Biotechnologies).

Immunoprecipitation assays were performed with anti-TACC3 (N-18, Upstate Biotechnology; H-300, Santa Cruz Biotechnologies), anti-TSC2 (C-20, Santa Cruz Biotechnology; clone 3G9D9, Zymed, Invitrogen) and anti-TSC1 (clone 3G9D9, Zymed, Invitrogen). Other antibodies used in this study were anti-LMNA (clone 133A2, Chemicon, Millipore), anti RASA1/GAP120 (clone B4F8, Upstate, Millipore), anti-pT389-S6K (Catalog #9205, Cell Signaling Technology), anti-CHFR (M01 clone 1H3-A12, Abnova), anti-CGN (H-180, Santa Cruz Biotechnologies), anti-PLK1 (aa 6-24, Chemicon, Millipore), anti-pS10-H3 (Catalog #06-570, Upstate, Millipore), anti-ARHGEF2 (aa 41-487) (Bakal et al., 2005) and anti-CP110 (aa 1-149, the gift of Brian David Dynlacht). Purified negative control IgGs of different species were purchased from Santa Cruz Biotechnologies. Epitope-tag antibodies were anti-FLAG M2 (Sigma-Aldrich), anti-GFP (clone JL-8, BD Biosciences), anti-GST (Sigma-Aldrich) and anti-MYC (clone 9E10, Sigma-Aldrich). Secondary HRP-linked antibodies were purchased from GE Healthcare, and fluor-linked antibodies were Alexa 488 or 546-594 nm anti-mouse and anti-rabbit, respectively (Molecular Probes, Invitrogen).

Table 1: List of primary antibodies

Antibody	*Dilution*	*Source*
α6-integrin (clone GoH3)	IFL 1:100	BD Biosciences
AURKA (IAK1 #610939)	IFL 1:500	BD Biosciences
AURKB (AIM-1 clone 6)	IFL 1:250	BD Biosciences
ARHGEF2 (aa 41-487)	WB 1:250	(Bakal et al., 2005)
CHFR (M01 clone 1H3-A12)	WB 1:250	Abnova
CGN (H-180)	WB 1:200	Santa Cruz Biotechnologies
CP110 (aa 1-149)	WB 1:500	(gift of Brian David Dynlacht)
FLAG M2	WB 1:1,000	Sigma-Aldrich
GFP (clone JL-8)	WB 1:500	BD Biosciences
GST	WB 1:2,000	Sigma-Aldrich
IHABP	IFL 1:400	Serum (gift of Volker Assmann)
LMNA (clone 133A2)	WB 1:50	Chemicon (Millipore)
MYC (clone 9E10)	WB 1:2,000	Sigma-Aldrich
NUP62 (clone 53)	IFL 1:500 WB 1:1,000	BD Biosciences
PLK1 (aa 6-24)	WB 1:1,000	Chemicon (Millipore)
pS10-H3 (#06-570)	WB 1:2,000	Upstate (Millipore)
pS2448-mTOR (#2971)	IFL 1:500	Cell Signaling Technology
pS939-TSC2 (#3615)	WB 1:1,000 IFL 1:500	Cell Signaling Technology
pT389-S6K (#9205)	WB 1:1,000	Cell Signaling Technology
RASA1/GAP120 (#B4F8)	WB 1:2,000	Upstate (Millipore)
TACC3 (H-300)	WB 1:250 IP 5µg IFL 1:50	Santa Cruz Biotechnologies
TACC3 (N-18)	WB 1:250	Santa Cruz Biotechnologies
TSC2 (clone 3G9D9)	IFL 1:500	Zymed (Invitrogen)
TSC2 (C-20)	WB 1:250 IP 5 µg	Santa Cruz Biotechnologies
TSC1 (clone 5C8A12)	WB 1:500 IFL 1:100	Sigma-Aldrich
ZO-1 (#61-7300)	IFL 1:50	Zymed (Invitrogen)

1.3. *Expression vectors*

To validate yeast two-hybrid (Y2H) interactions we first cloned the sequences of interest into expression vectors. Briefly, full-length open-reading frames (ORFs) were transferred into GST- and MYC-tagged Gateway-compatible vectors (pDEST-27 and pCMV-MYC-N-term tagged vectors, respectively) (**Figure 8**) (Invitrogen). First, we created PCR products of the fragments of interest in our study containing attB sites by using primers with a 25-base pair attB sequence plus four terminal guanines (G). Next, the PCR products were cloned into a Gateway DONR vector (i.e. a plasmid containing the gene of interest and flanked by Gateway attL recombination sites) using the BP method following manufacturer's protocol (Invitrogen). Having cloned the sequence of interest in the DONR vector, we next cloned the DNA insert into the destination vector (pDEST-27 or pCMV-MYC-N-term) by performing the LR reaction following manufacturer's protocol (Invitrogen). The pCMV-*MYC-HMMR* and pCMV-*GST-TACC3* constructs were obtained using Gateway Technology. The other tagged constructs used in this study were pCBF-*Flag-CP110-GFP*, pEGFP-N-*KIF1C* and pEGFP vectors expressing different domains of TSC2 (pEGFP-*TSC2*, pEGFP-*TSC2-HBD* and pEGFP-*TSC2-ΔHBD*), gifts from William Tsang, Reiner Lammers and Helena Goncharova, respectively.

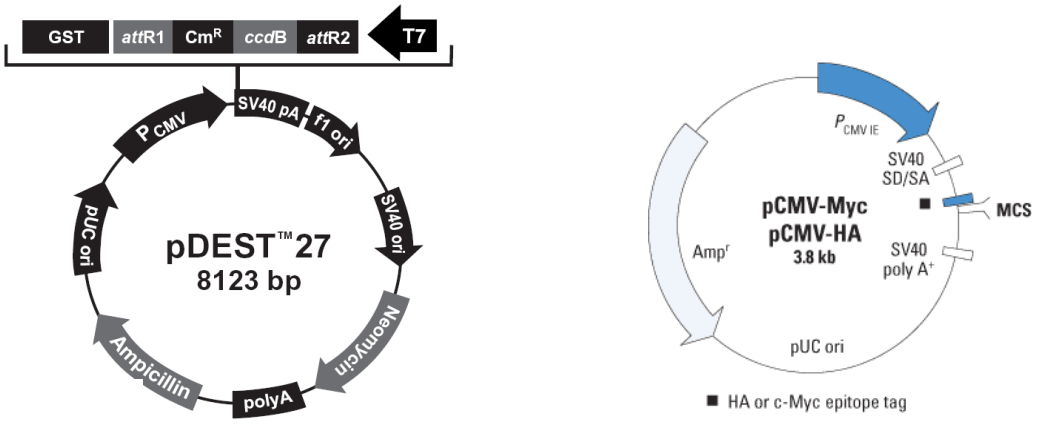

Figure 8: Gateway destination vectors

Structure of Gateway Technologies vector pDEST-27 (left panel). Structure of the pCMV-*MYC* vector from Clontech, which was converted to Gateway using the Gateway Vector Conversion System (Invitrogen) (right panel).

2 EXPERIMENTAL PROCEDURES

2.1. *Yeast two-hybrid screens*

The Y2H system is a molecular technique used to identify and characterize protein interactions, based on the observation that most transcription factors can be separated into a DNA-binding domain (DBD) and a transcriptional activation domain (AD) (Fields and Song, 1989). Thus, interacting proteins can be potentially identified (X-Y heterodimer or X-X homodimer) by generating two different hybrid proteins, one with X protein fused to the DBD and the other with protein Y fused to the AD (Walhout and Vidal, 2001), which together reconstitute a transcription factor that can activate the transcription reporter genes regulated by DBD sites.

Proteome-scale Y2H screens were performed following two different strategies, transformation or mating (Vidalain et al., 2004; Walhout and Vidal, 2001), and using two different cDNA libraries, of human fetal brain or spleen (ProQuest, Invitrogen). Three TACC3 baits were defined according to their protein domains (Gergely et al., 2000a; Piekorz et al., 2002; Still et al., 2004), with the C-term domain spanning aa 629-838 and cloned into the Gateway pDONR201 (Invitrogen) vector following manufacturer's protocol (Invitrogen) and using reverse transcriptase polymerase chain reaction (RT-PCR) products from healthy lymphocytes with the following primers:

Forward	***5'- GGGGACAAGTTTGTACAAAAAAGCAGGCTTGTCCACCGGACCTATAGT-3'***
Reverse	***5'-GGGGACCACTTTGTACAAGAAAGCTGGGTTCAGATCTTCTCCATCTTGGAGATGAGG-3'***

Baits were fully sequenced so that no changes relative to publicly available sequence information were observed. Products were transferred to the pPC97 yeast expression vector (Invitrogen) (**Figure 9**) to be fused with the DBD of GAL4. Constructs were transformed in MaV203 (Invitrogen) or AH109 (Clontech) yeast strains for screens using selective medium lacking histidine (HIS). The MaV203 yeast strain contains three GAL4-inducible reporter genes: *GAL1::lacZ*, *SPAL10::URA3* and $HIS3_{UASGAL1}$*::HIS3* (Vidal et al., 1996a; Vidal et al., 1996b). The AH109 yeast strain contains distinct *ADE2*, *HIS3*, *lacZ* and *MEL1* GAL4-inducible reporter genes. Yeast strains were supplemented with 10 mM (mating protocol) or 20 mM (transformation protocol) 3-amino-1,2,4-triazole (3-AT; Sigma-Aldrich) to test the interaction-dependent transactivation of the HIS3 reporter. Previously, baits were examined for self-activation at range of 10-80 mM concentrations of 3-AT. In total, using these conditions, more than 10 million transformants were

screened per bait. Positive colonies were grown in selective medium for three cycles (10-15 days) to avoid cDNA contaminants, prior to PCR amplification and sequence identification of preys (Vidalain et al., 2004).

- *Mating screening protocol*

Prior to screening, we performed amplification of the cDNA library (ProQuest, Invitrogen) containing the pPC86 vector (Invitrogen) (**Figure 9**) in Y187 (Clontech) yeast strain, which contains the *lacZ* and *MEL1* reporter constructs that are only expressed in the presence of *GAL4*-based protein interactions and is an ideal library host strain for AH109. Transformation of the cDNA library was performed as follows: an overnight (o/n) patch of Y187 yeasts grown in a YPD plate was inoculated in YPD liquid media (10 g yeast extract, 20 g bacto-peptone, 50 ml 40% glucose for 1 liter) for 5-6 h until the OD_{600} increased to 0.4-0.5 units. Cells were centrifuged for 5 minutes (min) at 2000 x g; the pellet was then washed twice in distilled water and subsequently with TE/LiAc solution (for 50 ml, 5 ml of 10x TE (100 mM Tris-HCl (pH 7.5, 10 mM EDTA) and 5 ml of 1 M LiAc) following centrifugation as before; next, the cell pellet was resuspended in TE/LiAc/PEG solution (TE/LiAc into 40 ml of 50% polyethylene glycol 3350) with 3 mg/ml of boiled salmon testes DNA used as carrier and 30 µg of the cDNA library (ProQuest, Invitrogen); the mix then was incubated at 30ºC for 30 min prior to a heat shock at 42ºC for 15 min; cells were then centrifuged to remove the TE/LiAc/PEG solution and resuspended in distilled water to be plated on YPD selective agar plates lacking tryptophan (TRP) and supplemented with ampicillin and chloramphenicol; cells were then incubated for two to three days at 30ºC prior to appearance of colonies. On the last day, colonies were scraped from plates, diluted in distilled water and stored as glycerol stocks.

For screening, the different TACC3 baits were grown o/n in AH109 yeast cells in YPD liquid media supplemented with ampicillin and chloramphenicol. The following day, an aliquot of the previously amplified cDNA library was incubated for 10 min at 30ºC in YPD media supplemented with glucose. In the meantime, OD_{600} of the o/n bait culture was measured (should be > 2-5 OD units) and 80 OD_{600} of the culture (e.g. for 3.6 OD_{600} we used 21 ml) were mixed with the library. The mix was centrifuged for 10 min at 2,500 x g. The pellet was resuspended in YPD liquid media and plated on YPD non-selective agar plates. The plates were incubated for 4 h 30 min at 30ºC. The grown culture was scraped under the flame using a Pasteur pipette and water. Final volume was centrifuged for 10 min at 2500 x g. The pellet was then resuspended in distilled water, plated on 10 mM 3-AT plates and

incubated at 30ºC. A 1/10,000 dilution of the final volume was also plated on YPD plates lacking leucine (LEU) and TRP to calculate mating efficiency. After five to six days, the colonies were picked and replicated to 3-AT plates ~4-5 times for three weeks. After the last replica, colonies were picked and incubated at 37ºC for 5 min and then at 95ºC for 5 min in a PCR machine for Zymolase digestion. Once cells were digested, the prey DNA were obtained by PCR using primers to the AD sequence and the termination sequence corresponding to the pPC97 vector. Next, PCR products were purified following manufacturer's protocol (Genomed GmbH) and sequenced using AD primers.

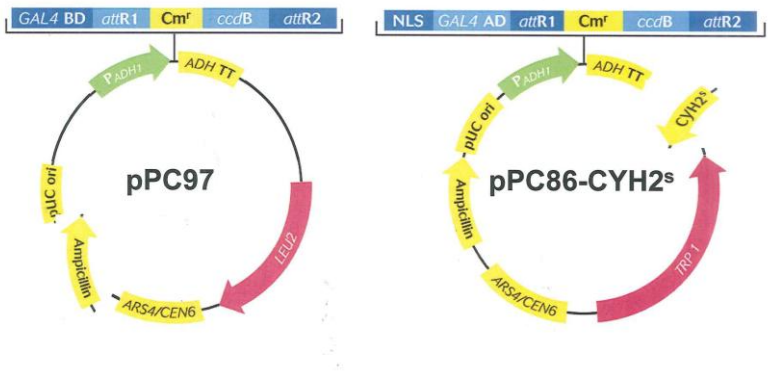

Figure 9: Y2H Gateway vectors

Figure shows structure of pPC97 (left panel) and pPC86 (right panel) used in this study for Y2H screening.

- *Transformation screening protocol*

The first step in this protocol was to transform the construct containing our bait of interest into the MaV203 yeast strain, as follows: an o/n culture of MaV203 yeasts in YPD liquid media supplemented with glucose was centrifuged for 5 min at 2000 x g; the pellet was then washed twice in distilled water and subsequently with TE/LiAc solution (for 50 ml, 5 ml of 10x TE (100 mM Tris-HCl (pH 7.5, 10 mM EDTA) and 5 ml of 1 M LiAc) following centrifugation as before; next, the cell pellet was resuspended in TE/LiAc/PEG solution (TE/LiAc into 40 ml of 50% polyethylene glycol 3350) with 10 mg/ml of boiled salmon testes DNA used as carrier and 50-100 ng of the bait construct; the mix then was incubated at 30ºC for 30 min prior to a heat shock at 42ºC for 15 min; cells were then centrifuged to remove the TE/LiAc/PEG solution and resuspended in distilled water to be plated on YPD selective (-LEU) agar plates; cells were then incubated for two to three days at 30ºC prior to appearance of colonies.

Once we had the yeast strain MaV203 transformed with our bait construct, we proceeded to the screening. A patch of the yeast strain was inoculated into YPD liquid selection media (-LEU) and grown o/n at 30ºC. The following day, OD_{600} of the 1:10 dilution of the o/n culture was measured. We next calculated the amount needed to inoculate a 250 ml YPD culture to give a final OD_{600} of 0.1. The medium with the inoculated culture was grown for ~5 h at 30ºC until OD_{600} increased to 0.35-0.6. Then, yeast cells were harvested by centrifugation at 2000 x g at 20ºC for 5 min and washed into distilled water. After a second centrifugation, cells were resuspended in TE/LiAc solution and centrifuged again. The pellet was resuspended in TE/LiAc solution in a total volume of 0.5 ml per 0.1 OD_{600}. At this point, we proceeded to transformation of the yeast strain with 20-30 µg of human fetal spleen or brain cDNA ProQuest library (Invitrogen) following the same protocol as described above. After transformation, cells were plated on 20 mM selection plates (-LEU, –TRP). A 1/10,000 dilution of the final volume was also plated on YPD selection plates (-LEU, -TRP) to calculate the library transformation efficiency. After five to six days colonies should be visible and can be picked and replicated to 3-AT plates 4-5 times for three weeks. After the last replica, colonies were picked for Zymolase digestion, PCR and product sequencing.

2.2. *Expression profile analysis*

Similarity of expression profiles was evaluated by computing the Pearson correlation coefficient (PCC) using normalized (gcRMA) expression levels of the GeneAtlas U133A human dataset (http://biogps.gnf.org) (Su et al., 2004). Comparisons were made for all possible microarray probe pairs and *p* values adjusted by the Bonferroni correction.

2.3. *Phylogenetic analyses*

Position-specific iterated BLAST (PSI-BLAST) (Altschul et al., 1997) searches were performed against proteins encoded in genomes deposited in Ensembl as of January 2008 (Flicek et al., 2008), using human TACC proteins. Parameters were set to a maximum of five interations and an e-value threshold of 0.0001. The phylogenetic pipeline used here is adapted from Huertas-Cepas *et al.* (Huerta-Cepas et al., 2007). Alignments of homologous sets of proteins were performed with MUSCLE 3.6 (Edgar, 2004) and trimmed to remove columns with gaps in more than 10% of the sequences, unless this procedure would remove more than one third of the positions in the alignment. In such cases the permitted percentage of sequences

with gaps is automatically increased until at least two thirds of the initial columns are conserved. Phylogenetic trees were reconstructed using Maximum Likelihood as implemented in PhyML v2.4.4 (Guindon and Gascuel, 2003). We used a discrete gamma-distribution model with four rate categories, in which invariant sites and the gamma shape parameter were estimated from the data. Four different evolutionary models were used (JTT, Dayhoff, VT and BLOSUM62) and the one best fitting the data according to the AIC criterion was selected (Akaike, 1973).

2.4. *Cell cycle synchronization with the double thymidine block protocol*

To arrest cell cultures at S phase, cells were seeded at 25-30% confluency and a DMEM F12 with 2 mM thymidine was added for 18 h (i.e. first block). Cultures were then trypsinized, washed twice with PBS for 10 min and seeded again in DMEM F12. Nine h later, DMEM F12 with 2 mM thymidine was added for the next 17 h (i.e. second block). Next, cultures were trypsinized, washed twice with PBS for 10 min and released into DMEM F12. The first time point (S phase) was collected after cell attachment was observed (1-5 h later depending on the cell line), the rest of the time points were collected at 2, 4, 6, 8 and 10 h. Cells were prepared as described in section 2.11.

2.5. *MT binding assay*

MT-binding assays were performed as previously described (Groisman et al., 2000). Briefly, HEK293 cells from six confluent 150 mm tissue culture dishes were collected by trypsinization and homogenized in 4 ml of PHEM buffer (60 mM PIPES, 25 mM HEPES, 1 mM EGTA, 1 mM MgAc, pH 6.8) supplemented with protease and phosphatase inhibitor cocktails (Sigma-Aldrich). The homogenate was clarified by centrifugation at 14,000 x g for 30 min, GTP was added to a final concentration of 1 mM, and taxol or nocodazole was added to a final concentration of 20 μM and 100 μM, respectively. The homogenates were incubated for 30 min at room temperature with rotation, layered onto an equal volume of 15% sucrose cushion in PHEM buffer, and centrifuged at 14,000 x g for 15 min. The supernatants and cushions were aspirated, the pellets were washed once in PHEM buffer, sample loading buffer was added, and resolved in 4-12% Bis-Tris NuPAGE gels using 1x MOPS running buffer (Invitrogen).

2.6. *Cytokinesis assay*

ELT3 cells (*Tsc2* mutant and hTSC2-reconstituted counterparts) were seeded on coverslips for 16-24 h before treatment with nocodazole. The day after, cells were treated with 70 ng/ml nocodazole for 8-12 h, released in fresh media without nocodazole for 90 min, and fixed with ice-cold methanol at different time points to 90 min. Immunofluorescence assays were performed as detailed above using anti-TUBA linked to Cy3 fluor (clone TUB 2.1, Sigma-Aldrich) co-stained with DAPI. Tsc1-deficient cells were treated similarly, permeabilized in 0.1% Triton X-100 in PBS for 30 min, blocked in this solution with 3% BSA for 30 min and mounted with GelMount (BioMedia) prior to direct immunofluorescence and counting.

2.7. *Cell fractionation analysis*

Cells (*Tsc2*$^{+/+}$*/Tp53*$^{-/-}$ and *Tsc2*$^{-/-}$*/Tp53*$^{-/-}$ MEFs) growing in p100 dishes at 80% confluence were trypsinized (3 min at 1750 x g) and washed twice with PBS. Next, the pellets were resuspended in 500 µl of buffer A (10 mM HEPES-KOH pH 7.9, 1 mM $MgCl_2$, 10 mM KCl and 0.5 mM dithiothretiol) containing protease and phosphatase inhibitors (Complete Protease Inhibitor Cocktail Tablets, Roche Diagnostics, and 5 mM NaF) and incubated for 10 min on ice. Cellular membranes were disrupted by 15 passages through a 23-gauge needle plus 10 passages through a 25-gauge needle. Then, cellular extracts were centrifuged for 5 min at 228 x g at 4ºC. The supernatant (cytoplasmic fraction) was collected and stored at -20ºC, while the pellet (nuclear fraction) was resuspended in buffer B (0.25 M sucrose, 10 mM $MgCl_2$ with protease and phosphatase inhibitors as above), homogenized by 10 passages through a 23-gauge needle and centrifuged for 5 min at 1,430 x g on a sucrose cushion (buffer C: 0.35 M sucrose, 0.5 mM $MgCl_2$ with protease and phosphatase inhibitors as above). Next, the pellets (purified nuclei) were resuspended in STM buffer (250 mM sucrose, 50 mM Tris-HCl pH 7.4, 5 mM $MgSO_4$ with protease and phosphatase inhibitors as above), DNAse (250 µg/ml) and RNAse (250 µg/ml). Pellets were incubated for 1 h on ice and centrifuged 10 min at 3,000 x g. The supernatants (S1) were collected and stored at -20ºC, while the pellets were resuspended in 1/5 LS/HS buffer (LS: 10 mM Tris-HCl ph 7.4, 0.2 mM $MgSO_4$ and HS: 2M NaCl in LS buffer) supplemented with phenylmethylsulfonyl fluoride (PMSF) and aprotinin. These pellets were incubated for 15 min on ice and centrifuged for 20 min at 8,000 x g. Finally, the supernatants were collected (S2) and the pellets resuspended in 1/5 LS/HS buffer following the same protocol as described above. After centrifugation, pellets containing the nuclear matrix were homogenized in STM buffer and subjected to Western blot analysis.

2.8. *Cell viability/proliferation assay*

Cell viability (as a measure of proliferation over time) was determined using a 3-(4,5-dimethylthiazol-2-yl)-2,5-diphenyl tetrazolium bromide (MTT) assay. This is a colorimetric assay that measures the reduction of yellow MTT by mitochondrial succinate dehydrogenase, producing an insoluble, colored (dark purple) formazan product. The cells are then solubilized with an organic solvent and the released, solubilized formazan reagent is measured spectrophotometrically. Since reduction of MTT can only occur in metabolically active cells the level of activity is a measure of the viability of the cells.

MCF7 cells transduced with the corresponding shRNA lentiviral particles were seeded into 24 well plates at a density of $1x10^4$ cells per well. Viability was then measured at days 1, 5 and 8. For every time point, we added a final concentration of 10 μM MTT per well and cells were incubated for 2 h at 37ºC. Next, the media was removed and the remaining formazan precipitate was diluted in 500 μl of DMSO. Optical density was measured at 570 nm.

2.9. *Three-dimensional culture of MCF10A cells on reconstituted basement membranes*

In the study of epithelial cell polarity and differentiation, MCF10A were grown as three-dimensional (3D) cultures in reconstituted basement membrane (rBM) (Geltrex™ from Invitrogen) (Debnath et al., 2003; Weaver et al., 1995). In these conditions, cells produce acini structures that recapitulate the tissue architecture *in vivo* with a hollow lumen and apicobasal polarization (Weaver et al., 1995).

Geltrex™ was thawed on ice in a refrigerator o/n. Working on ice, 40 μl Geltrex™ was added to each well in a sterile eight-well glass chamber slide. Slides were placed in a cell culture incubator to allow the basement membrane solidify for at least 15 min. While the Geltrex™ was solidifying, cells were trypsinized, counted, diluted in HuMEC media plus 2% Geltrex™ and plated to a final volume of 2,000 cells per well. Medium containing 2% Geltrex™ was changed every four days. For quantitation of growth, pictures were taken at days 6, 8 and 12. Bright-field images of acini were analyzed for size and shape with ImageJ software (National Institutes of Health). For shape analysis, the square of the inverse of circularity was plotted. At day 12 cells were fixed and prepared for immunofluorescence as described in subsequent sections.

2.10. *Co-affinity purification assays*

For co-affinity purification (co-AP) assays using Glutathione Sepharose 4B (GE Healthcare), ORFs were transferred from the DONR vector into the N-term GST-tagged Gateway destination vector pDEST-27 (Invitrogen) (**Figure 8**) as explained above (section 1.3, Materials). Plasmids (1.5 μg) were transfected into HEK293 cells in six-well format using Lipofectamine 2000 (Invitrogen) or FuGene® 6 (Roche Diagnostics). Cells were cultured for 48 h and lysates prepared in buffer containing 50 mM Tris-HCl, pH 7.5, 100-150 mM NaCl, 0.5% Nonidet P-40, 1 mM EDTA with protease and phosphatase inhibitors (Complete Protease Inhibitor Cocktail Tablets, Roche Diagnostics, and 5 mM NaF). Lysates were cleared twice by centrifugation at 13,000 x g before purification of protein complexes using glutathione-Sepharose beads (GE Healthcare) for one h at 4ºC. The glutathione beads were then washed three times with lysis buffer, and denatured at 70-95°C for 5-10 min prior to SDS-PAGE gel electrophoresis.

2.11. *Co-immunoprecipitation assays*

For co-immunoprecipitation (co-IP) assays, cells were harvested at subconfluent density and washed twice with PBS. Cell lysates were prepared in buffer containing 20 mM Tris-HCl (pH 8.0), 100-150 mM NaCl, 0.5% Nonidet P-40, 1 mM EDTA with protease and phosphatase inhibitors (Complete Protease Inhibitor Cocktail Tablets, Roche Diagnostics, and 5 mM NaF). In some assays supplementary phosphatase (10 mM NaF) or proteasome (MG-132, Sigma-Aldrich) inhibitors were added to the solutions. Cells were incubated in lysis buffer for 15 min at 4°C and clarified twice by centrifugation at 13,000 x g for 20 min. Protein concentrations in the clarified lysates were determined by the BioRad Bradford Protein Assay. Preclearing was carried out for one h at 4°C with Protein G Sepharose 4 Fast Flow (GE Healthcare). Immunoprecipitations using 2.5 to 5 μg of antibodies were performed at 4°C o/n. Samples were then incubated for one h at 4°C with Protein G Sepharose 4 Fast Flow (GE Healthcare), washed three times with lysis buffer, and denatured at 70-95°C for 5-10 min prior to SDS-PAGE gel electrophoresis.

2.12. *Western blotting*

For SDS-PAGE gel electrophoresis, samples were mixed in Laemmli loading buffer (60mM Tris-HCl pH 6.8, 2% (w/v) SDS, 10% glycerol, 0.2 mg/ml bromophenol blue and 0.1 M DTT), denatured at 70-95ºC for 5-10 min and loaded in tris-glycine-SDS PAGE gels. Proteins were separated by gel electrophoresis using the Bio-Rad mini

gel apparatus. Next, proteins were transferred to Invitrolon PVDF (Invitrogen) or IMMOBILON PVDF (Millipore) membranes using buffer containing 25 mM Tris base, 192 mM Glycine and 10 to 20% methanol (depending on the molecular weight of the proteins of interest) and using the Bio-Rad tank transfer system. Membranes were incubated for at least one h in blocking buffer with 5% low-fat dry milk in TBS-T (TBS with 0.1% Tween-20). For identification of TSC1 or TACC3, membranes were incubated in alternative blocking buffer: 2.5% low-fat dry milk; 2.5% BSA in TBS-T. All antibody incubations were carried out in blocking buffer o/n at 4ºC under constant agitation. Membranes were then washed three times for 10 min with TBS-T and probed for one h with horseradish peroxidase (HRP) labeled secondary antibodies, diluted in blocking buffer according to the manufacturer's instructions. After a three 10 min wash with TBS-T, target proteins were identified by detection of HRP-labeled antibody complexes with chemiluminescence using ECL or ECL-Plus Western blotting Detection kit (GE Healthcare) following standard protocols. In some cases, samples were resolved in NuPAGE Novex 4-12% Bis-Tris or 3-8% Tris-Acetate Gels (Invitrogen).

2.13. *Immunofluorescence*

Cells were seeded on glass coverslips, fixed with ice-cold methanol (Panreac) for 10 min at room temperature and permeabilized with 0.02% Tween-20 in PBS. Cells fixed on glass coverslips were incubated 45-60 min at room temperature with blocking buffer (4% FBS and 0.02% Tween-20 in PBS) and stained with the primary antibodies o/n at 4ºC. The day after, cells were washed three times with 0.02% Tween-20 in PBS for 20 min. Coverslips were incubated in secondary antibodies conjugated with either Alexafluor 488 or 594 (Invitrogen) for 30-45 min at room temperature. After three washes of 20 min with 0.02% Tween-20 in PBS, coverslips were mounted over DAPI-containing VECTASHIELD (Vector Laboratories). Immunofluorescences were observed on a confocal microscope (Olympus BX60) and the images were obtained using a SPOT RT Mono-2000 camera (Diagnostic instruments).

- *Immunofluorescence staining of MCF10A cells cultured in rBM*

Culture media was removed and wells washed with PBS to subsequently fix cells with ice-cold methanol for two h at -20ºC. Once fixed, cells were permeabilized with PBS containing 0.5% Triton X-100 for 10 min at 4ºC. After permeabilization, cells were rinsed three times with PBS containing 100 mM Glycine for 10 min per wash at room temperature. Then, cells were incubated for 45-60 min at room

temperature with blocking buffer (0.1% FBS, 0.02% Tween-20 and 10% goat serum in PBS) and stained with primary antibodies o/n at 4ºC. The day after, cells were washed three times with 0.02% Tween-20 in PBS for 20 min. Cells were incubated in secondary antibodies conjugated with either Alexafluor 488 or 594 (Invitrogen) for 30-45 min at room temperature. After three washes with 0.02% Tween-20 in PBS for 20 min, cells were stained with DAPI-containing VECTASHIELD (Vector Laboratories) and covered with glass coverslips. Preparations were observed on a confocal microscope (Olympus BX60) and the images were obtained using a SPOT RT Mono-2000 camera (Diagnostic instruments).

2.14. *shRNA design and viral preparation*

Five different shRNAs against TACC3 (shRNA-*TACC3*), TSC2 (shRNA-*TSC2*) and TSC1 (shRNA-*TSC1*) were purchased from Sigma-Adrich (St. Louis, MO). Five 21-nucleotide shRNA duplexes from five different parts of the human TACC3 mRNA (Gene Bank Accession No. NM_006342.1), human TSC2 mRNA (Gene Bank Accession No. NM_000548), and human TSC1 mRNA (Gene Bank Accession No. NM_000368) were designed by Sigma-Aldrich using the MISSION™ search database at www.sigma-aldrich.com/missionsearch, which is produced and distributed under license from the Massachusetts Institute of Technology. The shRNA sequences tested were as shown in Table 2. Long-term, stable gene silencing distinguishes short hairpin RNA constructs (shRNA) from other RNAi tools. The lentiviral shRNA constructs can easily transduce typically difficult cell lines, even non-dividing cells, and readily integrate the shRNA into the genome of these cells for stable gene silencing under selection with puromycin (www.sigmaaldrich.com).

HEK293T cells were used as the packaging cell line for virus production. Cells were co-transfected with the packaging vector psPAX2, the envelope vector pMD2.G and shRNA sequence or pLKO.1 shRNA empty vector (**Figure 10**), using FuGENE® 6 (Roche Diagnostics) as the transfection reagent in serum-free OPTI-MEM (Invitrogen). Transfected cells were incubated in standard conditions for 12-15 h. Next, the media was removed and replaced with fresh DMEM 10% FBS, and cultures were incubated for a further 24 h. The media was then harvested, centrifuged at 1,750 x g and passed through a 0.45 µm filter to remove any cellular debris. Virus supernatant was used immediately for transduction or aliquoted at -80ºC.

MCF7 and MCF10A cells were transduced with lentivirus as follows: the cells were plated at 70-80% confluency and transduced with shRNA lentiviral particles

and Polybrene® (Sigma-Aldrich) at a final concentration of 8 µg/mL; next, cells were incubated at 37ºC for 24 h. The day after, virus-containing media was replaced with fresh media, and 72 h after transduction the media was supplemented with 5 µg/ml puromycin for selection of infected cells (4-5 days).

The lentiviral-based generation of single cell clones for doxycycline (DOX)-inducible shRNA-mediated down-regulation of TACC3 expression used in this study has been previously described for HeLa cells (Schneider et al., 2007a) or will be published elsewhere for MCF7 and MCF10a cells (Schmidt et al., manuscript in preparation). For immunofluorescence analysis, infected cells were grown continuously under DOX (5 µg/ml) treatment.

Table 2: Target sequences used to down-regulate *TACC3*, *TSC2* and *TSC1* expressions

TRC#	*Description*	*Sequence*	*Validated*	*Used*
TRCN0000039733	TSC1 shRNA #33	CCGGCCACACATTTAATTCAGCTTTCTCGAG AAAGCTGAATTAAATGTGTGGTTTTTG	n/a	
TRCN0000039734	TSC1 shRNA #34	CCGGGCACTCTTTCATCGCCTTTATCTCGAG ATAAAGGCGATGAAAGAGTGCTTTTTG	Y	***
TRCN0000039735	TSC1 shRNA #35	CCGGGCCAAGAAAGACCACCTTCTTCTCGA GAAGAAGGTGGTCTTTCTTGGCTTTTTG	Y	
TRCN0000039736	TSC1 shRNA #36	CCGGGCAGCCATCTTGGAAGCATAACTCGA GTTATGCTTCCAAGATGGCTGCTTTTTG	Y	
TRCN0000039737	TSC1 shRNA #37	CCGGGCTACATATCATGGACTACAACTCGAG TTGTAGTCCATGATATGTAGCTTTTTG	n/a	
TRCN0000040178	TSC2 shRNA #78	CCGGCGACGAGTCAAACAAGCCAATCTCGA GATTGGCTTGTTTGACTCGTCGTTTTTG	Y	***
TRCN0000040179	TSC2 shRNA #79	CCGGGCTCATCAACAGGCAGTTCTACTCGA GTAGAACTGCCTGTTGATGAGCTTTTTG	Y	
TRCN0000040180	TSC2 shRNA #80	CCGGCGCTATAAAGTGCTCATCTTTCTCGAG AAAGATGAGCACTTTATAGCGTTTTTG	n/a	
TRCN0000040181	TSC2 shRNA #81	CCGGCCAACGAAGACCTTCACGAAACTCGA GTTTCGTGAAGGTCTTCGTTGGTTTTTG	Y	
TRCN0000040182	TSC2 shRNA #82	CCGGGAGGGTAAACAGACGGAGTTTCTCGA GAAACTCCGTCTGTTTACCCTCTTTTTG	Y	
TRCN0000062023	TACC3 shRNA #23	CCGGCCACGGAGCCGCTGTCCCCGCCTCGA GGCGGGGACAGCGGCTCCGTGGTTTTTG	n/a	
TRCN0000062024	TACC3 shRNA #24	CCGGGCAGTCCTTATACCTCAAGTTCTCGAG AACTTGAGGTATAAGGACTGCTTTTTG	n/a	
TRCN0000062025	TACC3 shRNA #25	CCGGCGCACAGGATTCTAAGTCCTACTCGA GTAGGACTTAGAATCCTGTGCGTTTTTG	n/a	
TRCN0000062026	TACC3 shRNA #26	CCGGGCTTGTGGAGTTCGATTTCTTCTCGAG AAGAAATCGAACTCCACAAGCTTTTTG	Y	***
TRCN0000062027	TACC3 shRNA #27	CCGGCCAGGAAGTTCTGAGAACCAACTCGA GTTGGTTCTCAGAACTTCCTGGTTTTTG	n/a	

Y: sequence validated for knockdown by Sigma-Aldrich

***: sequence used for gene knockdown in this study

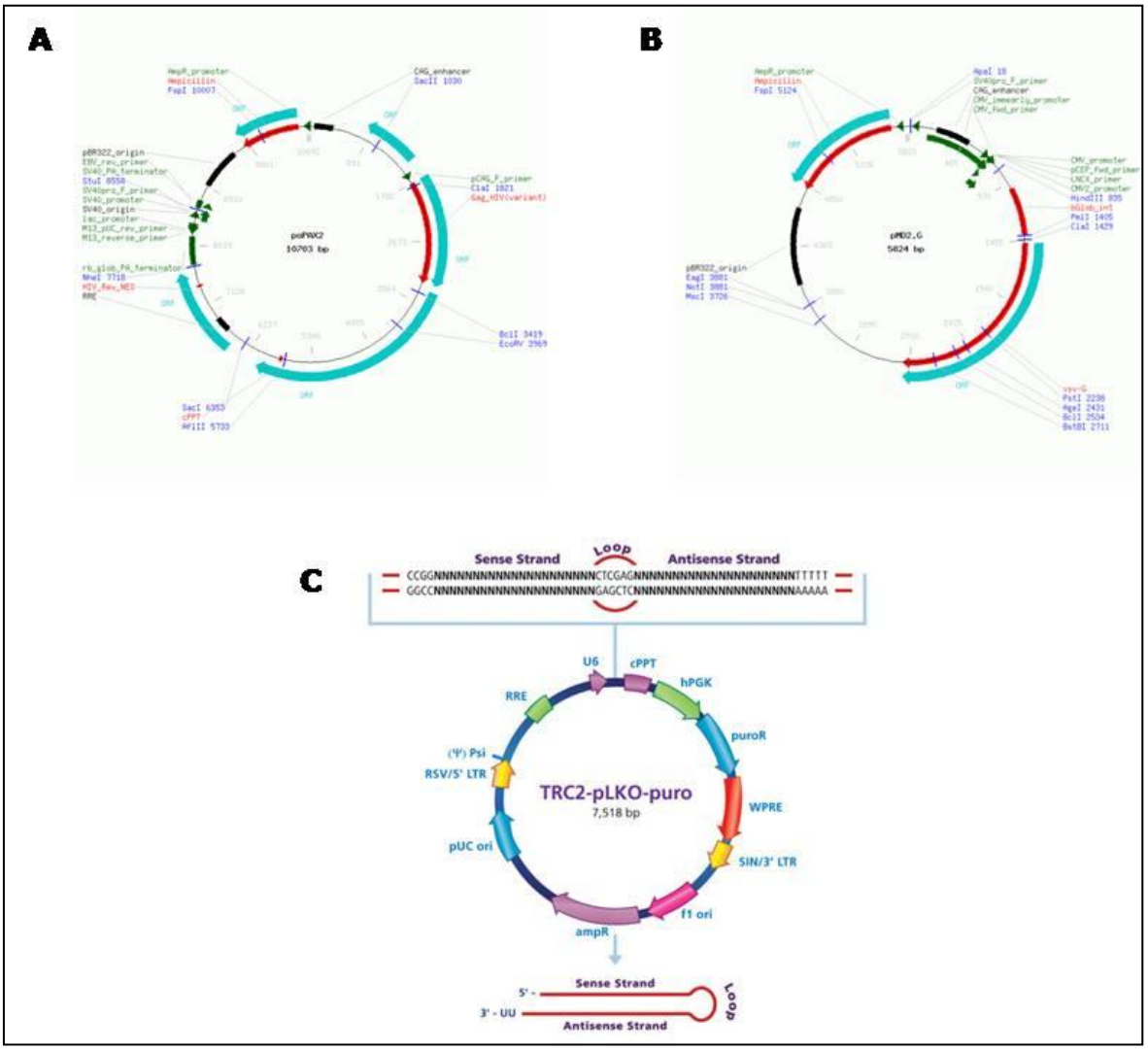

Figure 10: Vectors used for lentiviral preparation

Figure shows the schematic structure of (**A**) the lentiviral packaging vector psPAX2, (**B**) the lentiviral envelope vector pMD2.G and (**C**) the pLKO.1-puro vector.

RESULTS

1 A high-confidence TACC3 interactome network linked to centrosome biology

In humans, all three TACC members have been linked to carcinogenesis (Conte et al., 2002; Conte et al., 2003; Chen et al., 2000; Raff, 2002; Still et al., 1999a; Still et al., 1999b), and the study of this family of proteins is starting to offer a variety of promising applications related to cancer therapies; TACC3 has recently been described as a novel prognostic maker in non-small cell lung cancer (Jung et al., 2006) and as a potential biomarker in ovarian cancer (Peters et al., 2005). To gain insight into TACC functions and their involvement in neoplasia we performed a Y2H screen using the conserved domain of TACC3 as bait.

Sixteen different and mostly novel interactions were identified with the TACC domain as bait, including the TACC3 homodimer and TACC1 and TACC2 heterodimers through the C-term region of the corresponding proteins (**Figure 11**).

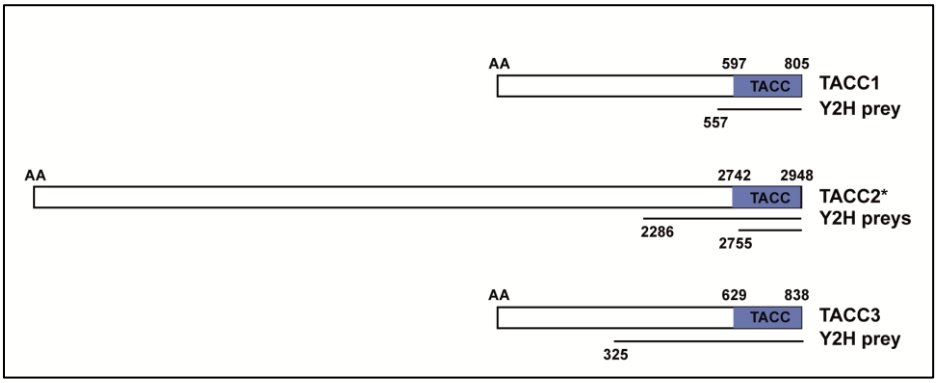

Figure 11: Y2H results for TACC3-TACC homo and heterodimers

Blue boxes show the aproximate boundaries of the corresponding TACC domains (amino acids, AA). Bottom lines and AA indicate the overlap with the TACC3-Y2H preys. Asterisk indicates the largest putative isoform of TACC2 (NP_996744).

Diverse molecular and functional evidence, including co-affinity purification (co-AP) and endogenous co-immunoprecipitation (co-IP) assays, supports the high confidence of this interactome. First, two interologs (i.e. orthologous pairs of interacting proteins in different organisms (Matthews et al., 2001)) were identified: with ch-TOG/CKAP5, conserved interaction with TACC ortholog in *S. pombe* (Sato et al., 2004), *C. elegans* (TAC-1) (Bellanger and Gonczy, 2003; Srayko et al., 2003), *D. melanogaster* (Cullen and Ohkura, 2001; Lee et al., 2001) and *X. laevis* (Kinoshita et al., 2005; O'Brien et al., 2005; Peset et al., 2005); and with FAM161B, conserved interaction with TAC-1 (FAM161B putative ortholog: Y38H6C.14, hypothetical protein NP_507957) (Li et al., 2004). In addition, KIF1C,

another newly identified physical interactor of TACC3, has a homolog (KLP-1) at "two-hop" interactions of TAC-1 (**Figure 12**), which suggests the identification of an evolutionarily conserved TACC interaction module.

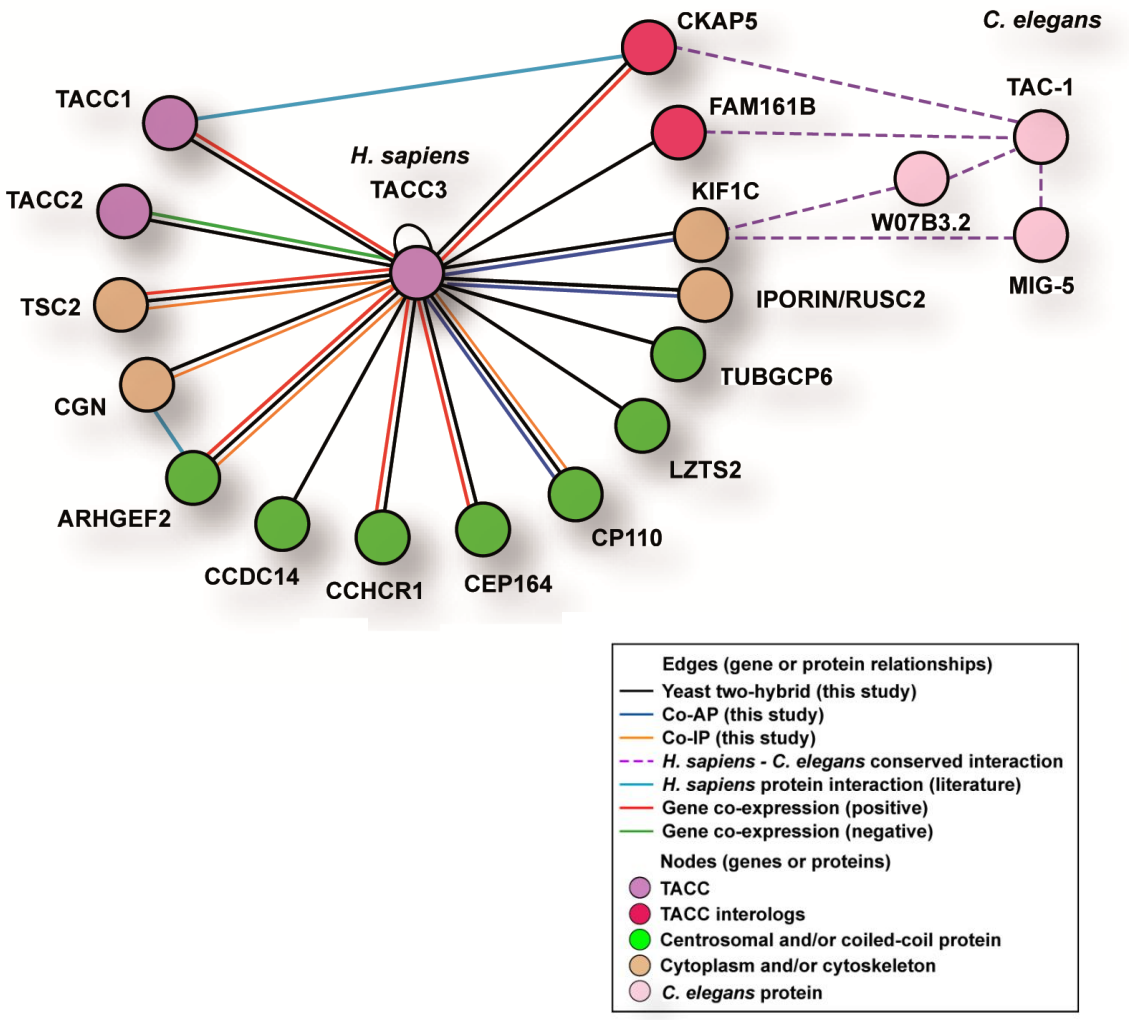

Figure 12: A high-confidence TACC3 interactome network

The figure shows the resulting network from the Y2H screen, containing transcript and protein associations represented by differently colored edges as detailed in the right panel. Discontinuous lines show interactions for *C. elegans* orthologs. Blue lines show previously reported interactions in humans (Aijaz et al., 2005; Lauffart et al., 2002). Protein function assignment is based on Gene Ontology (GO) biological process terms.

The fact that no additional interologs were detected—in particular relative to TAC-1, which essentially contains the TACC domain—may be due to technical limitations and/or evolutionary differences. Phylogenetic analysis indicated that human TACCs probably resulted from two consecutive duplications occurring after the divergence of vertebrates and uro-chordates, and that TACC1 and 2 originated from the most recent of these duplications and are, therefore, more evolutionarily related to each other than to TACC3 (**Figure 13**) (Still et al., 2004). This analysis also suggested accelerated evolution of TACCs among coiled-coil domain-containing proteins, which may further explain interactome differences across species (**Figure 14**).

The similarity of gene expression profiles for 7 of the 12 *TACC3*-Y2H prey gene pairs, measured with the Pearson correlation coefficient (PCC) across a large number of normal human samples (Su et al., 2004), is further evidence of the high-confidence of the interactome (**Figure 12**; $|PCC| > 0.30$, Bonferroni-corrected *P* values < 0.05). The primary area of similarity was positive co-expression, which suggests synergistic roles in centrosome biology.

*(The phylogenetic analyses represented in **Figure 13** and **Figure 14** were performed in collaboration with Toni Gabaldón from the Center of Genomic Regulation at the Barcelona Biomedical Research Park)*

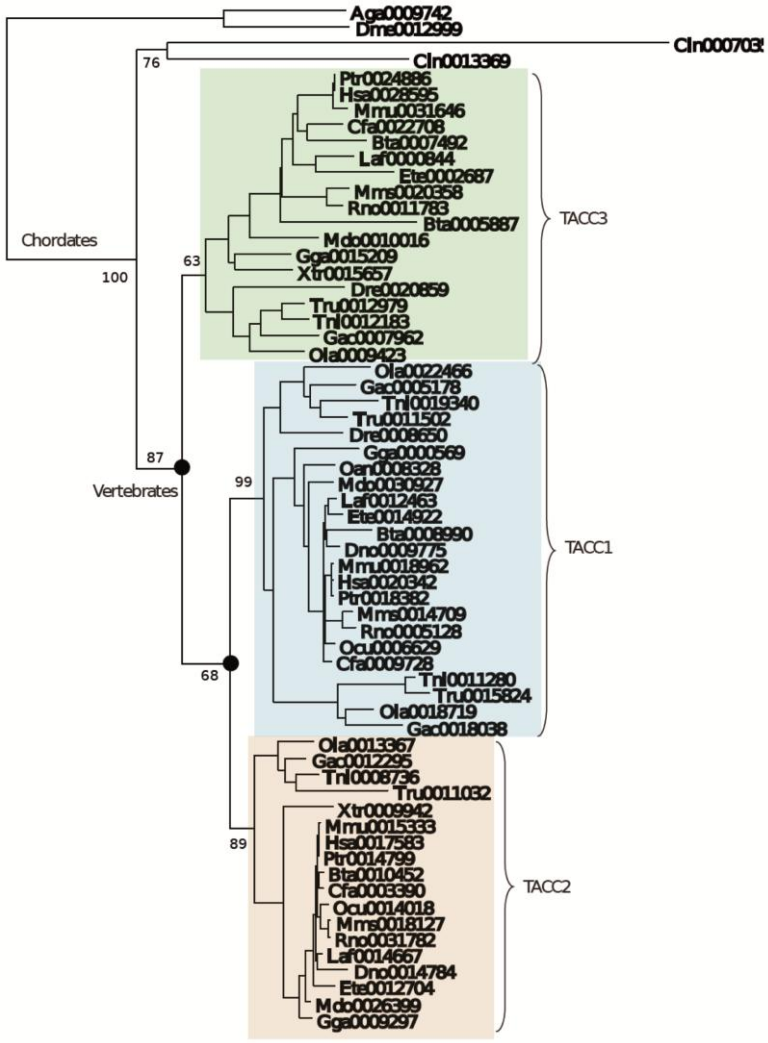

Figure 13: Phylogenetic tree representing the evolutionary relationships among human TACCs and related proteins

Duplication events at the base of vertebrates leading to the three TACC paralogous groups are indicated by black circles. Members of each of the TACC paralogous groups are indicated by colored boxes. Noteworthy is the presence of two paralogous copies of TACC1 in fish. Bootstrap support (over 100 replicates) is indicated for the main groupings. Three-letter codes at the begining of the sequence identifier indicate the organism source: *Anopheles gambiae* (Aga), *Bos taurus* (Bta), *Canis familiaris* (Cfa), *Ciona intestinalis* (Cin), *Danio rerio* (Dre), *Dasypus novemcinctus* (Dno), *Drosophila melanogaster* (Dme), *Echinops telfairi* (Ete), *Gallus gallus* (Gga), *Gasterosteus aculeatus* (Gac), *Homo sapiens* (Hsa), *Oryzias latipes* (Ola), *Pan troglodytes* (Ptr), *Rattus norvergicus* (Rno), *Loxodontha africana* (Laf), *Macaca mulata* (Mmu), *Monodelphis domestica* (Mdo), *Mus musculus* (Mms), *Oryctolagus cuniculus* (Ocu), *Takifugu rubripes* (Tru), *Tetraodon nigroviris* (Tni) and *Xenopus tropicalis* (Xtr). The corresponding sequences can be downloaded from PhylomeDB (www.phylomedb.org).

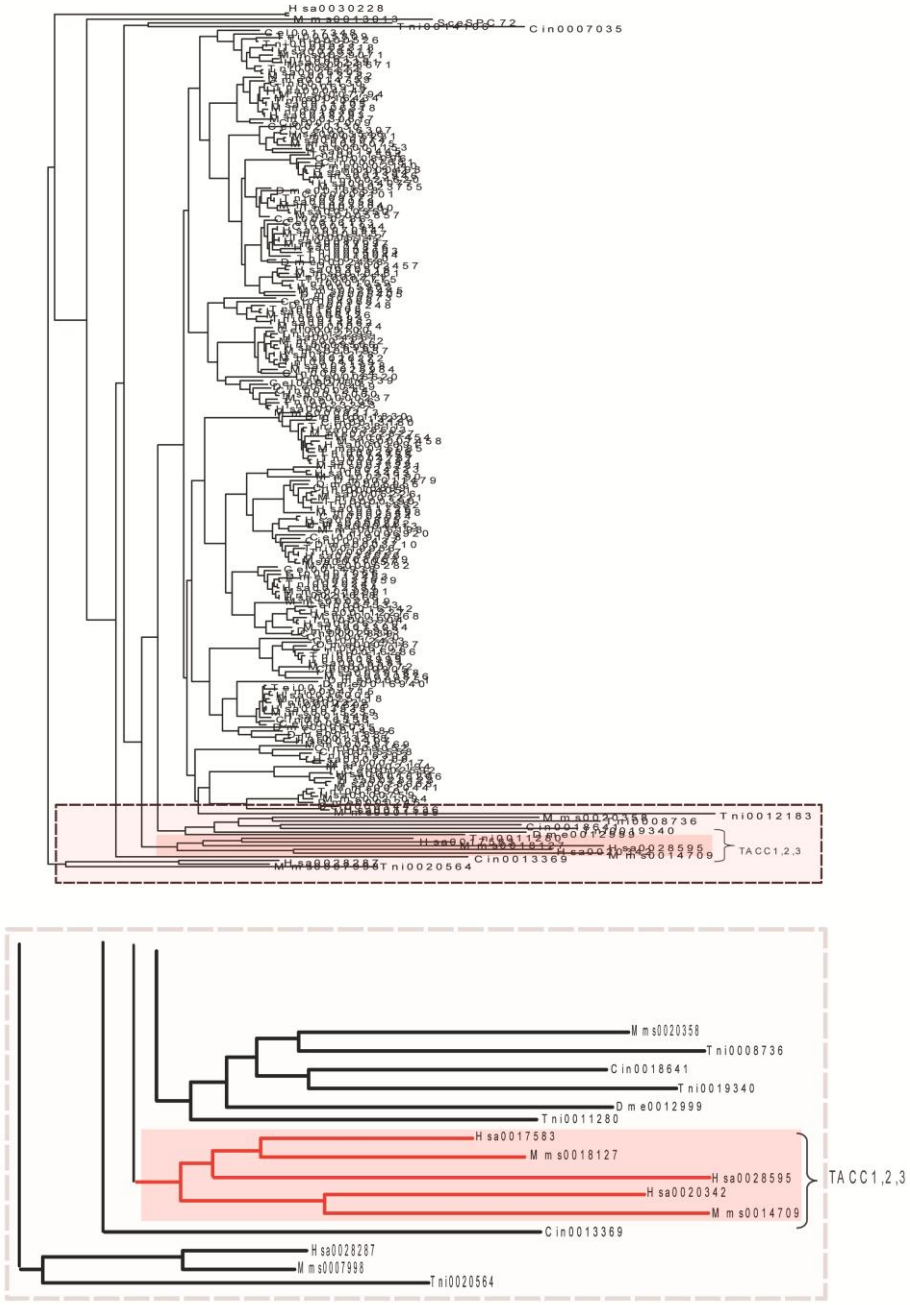

Figure 14: Phylogenetic analysis of TACCs within coiled-coil motif-containing proteins (large tree)

Homologous proteins from a selected group of species were retrieved with PSI-Blast searches starting from each human TACC representative. All TACC representatives cluster within a monophyletic partition in the tree (see detail). High evolutionary rates affecting TACCs are apparent from the relatively long branches leading to these proteins. Their specific position within the tree is perhaps the result of long-branch attraction. Three-letter codes as in Figure 13. The corresponding sequences can be downloaded from PhylomeDB (www.phylomedb.org).

Analysis of Gene Ontology (GO) term annotations in the TACC3 interactome relative to all human coding genes identified significant over-representation of MT-associated biological processes (**Table 3**), which include important regulators of cilia formation (centrosomal protein 164 kDa (CEP164) (Graser et al., 2007) and centrosomal protein 110 kDa (CP110) (Tsang et al., 2008)) and cytokinesis (RHO/RAC guanine nucleotide exchange factor 2 (ARHGEF2/GEF-H1) (Birkenfeld et al., 2007), leucine zipper, putative tumor suppressor 2 (LAPSER1/LZTS2) (Sudo and Maru, 2007) and TACC1 (Delaval et al., 2004)). In particular, CP110 is a centrosomal protein involved in centrosome duplication (Chen et al., 2002), cilia growth regulation in growing cells (Tsang et al., 2008), and its deregulation may contribute to genomic instability (Chen et al., 2002; Spektor et al., 2007; Tsang et al., 2008). CEP164 has recently been localized to the mature centriole and shown to regulate primary cilia formation (Graser et al., 2007). Consistent with the involvement of TACCs in mitosis regulation, some of the TACC3 interactors described in this study have been shown to play a role in cytokinesis. The tumor suppressor LAPSER1 is present in the centrosome and midbody, and regulates central spindle organization and progression of cytokinesis (Sudo and Maru, 2007). TACC1 forms a complex with AURKB (Delaval et al., 2004), the major regulator of cytokinesis (Tatsuka et al., 1998; Terada et al., 1998). Loss of AURKB seems to affect TACC1 localization to the midbody, leading to abnormal cytokinesis completion, which suggests a possible coordinated role of both proteins in this process (Delaval et al., 2004).

Table 3: Over-represented GO biological process terms in the TACC3 interactome
(False discovery rate (FDR)-adjusted *P* values < 0.05)

Microtubule-based process
Microtubule cytoskeleton organization and biogenesis
Metabolic process
Cytoskeleton organization and biogenesis
Cellular metabolic process
Centrosome organization and biogenesis
Primary metabolic process
Microtubule-organizing center organization and biogenesis
Negative regulation of phosphoinositide 3-kinase cascade
Microtubule nucleation
Macromolecule metabolic process
Cell cycle

The TACC3 interactions identified in the Y2H system were further evaluated in complementary or independent biochemical assays. First, some of the interactions were corroborated by co-APs of fusion proteins in HEK293 cells as shown in **Figure 15**. In this assay, cells were co-transfected with GST-tagged full-length human TACC3 or GST-only as a negative control and the Y2H prey cloned into a different tagged construct (see Methods). This analysis identified co-AP of TACC3 with the centrosomal protein CP110. We also verified the interaction with KIF1C, a kinesin family member, plus-end enriched MT motor (Kopp et al., 2006) and recently identified in a large functional genomic screen as a positive modulator of ciliogenesis (Kim et al.). In addition, co-AP assays revealed a novel physical interaction between TACC3 and the putative TACC homolog RHAMM (**Figure 15B**). Consistently with TACC3 known functions, RHAMM is a centrosomal protein involved in MT stabilization (Maxwell et al., 2003).

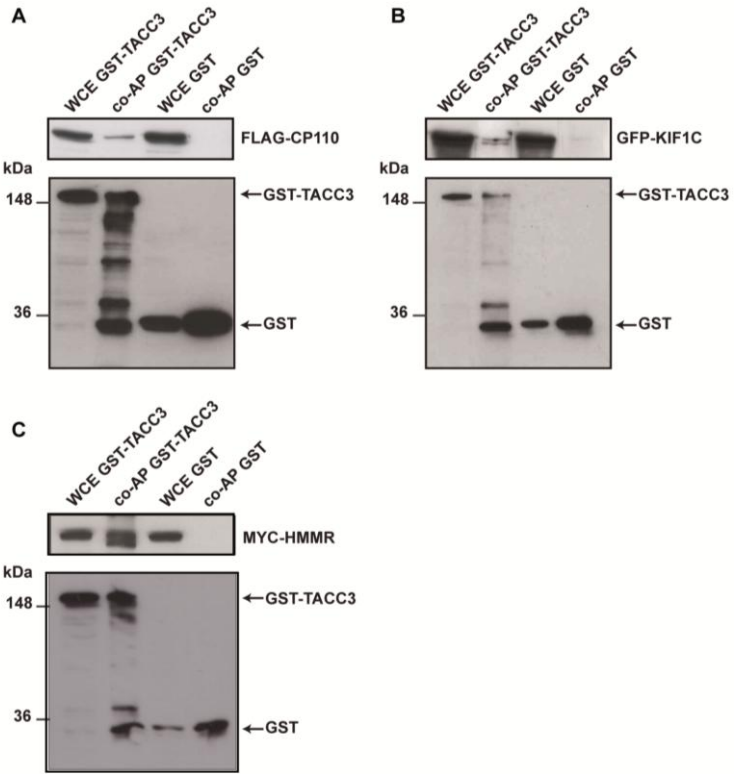

Figure 15: Validation of TACC3 interactions by co-APs

Confirmation of TACC3 protein interactions by co-AP in HEK293 extracts. HEK293 cells were co-transfected with (**A**) FLAG-CP110, (**B**) GFP-KIF1C or (**C**) MYC-HMMR, and GST-tag full length TACC3 or GST-only constructs. Upper panels in (**A**), (**B**) and (**C**) show immunoblot analysis of the GST pull-down assay using anti-FLAG, anti-GFP and anti-MYC antibodies, respectively. Bottom panels show respective pull-down assays blotted against GST antibody as a control. WCE, whole cell extract, co-AP, co-affinity purification and molecular weight (kDa; kilodaltons) are shown.

Additionally, co-IPs in HEK293 cell extracts identified complexes between TACC3 and ARHGEF2/GEF-H1, CGN, CP110 (**Figure 16**) or TSC2 (**Figure 17A**). ARHGEF2, a guanine nucleotide exchange factor for RHOA, and CGN, a junctional adaptor, were previously shown to interact physically (Aijaz et al., 2005) controlling at some point epithelial proliferation and differentiation. These data further support the detection of true positive interactions for TACC3. In the study of the interaction between TACC3 and CGN, cells were treated with nocodazole as shown in **Figure 16B**. Nocodazole treatment increased the interaction between the two proteins, suggesting a G2/M-checkpoint dependency.

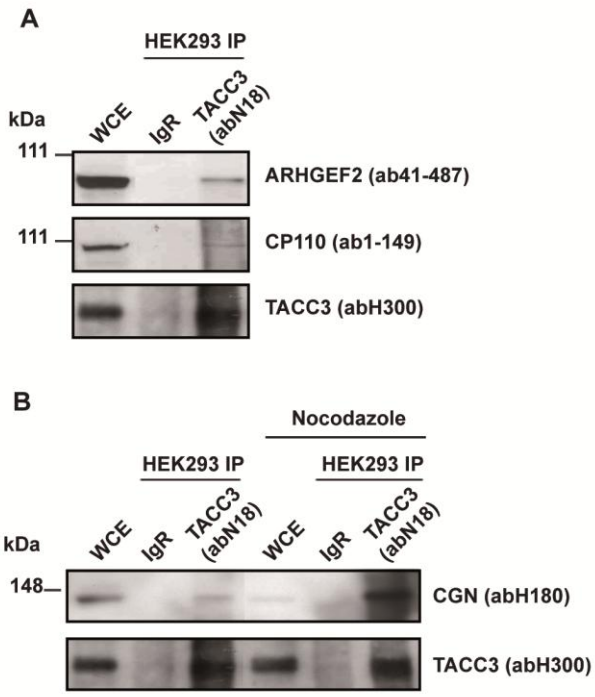

Figure 16: Validation of TACC3 interactions by co-IP

Results show endogenous co-IPs in HEK293 cells for (**A**) ARHGEF2 and CP110 in normal conditions and (**B**) for CGN in cells treated with nocodazole. WCEs and normal purified immunoglobulin negative control (IgG R; rabbit) are shown. The antibodies (ab) used for each experiment are shown in parentheses.

The interaction between TACC3 and TSC2 was detected reciprocally using different subconfluent and unsynchronized cell cultures and specific antibodies in co-IP assays (**Figure 17** and subsequent sections). However, unlike endogenous levels of TSC2, our first results showed a weak interaction between TACC3 and TSC2 (**Figure 17A**), suggesting that the TACC3-TSC2 complex formation may be condition/location-dependent or transient. Protein complexes of TACC3-TSC2 were identified in HEK293 and MCF7 extracts (**Figure 17**), and in cell cycle-synchronized HeLa extracts (subsequent sections). In addition, complexes of TACC3 and phospho-Ser939 (pS939)-TSC2 were detected in BT474 extracts (**Figure 17B**), which are known to contain abundant phosphorylated TSC2 as compared to MCF7 (Ju et al., 2007).

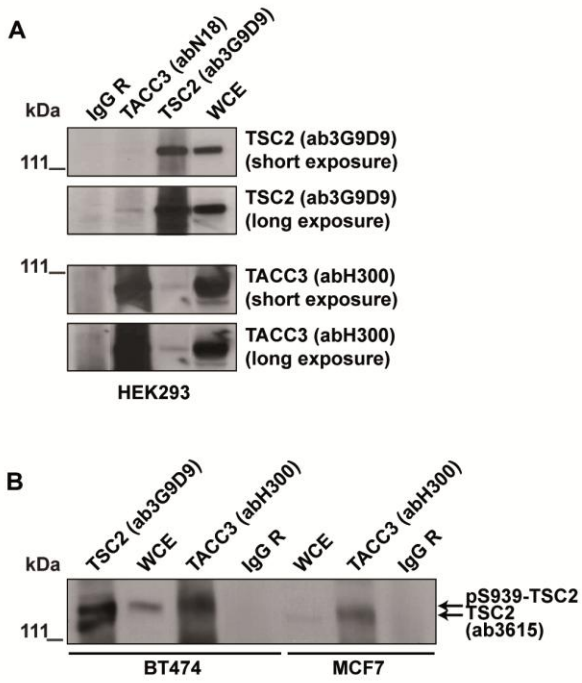

Figure 17: Validation of TACC3-TSC2 interaction by co-IP

(**A**) Western blot results showing reciprocal co-IPs of TACC3 and TSC2 in HEK293 extracts. (**B**) Panel shows results of a high-resolution Western blot where TACC3 co-IP with pS939-TSC2—in addition to possibly unphosphorylated TSC2 as compared to WCEs—can be resolved (detected with anti-pS939-TSC2 antibody) according to expected differences between BT474 and MCF7 cells. WCE and normal purified immunoglobulin negative control (IgG R; rabbit) are shown. Antibodies used for each experiment are shown in parentheses.

Once we had confirmed the interaction between TACC domain in TACC3 and TSC2, our next goal was to identify the specific interacting region in TSC2. We performed co-AP assays using GST-TACC3 and pEGFP vectors expressing different domains of TSC2. These vectors were kindly provided by Dr. Goncharova (Goncharova et al., 2004). The results suggested that the N-term region (aa 1-460), but not the rest of the protein (data not shown), mediates the interaction (**Figure 18**). This TSC2 fragment contains the TSC1-binding domain and a coiled-coil motif (TSC2 hamartin-binding domain; TSC2-HBD). Interestingly, the TSC2-HBD was previously shown to interact with TSC1 within its RHO-activation domain (Hodges et al., 2001) and to be necessary for the regulation of the cytoskeleton and cell adhesion (Astrinidis et al., 2002; Goncharova et al., 2004). In particular, TSC2 was likely to be responsible for stress fiber disassembly and focal adhesion remodeling through its interaction with TSC1 (Goncharova et al., 2004). Together, our observations delineate a high-confidence TACC3 interactome network which includes TSC2 and is linked to centrosome biology.

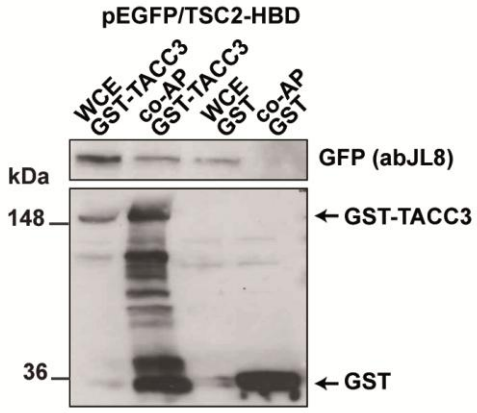

Figure 18: TSC2 N-term region mediates TACC3 interaction

Co-AP of GST-TACC3 and pEGFP-TSC2-HBD in HEK293.Top panel shows Western blot results using an anti-GFP antibody directed against GFP-TSC2-HBD. Bottom panel shows results of the same blot probed with anti-GST antibody. Results of WCEs and the co-AP assays are shown: arrows point to WCEs/co-APs GST-TACC3 and GST-only.

2 TACC3 and TSC2 localize to the nuclear envelope and their depletion causes morphological alterations of this structure

The identification of the tumor suppressor TSC2 as a novel TACC3 interactor supports its involvement in MT-dependent structures and processes (Astrinidis et al., 2002; Goncharova et al., 2004; Jiang and Yeung, 2006). An *in vitro* MT-binding assay using taxol and nocodazole for MT stabilization and depolymerization, respectively, and PLK1 and α-tubulin (TUBA) as controls showed that fractions of TSC2 and its heterodimeric partner TSC1 are associated with MTs (**Figure 19**). This finding may be linked to previous work indicating abnormal vesicular trafficking due to MT disorganization in Tsc2-deficient cells (Jiang and Yeung, 2006). Together, previous results and our confirmed MT association of TSC1 and TSC2 suggest a role of TSC2/mTOR in regulation of MT organization.

*(The MT-binding assay represented in **Figure 19** was performed in collaboration with Aristotelis Astrinidis from the Drexel University College of Medicine)*

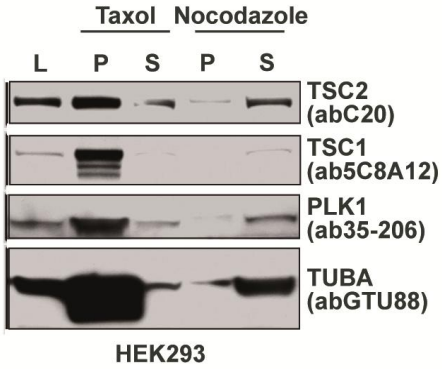

Figure 19: MT association of TSC1 and TSC2

Figure shows Western blot results of a MT-binding assay of TSC2 and TSC1, and appropriate controls PLK1 and TUBA, in HEK293. Sample load (L, 1/100 of input), pellets (P) and supernatants (S, 1/100 of input) are shown.

To further investigate the association of TSC2 with cellular structures, we examined its subcellular localization in HeLa cells and murine embryonic fibroblast (MEF) cultures derived from littermate embryos with the *Tsc2*$^{-/-}$/*Tp53*$^{-/-}$ genotype or from controls with the *Tsc2*$^{+/+}$/*Tp53*$^{-/-}$ genotype. These analyses suggested localization of TSC2/Tsc2 at the nuclear envelope in interphase cells as shown in **Figure 20A**. In support of this hypothesis, TSC2 co-immunoprecipitates with the nuclear pore subunit NUP62 (**Figure 20B**), which in turn interacts physically with centrosome- and nuclear envelope-associated proteins identified in the RHAMM interactome (Pujana et al., 2007).

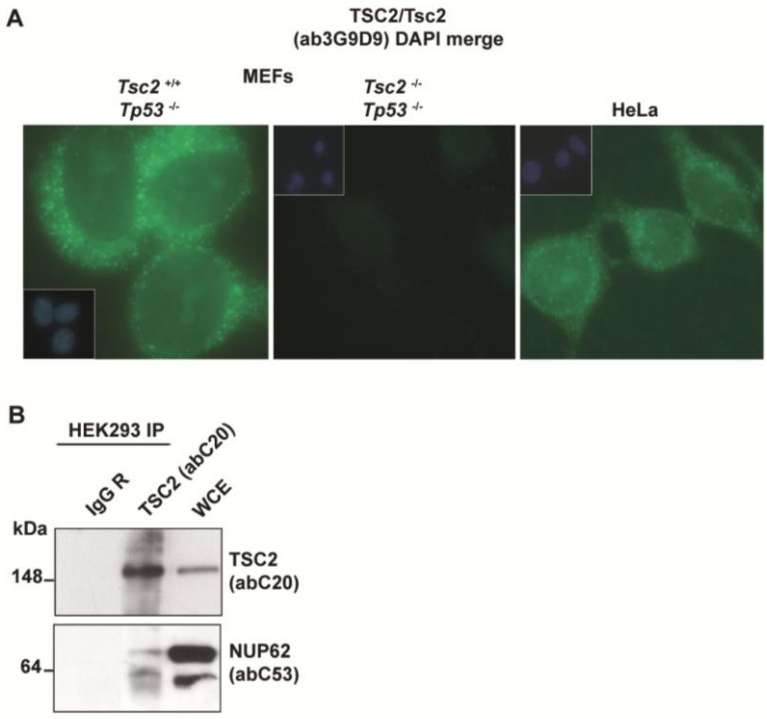

Figure 20: Nuclear envelope localization of TSC2/Tsc2

(**A**) Figure shows the subcellular immunolocalization of TSC2/Tsc2 in MEFs (*Tsc2*$^{+/+}$/*Tp53*$^{-/-}$ and *Tsc2*$^{-/-}$/*Tp53*$^{-/-}$) and HeLa cells. (**B**) Western blot results of endogenous IP of TSC2 in HEK293 extracts showing the nuclear pore subunit NUP62 immunoprecipitation.

Having suggested the nuclear envelope TSC2 localization, TACC3 was also found to localize at this structure in unsynchronized cultures (**Figure 21**). Importantly, TAC-1 was previously found to interact physically with components of the nuclear pore (NPP-1) and lamina (LMN-1) (Boxem et al., 2008).

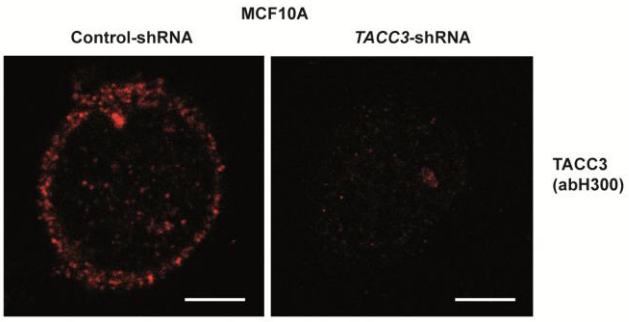

Figure 21: Nuclear envelope localization of TACC3

Figure shows subcellular immunolocalization of TACC3 analyzed by confocal microscopy in MCF10A cells. A lentiviral shRNA expression system was used in this study. Left panel shows MCF10A cells transduced with pLKO.1-based scrambled control construct; right panel shows MCF10A cells transduced with *TACC3*-shRNA construct. Scale bars represent 5 µm.

To biochemically confirm the nuclear localization of TACC3 and TSC2, we performed a cellular fractionation assay (see Methods) using *Tsc2*$^{-/-}$/*Tp53*$^{-/-}$ and *Tsc2*$^{+/+}$/*Tp53*$^{-/-}$ MEFs. Consistently with our previous observations in immunofluorescences, Tsc2 and Tacc3, but not Tsc1, co-purified with the major structural component of the inner nuclear membrane, lamin A (Lmna) (**Figure 22**).

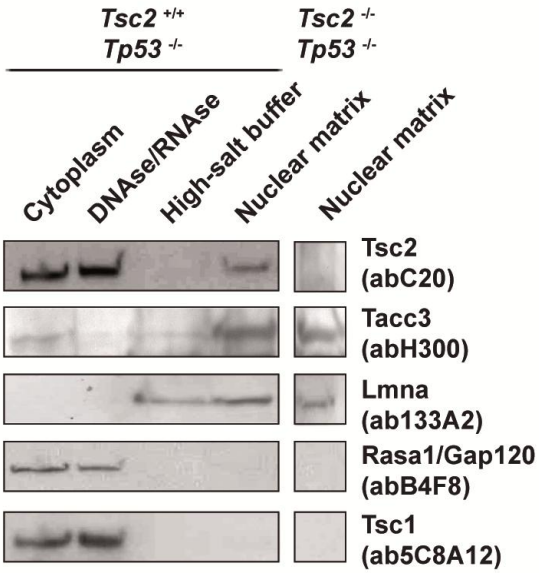

Figure 22: Tacc3 and Tsc2, but not Tsc1, co-purify with the nuclear fraction

Co-purification of Lmna, Tacc3 and Tsc2 in *Tsc2*$^{+/+}$/*Tp53*$^{-/-}$ compared to *Tsc2*$^{-/-}$/*Tp53*$^{-/-}$ MEFs. Fractionation and Western blot analyses are shown for the cytoplasm, DNAse/RNAse-treated nuclear preparations, high-salt extraction buffer nuclear preparations and the remaining pellet, which mainly represents the nuclear matrix. Controls for the purity of the cytoplasmic (Rasa1/Gap120) and nuclear matrix (Lmna) fractions are shown.

Perturbation of centrosome and/or nuclear envelope proteins may cause morphological alterations of the envelope structure (Bonne et al., 1999; Dawe et al., 2009; Luke et al., 2008; Malone et al., 2003). Several human diseases are associated with nuclear envelope protein defects (Worman et al., 2009), being mutations in *LMNA* the most frequent cause (Capell and Collins, 2006). In addition, taxol treatment of cell cultures causes dramatic unraveling of the nuclear LMNA and disorganization of nuclear pore structures (Theodoropoulos et al., 1999). Consistent with TACC3 and TSC2 nuclear localization, morphological alterations of the envelope in Tacc3- and Tsc2- but not Tsc1-deficient MEFs were detected using Nup62 immunostaining (**Figure 23** shows representative fluorescence microscopy images of Tacc3- and Tsc2-deficient MEFs and controls).

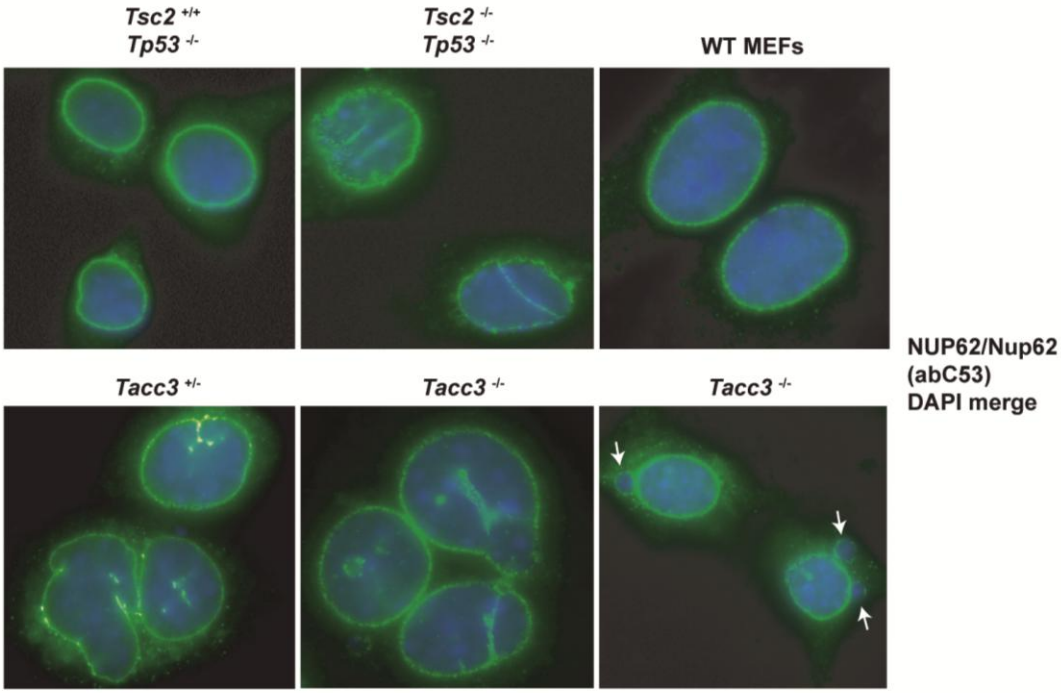

Figure 23: Morphological alterations of the nuclear envelope in Tacc3- and Tsc2-deficient MEFs

Figure shows abnormal nuclear envelope structures in *Tsc2*$^{-/-}$/*Tp53*$^{-/-}$, and *Tacc3*$^{+/-}$ and *Tacc3*$^{-/-}$ cells, revealed by Nup62 immunofluorescence. Bottom right panel shows micronuclei figures (arrows) in *Tacc3*$^{-/-}$ cells.

Moreover, Tacc3-deficient MEFs showed micronuclei figures at a frequency of 4.6 ± 1.5%, which were barely observed in wt MEFs similarly immortalized (0.3 ± 0.5%; these results correspond to a typical experiment of four replicates with > 200 cells counted each) (**Figure 23**). Among the different nuclear abnormalities described in the bibiliography, the presence of micronuclei (i.e. chromatin-

containing, membrane bound bodies that can be present in addition to the normal nucleus of the cell) has been frequently observed in cancer cells (Gisselsson et al., 2001; Kalitsis et al., 2000). However, micronuclei figures were not observed in Tsc2- or Tsc1-deficient MEFs (data not shown). Taken together, these results suggest a specific role of TSC2 in maintaining proper nuclear envelope structure, possibly involving TACC3.

3 pS939-TSC2 localizes to cytokinetic structures in a TACC3-dependent manner

Given the physical interaction between TACC3 and TSC2, and the key role of TACC3 in regulation of cell division (Albee and Wiese, 2008; Gergely et al., 2003; Kinoshita et al., 2005; Schneider et al., 2007b; Yao et al., 2007), we next analyzed the subcellular localization of TACC3 and TSC2 along the cell cycle. We performed immunofluorescence analysis of mammary epithelial cells using the centrosomal protein RHAMM as a control. Initially, studies in non-synchronized telomerase-immortalized human mammary epithelial cells (HME/TERT) revealed that TSC2 clearly localized to the midbody and to the cleavage furrow at cytokinesis (**Figure 24**). We also analyzed TACC3 (total and phosphor-Ser558 (S558)) localization during cell division, using AURKA as a control. Total TACC3 immunostaining confirmed mitotic spindle localization, while pS558-TACC3, which is an AURKA phosphorylation site (LeRoy et al., 2007), localized to the spindle poles (**Figure 25**). To confirm antibody specificity for the phosphorylated form of TACC3 we treated HeLa cells with nocodazole, obtaining a rich population of mitotic cells and, therefore, increasing the presence of pS558-TACC3 in the centrosomes (LeRoy et al., 2007). A different migration band corresponding to pS558-TACC3 was observed in Western blot results, as shown in **Figure 25**.

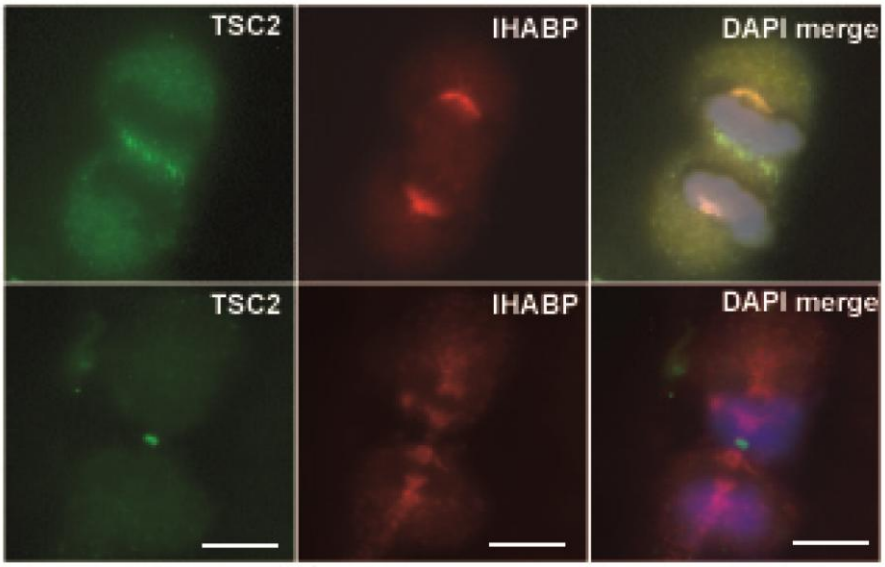

Figure 24: Subcellular localization of TSC2 during cell division

Immunofluorescence of HME/TERT showing TSC2 (tuberin, clone 3G9D9) staining at the midbody (upper panel) and the cleavage furrow (bottom panel). RHAMM staining with IHABP antibody was used as a control. RHAMM localizes at the mitotic spindle poles (upper panel) and at the remaining microtubule (bottom panel). Scale bars represent 10 µm.

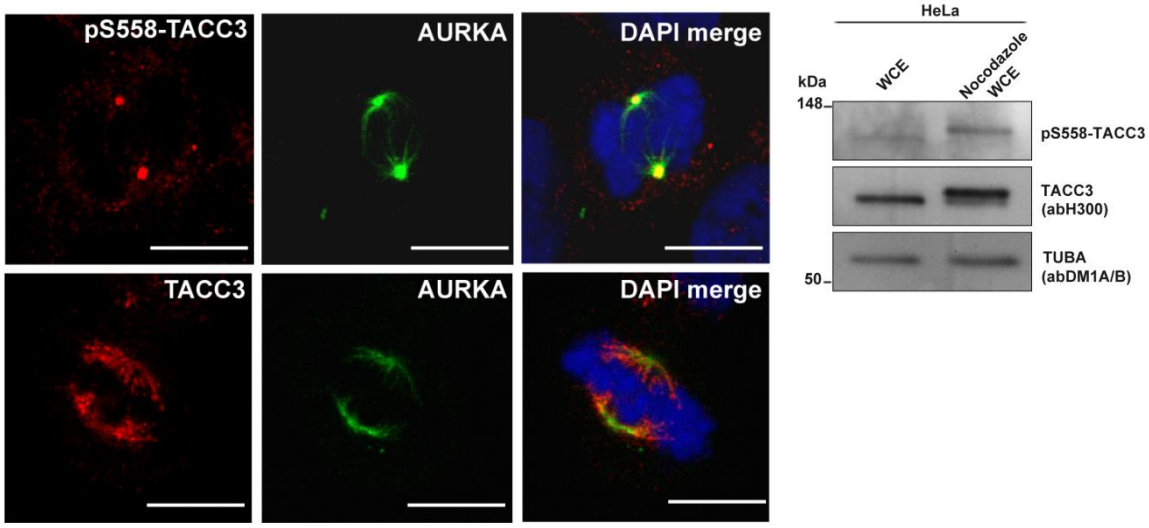

Figure 25: Subcellular localization of total- and pS558-TACC3 during cell division

Immunofluorescence of HeLa cells showing pS558-TACC3 staining at the spindle poles (upper panel) and total-TACC3 (H300) staining at the mitotic spindle (bottom panel). AURKA (IAK1 #610939) staining was used as a control. AURKA localizes at the mitotic spindle poles (upper panel) and at mitotic spindles (bottom panel). Scale bars represent 10 µm. Right panel shows Western blot of HeLa cells in normal conditions and HeLa cells treated with nocodazole, blotted against pS558-TACC3 (New England Peptide) and TUBA.

To corroborate these preliminary results, we next analyzed TACC3 and TSC2 (total and pS939) during cell division by confocal laser scanning microscopy in four cell lines (BT474, HeLa, MCF7 and MCF10A). In metaphase, TACC3 and total-TSC2 localized at the spindle MTs and poles, while pS939-TSC2 was specifically detected at the poles (**Figure 26A**). In telophase and cytokinesis, both total- and pS939-TSC2 were particularly strong at the cleavage furrow, while TACC3 localized in the pericentrosomal region and at the remaining polar spindle MTs in the midbody (**Figure 26B**).

*(The confocal laser scanning experiments corresponding to **Figure 26**, **Figure 28** and **Figure 29** were performed in collaboration with Stephan Schmidt from the Department of Biochemistry and Molecular Biology II at Heinrich-Heine University, Düsseldorf)*

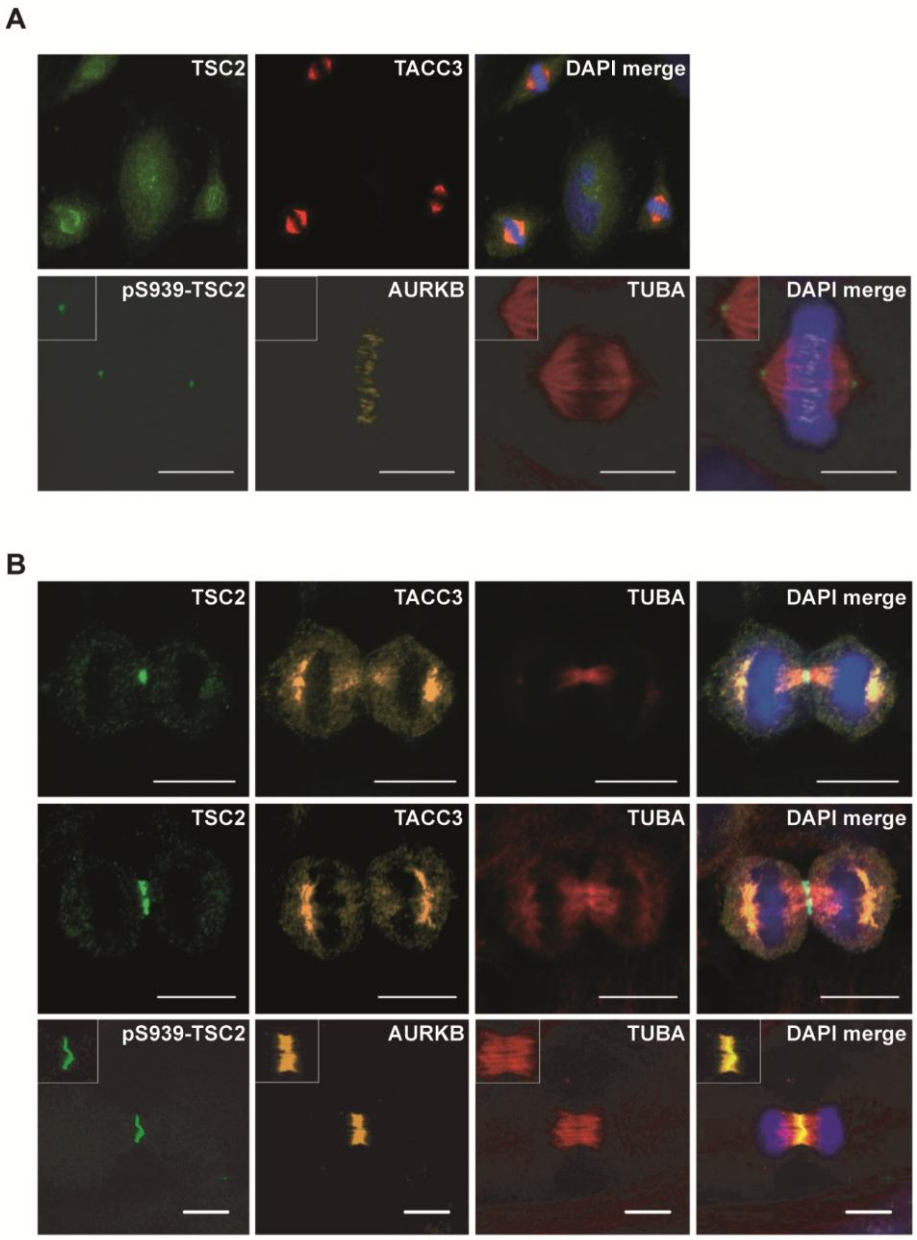

Figure 26: Subcellular localization of TACC3 and TSC2 during mitosis and cytokinesis

(**A**) Localization of TACC3 and TSC2 at mitotic spindle microtubules and poles, and of pS939-TSC2 at spindle poles. Representative fluorescence (top panels) or confocal laser scanning (bottom panels, scale bars 10µm) microscopy images are depicted. Nuclei were stained with DAPI and microtubules with an anti-TUBA antibody. (**B**) Localization of TACC3 in pericentrosomal areas and at the remaining spindle microtubules in the midbody during cytokinesis, and of TSC2 and pS939-TSC2 at the cleavage furrow. Control staining using ab against AURKB and TUBA is shown. Representative confocal laser scanning microscopy images are depicted. Scale bars represent 10 µm.

Given the observed interaction through TSC2-HBD (**Figure 18**), we hypothesized the existence of dynamic associations between TACC3, TSC1 and TSC2. To test this hypothesis, we synchronized HeLa cells by double thymidine block. Using PLK1 as a mitotic maker, we observed that TACC3-TSC2 complexes were mostly evident through mitosis (4-10 h after release), while TSC1-TSC2 complexes appeared more strongly in S-G_2/M (2 and 4 h after release) (**Figure 27**). Unfortunately, we were unable to obtain stronger interaction bands for TACC3 or TSC2 reciprocal co-IPs as shown in **Figure 27** (left panels). We believe that this could be due to a transient, and possibly dependent of biochemical modifications, interaction between the two proteins, which makes it difficult to obtain better evidence. However, taken together, these data are consistent with co-IP results in unsynchronized cell cultures (**Figure 17**) and suggest a role for TACC3-TSC2 in regulation of cell division.

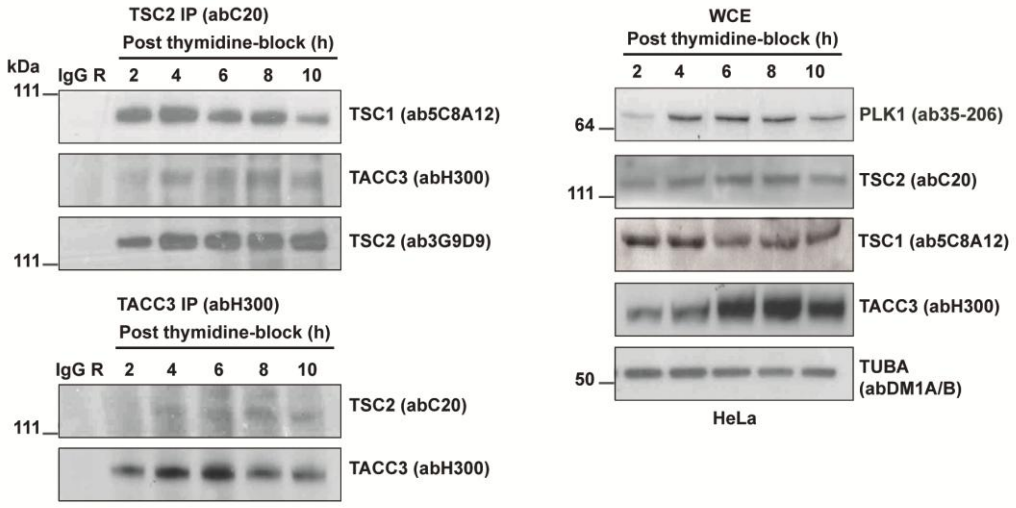

Figure 27: TACC3-TSC2 interaction through the cell cycle

Cell cycle synchronization and co-IP assay in HeLa cultures using a double thymidine block protocol. Results are shown for TSC2 and TACC3 co-IPs, including IgG controls, and for protein levels across the corresponding WCEs (PLK1 as mitotic marker). Time points (h) of post-thymidine block release are indicated.

Having established a dynamic association between TACC3 and TSC2, we next evaluated the dependence on TACC3 for TSC2 localization during cell division. A doxycycline (DOX)-regulated shRNA system allowing almost complete depletion of TACC3 in HeLa cells was used (Schneider et al., 2007b). Depletion of TACC3 in HeLa cells correlated with loss of reactivity of pS939-TSC2 at spindle poles and intercellular bridges during cytokinesis (**Figure 28**). Two phosphorylated forms of mTOR—pS2448- and pS2481-mTOR—have been described as localizing to mitotic and cytokinetic structures (Vazquez-Martin et al., 2009a; Yaba et al., 2008). In this context, the AMP-activated protein kinase (AMPK)—a key regulator of metabolism and proliferation that acts upstream of the TSC1-TSC2 complex—has also been shown to localize to several mitotic structures throughout all of the mitotic stages and cytokinesis (Vazquez-Martin et al., 2009c), and has been suggested as a putative novel tumor suppressor of the mitotic/cytokinetic phase of the cell cycle (Vazquez-Martin et al., 2009b).

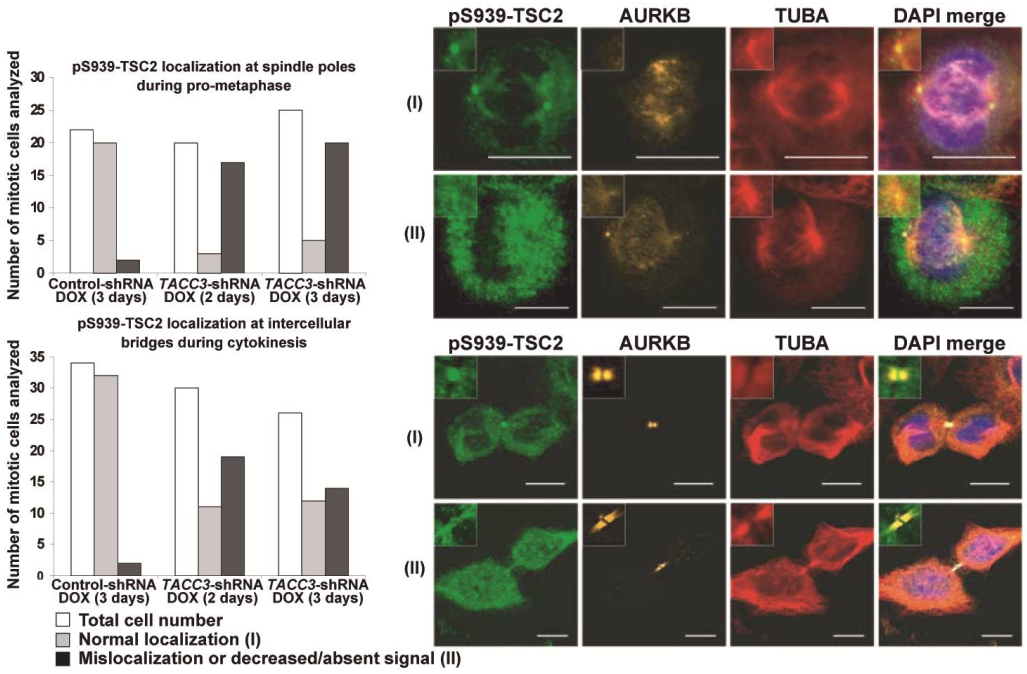

Figure 28: TACC3-dependent subcellular localization of pS939-TSC2 during cell division

Loss of pS939-TSC2 reactivity and/or localization in TACC3-depleted HeLa cells at days 2 and 3 of DOX-induced shRNA expression. Graphs show absolute numbers of cell counts as indicated and representative images of TACC3-depleted HeLa cells are shown in right panels. Upper panels represent analysis of pS939-TSC2 localization at spindle poles and lower panels represent analysis of pS939-TSC2 localization at the cytokinetic cleavage furrow. Scale bars represent 10 µm.

To determine whether other TSC2-related proteins were affected by TACC3 depletion, we performed the same experiment described above and examined TSC1 and pS2448-mTOR localization during cell division. However, in contrast to pS939-TSC2, we did not observe alterations of either TSC1 or pS2448**-**mTOR (**Figure 29**), which further supports a specific function of TSC2 in relation to TACC3 during cell division.

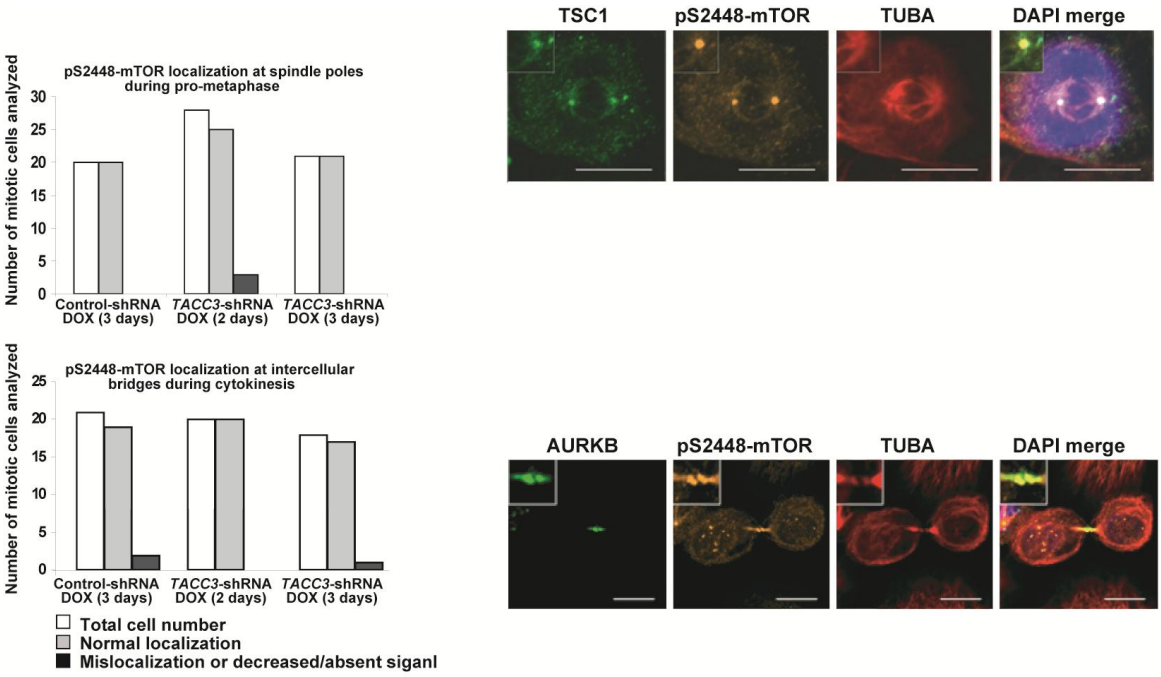

Figure 29: Localization of pS2448-mTOR during cell division is not affected in TACC3-depleted HeLa cells

Loss of pS2448-mTOR reactivity and/or localization in TACC3-depleted HeLa cells at days 2 and 3 of DOX-induced shRNA expression. Graphs show absolute numbers of cell counts as indicated and representative images of TACC3-depleted HeLa cells are shown in right panels. Top panels represent analysis of pS2448-mTOR localization at spindle poles and bottom panels represent analysis of pS2448-mTOR localization at the cytokinetic cleavage furrow. Scale bars represent 10 µm.

4 TACC3 or TSC2 deficiency results in cytokinetic delay and increased appearance of binucleated cells

Consistent with loss of pS939-TSC2 localization to cytokinetic structures in TACC3-depleted cells, abnormally elongated abscission was a common phenotype observed in unsynchronized Tacc3- and Tsc2-deficient MEFs detected by AURKB immunostaining (**Figure 30**). When abscission fails, cytokinesis remains incomplete, and the cleavage furrow regresses, thus leading to the formation of binucleated cells (reviewed in (Glotzer, 2005)). Consistently, higher percentages of binucleated cells were observed in Tacc3-deficient and Tsc2-deficient MEFs relative to wt counterparts (*Tacc3*$^{-/-}$ 8.5 ± 3.2%; *Tacc3*$^{+/-}$ 6.8 ± 3.1%; wt, immortalized MEFs 2.0 ± 1.0%; and, *Tsc2*$^{-/-}$/*Tp53*$^{-/-}$ 6.6 ± 2.1%; *Tsc2*$^{+/+}$/*Tp53*$^{-/-}$ 2.6 ± 1.5%; these percentages illustrate mean values of three replicates with > 500 cells counted each) (**Figure 31**). Disruption of the expression of various mitotic proteins (e.g. BRCA2 (Daniels et al., 2004), AURKB (Terada et al., 1998) or KIF23 (Zhu et al., 2005)) has consistently been shown to interrupt cytokinesis and increase binucleated cell formation. These results suggest a role for TACC3 and TSC2 in regulating cytokinesis and are consistent with previously reported tetraploidization Eker rat leiomyoma tumor cells (ELT3) with a germline *Tsc2* mutation (Gui et al., 2007).

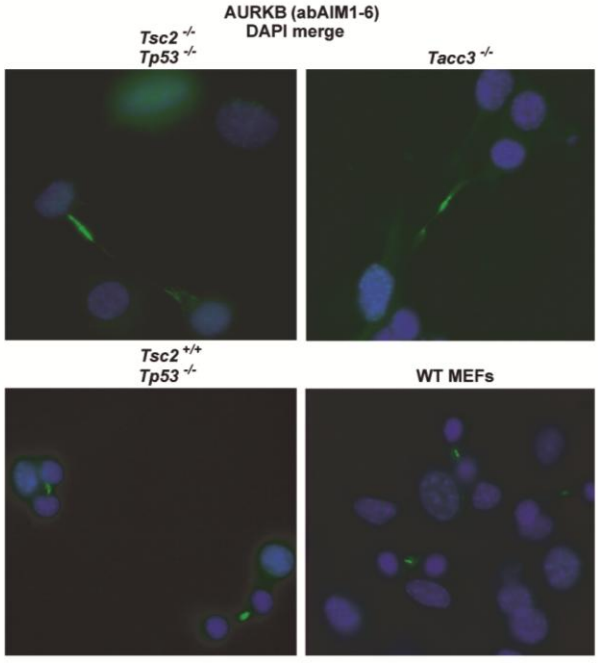

Figure 30: Tacc3- and Tsc2-deficient MEFs show abnormal cytokinesis compared to controls

Aberrant (elongated) abscission in Tsc2$^{-/-}$/Tp53$^{-/-}$ and Tacc3$^{-/-}$ cells compared to wt counterparts as indicated by immunofluorescence staining for the passenger protein AURKB.

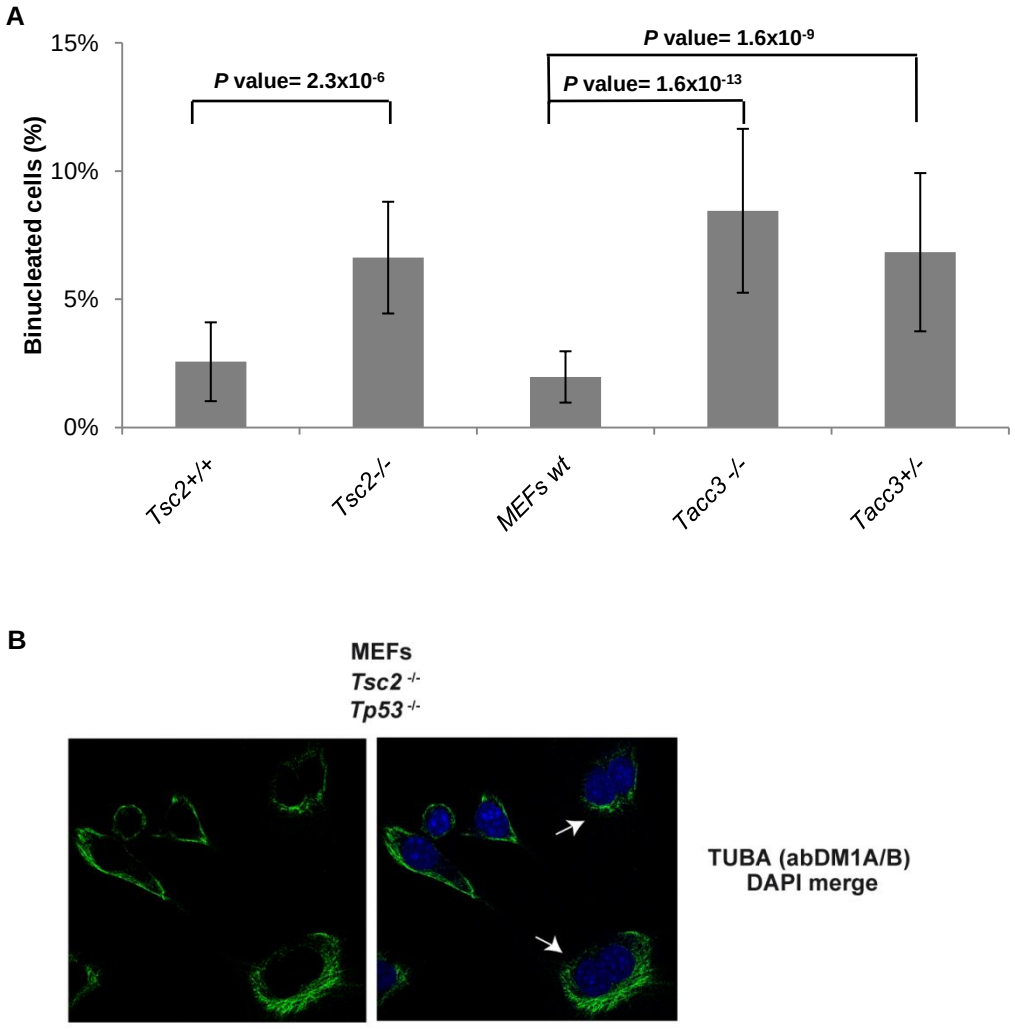

Figure 31: Tacc3-deficient and Tsc2-deficient MEFs present higher percentages of binucleated cells relative to wild-type counterparts

(**A**) Graph shows representation of binucleated cells (%) in MEF cultures of the *Tsc2*$^{-/-}$, *Tacc3*$^{-/-}$, *Tacc3*$^{+/-}$ genetic background relative to corresponding wild-type. MEFs were fixed and stained with anti-TUBA ab and DAPI, and the percentage of multiple nuclei was calculated by direct counting of > 500 cells from each cell line. The graph shows the mean and standard deviation (*P* values computed with chi-square test). (**B**) Panel shows binucleated *Tsc2*$^{-/-}$ MEFs (white arrows) detected by staining with TUBA and DAPI.

Next, ELT3 cells were used to evaluate the effects of Tsc2-defiency on cell division in synchronized cultures. We performed a cytokinesis assay in which cells were arrested with nocodazole for 8-12 h, released and analyzed at different time points. Tsc2-deficient ELT3 cells exhibited significant delay in completion of cytokinesis relative to human TSC2 (hTSC2)-reconstituted cells (**Figure 32** shows a typical experiment with total > 500 cells counted at each time-point; two-tailed *t*-test at 90 min *P* value = 0.005).

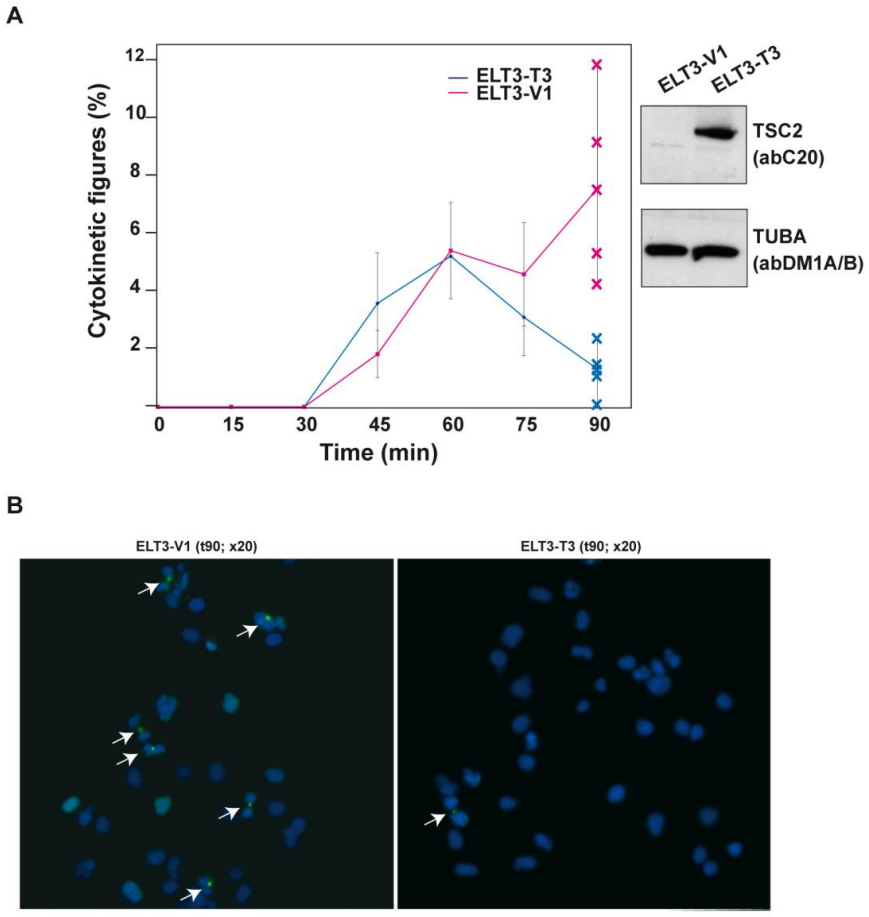

Figure 32: Tsc2-deficiency causes delay in cytokinesis progression

Figure shows evaluation of cytokinesis progression in ELT3-V1 (Tsc2-deficient, vector control) relative to ELT3-T3 (hTSC2-reconstituted) cells using nocodazole synchronization protocol. (**A**) Graphical representation of the percentages of cytokinetic figures in cells after nocodazole release over time (min). Results are shown for a typical experiment of three independent replicas. Curves include the mean and standard deviation calculated from five independent microscopy fields with counting each >100 cells at each time point. Percentages of cytokinetic cells at 90 min after nocodazole release are shown with colored crosses as indicated for each cell line. Right panel shows the confirmation of the TSC2/Tsc2 status of ELT3 cells before and after hTSC2 reconstitution. (**B**) Representative fluorescence microscopy images (x20) in ELT3-V1 relative to ELT3-T3 cells at 90 min with cytokinetic figures marked with arrows, using AURKB immunostaining.

In agreement with the delayed cytokinesis observed in Tsc2-deficient MEFs, slower completion of cytokinesis after nocodazole release was also observed in Tsc1-deficient compared to human TSC1 (hTSC1)-reconstituted MEFs (**Figure 33**) and, consistently, Tsc1-deficient cells also showed increased incidence of binucleation in unsynchronized cultures relative to wt cells (**Figure 34**). However, aberrant cytokinetic figures (i.e. elongated abscission) were not observed at an increased frequency in Tsc1-deficient cells (**Figure 34**), which suggests complementary but not fully redundant functions of TSC1 and TSC2 in cell division, with TACC3-mediated localization of pS939-TSC2 at cytokinetic structures.

*(The cytokinesis assay represented in **Figure 33** was performed in collaboration with Aristotelis Astrinidis from the Drexel University College of Medicine)*

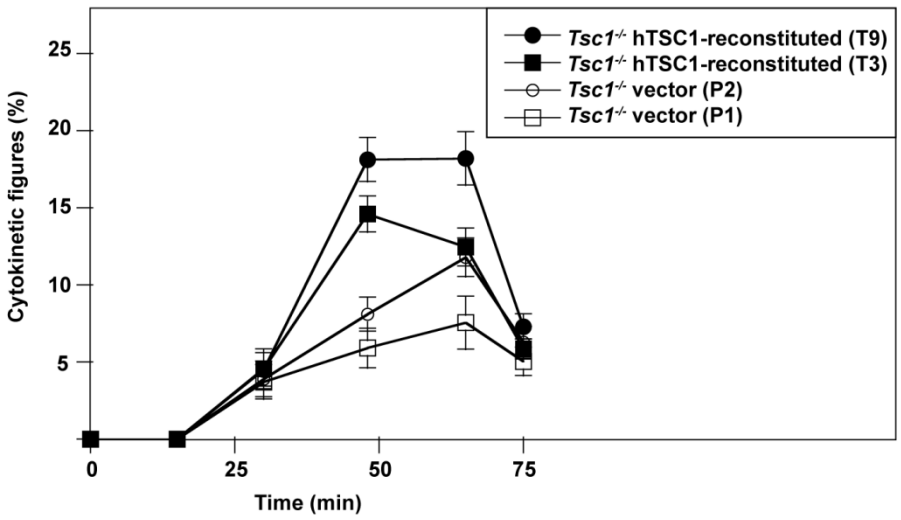

Figure 33: Tsc1-deficiency causes delay in cytokinesis progression

Graphical representation of cytokinetic figures (%) in MEF cultures of the *Tsc1*$^{-/-}$ genetic background reconstituted with hTSC1 (T3 and T9) or vector controls (P1 and P2), and synchronized with nocodazole. Mean and standard deviation are shown.

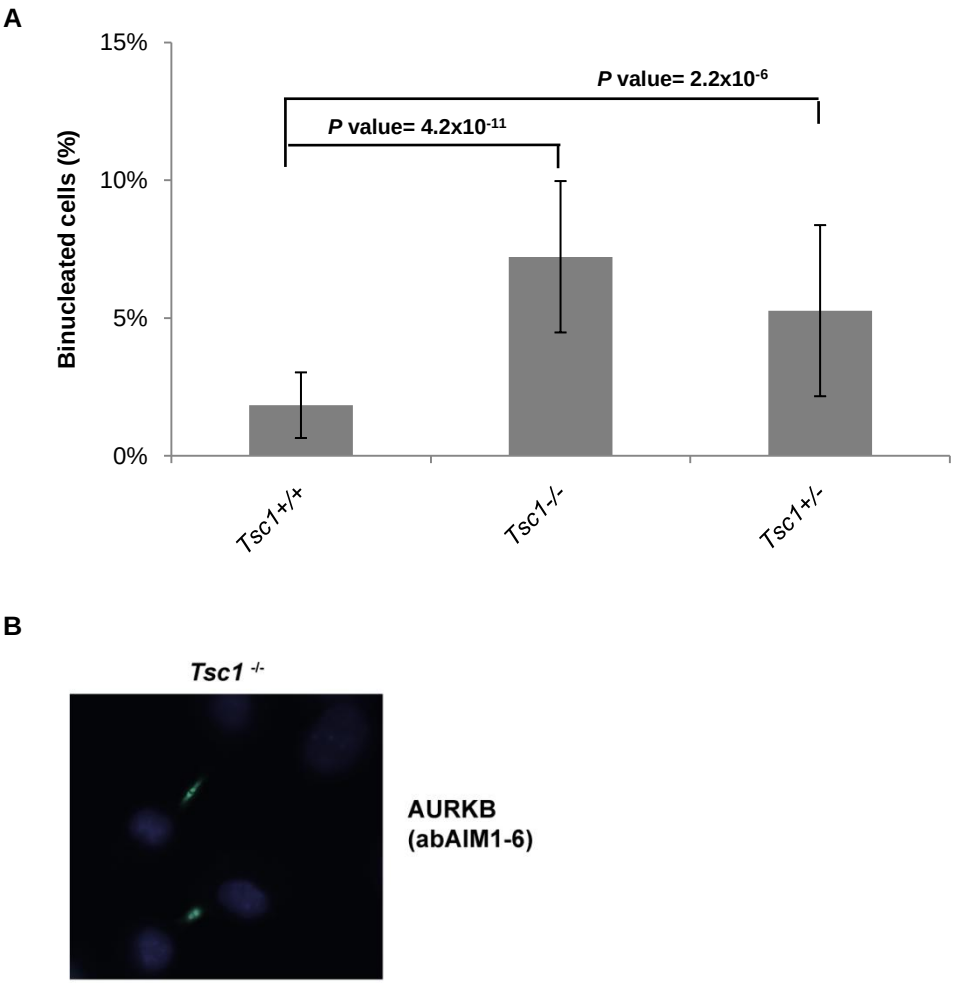

Figure 34: Tsc1-deficient MEFs present high percentage of binucleated cells but not aberrant cytokinesis

(**A**) Graph shows representation of binucleated cells (%) in MEF cultures of the *Tsc1*$^{-/-}$ genetic background relative to corresponding wt. MEFs were fixed and stained with anti-TUBA and DAPI, and the percentage of multiple nuclei was calculated by direct counting of > 500 cells from each cell line. The graph shows the mean and standard deviation (*P* values computed with chi-square test). (**B**) Panel shows normal abscission figures in Tsc1-deficient MEFs detected by AURKB immunostaining.

If TACC3-TSC2 interaction is biologically relevant *in vivo*, the cytokinetic abnormalities observed in ELT3 cell cultures should correlate with detectable alterations of gene expression in epithelial tissues of Eker rats compared to controls. To test this hypothesis, we evaluated association of cell cycle-related gene sets (i.e. sets for G_1/S, S, G_2, G_2/M and M/G_1 phases (Whitfield et al., 2002)) in a genome-wide expression dataset of Eker rat kidneys and controls (Stemmer et al., 2007) using the non-parametric approach in the Gene Set Enrichment Analysis (GSEA) tool (Subramanian et al., 2005). The GSEA is a computational method that determines whether an a priori defined set of genes shows statistically significant, concordant differences between two biological states. This analysis revealed that Eker rat kidneys had higher expression of genes involved in cytokinesis and mitotic exit (M/G_1 set, *P* value = 0.04, **Figure 35**) than normal rat kindeys; however, other cell cycle-related gene sets showed no difference (*P* value > 0.20). This observation further supports the critical role of TSC2/Tsc2 in cytokinesis and suggests relevant consequences in pathology.

*(The analysis represented in **Figure 35** was performed by Núria Bonifaci, a member of our research group)*

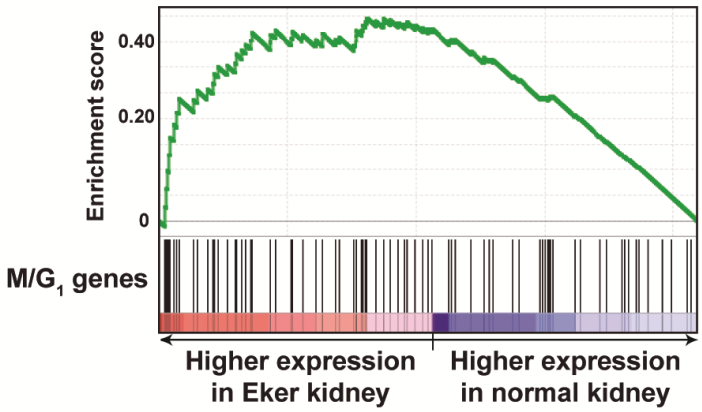

Figure 35: Association of M/G1 genes with Eker status

The GSEA output is shown including enrichment score and M/G1 gene (i.e. genes with periodic expression and a peak at M/G1 (Whitfield et al., 2002)) positions in the whole-genome ordered gene list according to the signal-to-noise expression ratio between Eker and normal kidneys.

5 *TSC2* acts epistatically to *TACC3* in the control of cell viability

To decipher the underlying TACC3-TSC2 relationship in control of cell division, we examined the existence of genetic interactions. We use the term "genetic interaction" to define a phenomenon where the effect of one gene is modified by another gene. Then, the gene whose phenotype is expressed is said to be "epistatic". For this purpose, lentiviral shRNA constructs were transduced into MCF7 cells, and the effects of single gene depletions were compared to those of simultaneous depletion of TACC3 and TSC2 in a cell viability assay (time course of viable cells measured using a methylthiazol tetrazolium (MTT) assay). Depletion of TSC2 significantly increased viability relative to the pLKO.1 control, whereas loss of TACC3 had the opposite effect (**Figure 36A**, the graph shows the typical results of three independent experiments in MCF7 cultures; ANCOVA Bonferroni-corrected *P* values < 0.005). Interestingly, simultaneous depletion of TSC2 and TACC3 rescued the reduced viability observed in the TACC3-depleted cells to a level similar to that observed in the presence of TSC2 depletion only (Bonferroni-corrected $P = 0.09$). Taken together, these data suggest that *TSC2* acts epistatically to *TACC3* in regulation of cell viability.

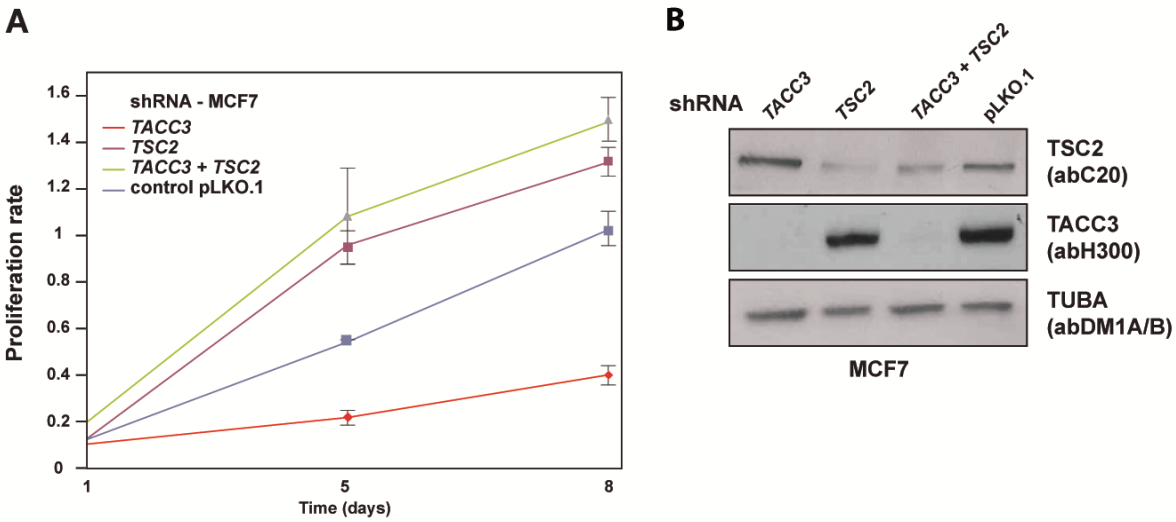

Figure 36: *TACC3-TSC2* epistatic relationship

(**A**) Results of a typical cell proliferation assay in MCF7 cells depleted of TACC3, TSC2, or TACC3 and TSC2 simultaneously, or transduced with a pLKO.1-based scrambled control construct. The graph shows the relative proliferation rate (number of viable cells measured using MTT conversion) over one, five and eight days after transduction with the corresponding lentiviral construct(s). (**B**) Western blot results showing depleted proteins in WCEs.

Sensing the integrity of the MT network and the nuclear envelope structure contributes to an early mitotic checkpoint mediated by CHFR (Scolnick and Halazonetis, 2000; Summers et al., 2005), which is a regulator of AURKA (Yu et al., 2005). As an E3 ubiquitin ligase, CHFR targets AURKA for ubiquitination and degradation, thus ensuring proper mitotic progression (Yu et al., 2005). In keeping with the putative role of TACC3 and TSC2 in MT dynamics and nuclear envelope structure (**Figures 20-23**), levels of CHFR and cyclin B1 (CCNB1) were higher in MCF7 cells after shRNA-mediated depletion of either TSC2 or TACC3 (**Figure 37**). Accumulation of CCNB1 is consistent with previous observations of cell cycle-dependent regulation and depletion studies of TACC3 expression (Jeng et al., 2009; Schneider et al., 2007b; Yao et al., 2007). However, simultaneous depletion of TSC2 and TACC3 did not cause an accumulation of CHFR or CCNB1 (**Figure 37**), which is consistent with an epistatic relationship (**Figure 36**). Accumulation of CHFR/CCNB1 and activation of the early mitotic checkpoint in TSC2-depleted cells may be compatible with increased proliferation due to the concomitant increase in mTOR signaling and translation. Whereas TSC2 depletion resulted in an increase in phosphorylation of ribosomal protein S6 kinase (pT389-S6K), as expected, TACC3-depleted cells showed lower levels of this marker (Fig. 5B). Consistent with an epistatic relationship, simultaneous depletion of both proteins resulted in increased pT389-S6K (**Figure 37**).

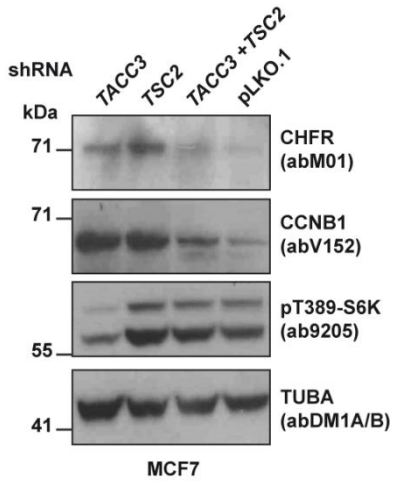

Figure 37: *TACC3-TSC2* convergence to the early mitotic checkpoint mediated by CHFR

Analysis of early mitosis checkpoint activation by accumulation of CHFR and CCNB1 in MCF7 cultures depleted of TACC3 or TSC2 versus TACC3 and TSC2 simultaneously, or pLKO.1 control transduced cells. Evaluation of the pT389-S6K (p70/p85) in these conditions is shown.

To determine whether aberrant mTOR signaling in Tsc2-deficient cells leads to perturbation of Tacc3 expression, protein levels were assayed in rapamycin-treated Tsc2-deficient MEFs and ELT3 cells and compared to DMSO-treated controls. These assays revealed that inhibition of mTOR signaling significantly increases Tacc3 levels (**Figure 38**). Together, these observations support the convergence of *TACC3*/TACC3 and *TSC2*/TSC2 in nuclear envelope structure integrity and cell division control through genetic and molecular interactions.

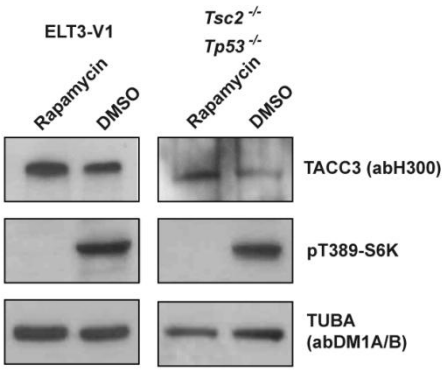

Figure 38: mTOR/TSC mediated regulation

Figure shows the effect of rapamycin treatment on Tacc3 levels in Tsc2-deficient cell lines. Tsc2-deficient ELT3 leiomyoma extracts (ELT3-V1, left panels) and $Tsc2^{-/-}Tp53^{-/-}$ MEF extracts (right panels) are shown. Blotting against pT389-S6K is used as a control of mTOR signaling and TUBA as a loading control.

6 Depletion of TACC3 or TSC2 results in abnormal cellular organization and loss of cell polarity

Given the observed involvement of TACC3 and TSC2 in cell division and proliferation, and the epistatic interaction between the two proteins, our next aim was to determine the role of this relationship in regulating tissue architecture, which is commonly disrupted in TSC patients (reviewed in (Napolioni and Curatolo, 2008)). We first performed single depletions of TACC3, TSC2 and TSC1 using lentiviral shRNA preparations and measured growth dynamics during apicobasal differentiation, which can be modeled by culture of MCF10A cells in reconstituted basement membrane (rBM) (Debnath et al., 2003). Depletion of either TACC3 or TSC2 resulted in phenotypically abnormal cell clusters under bright-field examination, whereas after TSC1 depletion we did not observe substantial phenotypical abnormalities (**Figure 39A**). Shape and size were analyzed, and we observed that clusters were, on average, significantly larger than controls, while no major changes in shape were seen (**Figure 39B**).

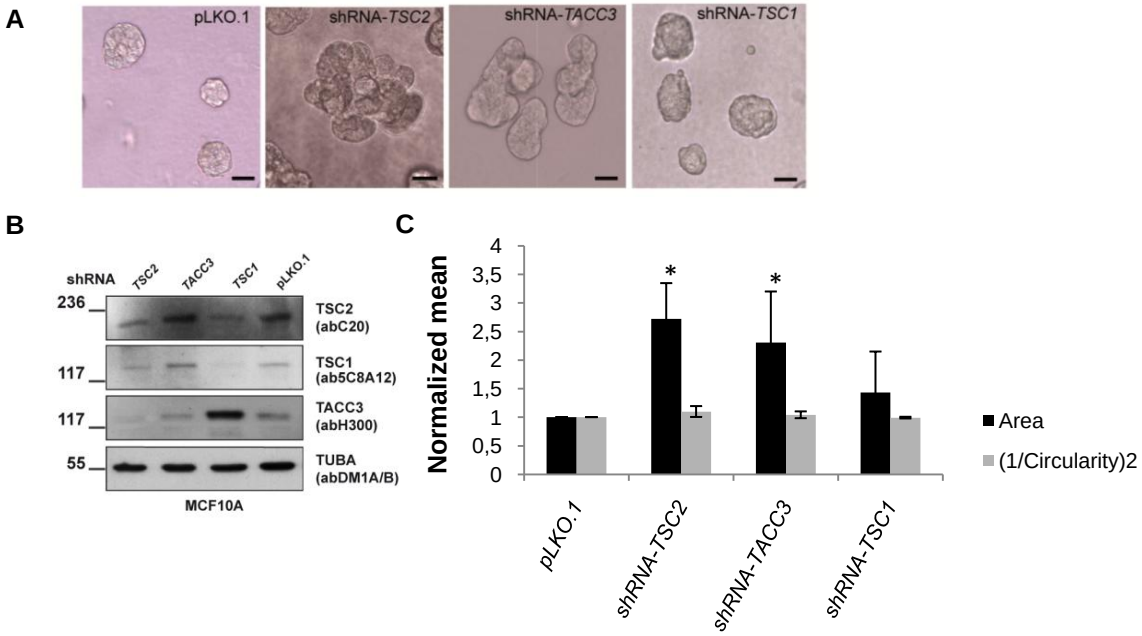

Figure 39: Depletion of TACC3 and TSC2, but not TSC1, impair apicobasal polarization

(**A**) Figure shows representative bright-field images from control vector pLKO.1, shRNA-*TSC2*, shRNA-*TACC3* and shRNA-*TSC1* transduced cultures eight days after seeding. Magnification is equivalent for all images and scale bars represent 20 µm. (**B**) Western blot results showing depleted proteins in WCEs. (**C**) Architecture of acini-like spheroids (hereafter termed acini) was quantified from bright-field images of cultures treated as described above. For comparison between experiments, all values were normalized to untreated cultures within experiments and differences assessed statistically relative to pLKO.1. Graph shows means and standard errors from four independent experiments. Asterisks indicate significant differences (two-sided *t*-test $P < 0.05$) from controls.

Examination of cytoskeletal elements by confocal scanning at day 12 revealed aberrant structural organization of TACC3- and TSC2-, but not TSC1-depleted acinar structures. We used ZO-1 and α6-integrin as markers of apical and basal polarity, respectively (Fogg et al., 2005; Koukoulis et al., 1991; Plachot and Lelievre, 2004). As shown in **Figure 40**, transduced clusters showed no expression of ZO-1 and presented an abnormal distribution of α6-integrin, futher suggesting a role for TACC3 and TSC2 in apicobasal polarity.

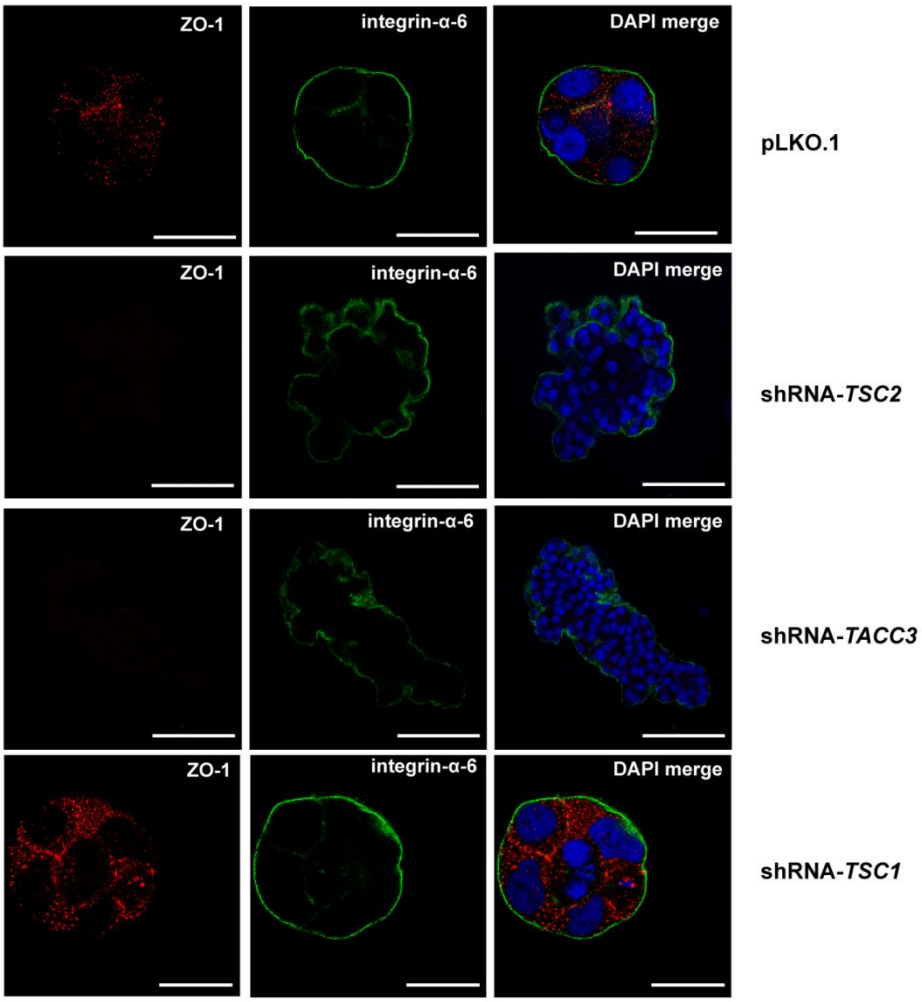

Figure 40: Depletion of TACC3 and TSC2, but not TSC1, affects apicobasal polarity

Figure shows confocal laser scanning analysis of the apical marker ZO-1 and the basal marker α6-integrin in TACC3, TSC1 and TSC2-depleted cultures fixed at day 12. Scale bars represent 20 µm.

Having established the effects of single depletions, we investigated the phenotype under simultaneous depletion of TACC3 and TSC2, and TACC3 and TSC1 (**Figure 41**). Surprisingly, as shown in the Western blot illustrated in **Figure 41B**, even though shRNA-*TACC3* lentiviral particles were known to be efficient, we observed that simultaneous depletion together with either TSC2 or TSC1 increased TACC3 expression to levels similar to that observed in the controls. This effect was also observed after single TSC1 depletion (**Figure 39B**). Thus, in MCF10A cells TACC3 expression may be regulated by the TSC/mTOR pathway, but this hypothesis warrants further investigations.

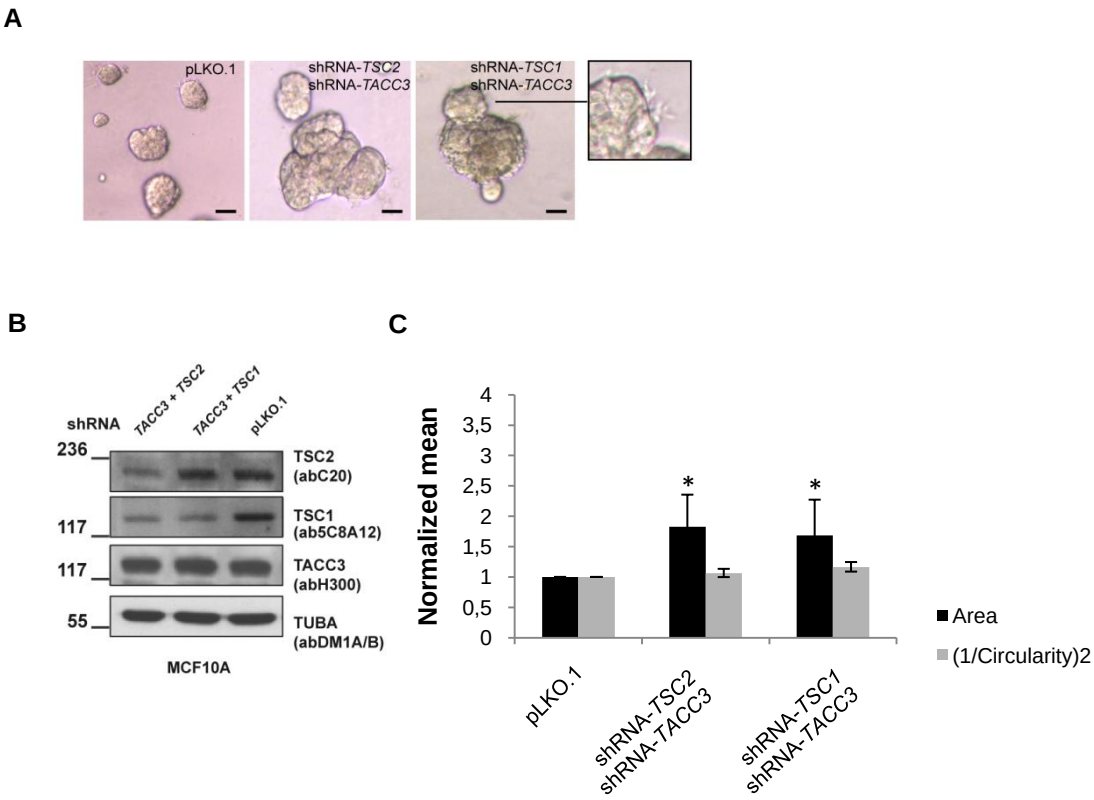

Figure 41: Simultaneous depletion of TACC3/TSC2 and TACC3/TSC1 impairs apicobasal polarization

(**A**) Figure shows representative bright-field images from control vector pLKO.1, shRNA-*TACC3*/shRNA-*TSC2* and shRNA-*TACC3*/shRNA-*TSC1* transduced cultures eight days after seeding. Magnification is equivalent for all images and scale bars represent 20 µm. (**B**) Western blot analysis of depleted proteins in WCEs. (**C**) Architecture of acini-like spheroids (hereafter termed acini) was quantified from bright-field images of cultures treated as described above. For comparison between experiments, all values were normalized to untreated cultures within experiments and differences assessed statistically relative to pLKO.1. Graph shows means and standard errors from two independent experiments. Asterisks indicate significant differences (two-sided *t*-test $P < 0.05$) from controls.

In contrast to viability in MCF7 cells (**Figure 36**), no epistatic or other type of interaction was observed in this study between TSC1/2 and TACC3. Notably, simultaneous depletion of TACC3 and TSC2 did not rescue differentiation. In fact, equivalent acini alterations were observed for single and double TACC3/TSC2 depletions. Importantly, simultaneous depletion of TACC3 and TSC1 resulted in a more severe phenotype than that observed in single TSC1 depletion. Shape and size were analyzed and we observed that clusters were, on average, larger than controls, although not to the same degree as after single depletions (**Figure 41B**). In this case, no major changes in shape were seen, but we observed irregular morphology of the basolateral acinar domain, suggesting some perturbation of this structure. Confocal scanning analysis of double-depleted structures using ZO-1 and α6-integrin as markers of apical and basal polarity, respectively, was consistent with previous observations in single depletions (**Figure 42**).

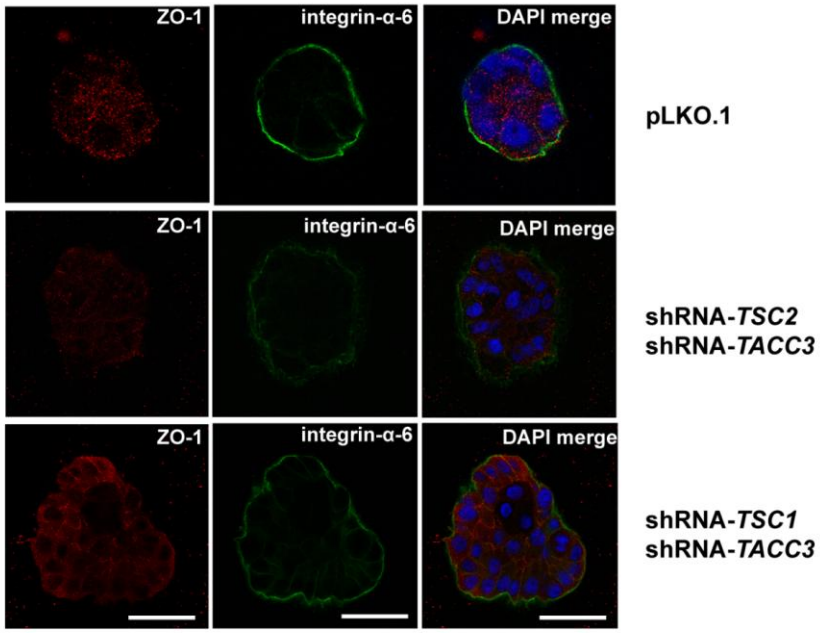

Figure 42: Simultaneous depletion of TACC3/TSC2 and TACC3/TSC1 affects apicobasal polarity

Figure shows confocal laser scanning analysis of the apical marker ZO-1 and the basal marker α6-integrin in TACC3/TSC2 and TACC3/TSC1-depleted cultures fixed at day 12. Scale bars represent 20 μm.

Interestingly, simultaneous depletion of TACC3 and TSC2 showed more severe disruption of the basolateral domain revealed by α6-integrin staining. This observation was consistent with the presence of abnormal projections at the basolateral domain identified in brightfield images (**Figure 41A**). Together, these results reveal new roles for the TACC3-TSC module in epithelial apicobasal differentiation, suggesting a possible involvement in tissue architecture and, therefore, pathology.

DISCUSSION

Discussion

The TACC family of proteins is characterized by an evolutionarily conserved coiled-coil domain (Gergely et al., 2000a). All TACCs have been localized to the centrosome at varying times throughout the cell cycle and, when perturbed lead to centrosome abnormalities and dysfunction (Gergely, 2002; Gergely et al., 2000a). In mammals, three members of the TACC family have been identified, TACC1, TACC2 and TACC3, showing expression alteration in many cancer types (Still et al., 1999a; Still et al., 1999b). Several studies involving TACC3 in centrosome biology and MT stabilization had been published at the time this project was begun (Kinoshita et al., 2005; Peset et al., 2005; Piekorz et al., 2002; Raff, 2002; Still et al., 2004; Still et al., 1999b). To gain insight into the role of TACCs in centrosome biology and, ultimately, human pathology, we screened for protein physical interactions of TACC3 using the TACC domain as bait.

The TACC3-centered interactome reveals physical interactions that are consistent with known molecular and functional associations of TACCs across species (Peset and Vernos, 2008) (**Figure 12**). Two known conserved interactions have been identified in this study: with ch-TOG/CKAP5 and with FAM161B. The MT-binding protein ch-TOG/CKAP5 has been found to interact with TACC ortholog in *S. pombe* (alp7), *C. elegans* (TAC-1), *D. melanogaster* (D-TACC) and *X. laevis* (tacc3) (Peset and Vernos, 2008). Ch-TOG/CKAP5 is essential for MT stability (Kinoshita et al., 2002), and previous studies report that TACC proteins are required for proper recruitment of ch-TOG/CKAP5 to the centrosome (Bellanger and Gonczy, 2003; Cullen and Ohkura, 2001; Kinoshita et al., 2005; Le Bot et al., 2003; Lee et al., 2001; Sato et al., 2004; Srayko et al., 2003). The interaction with the predicted protein FAM161B is conserved in *C. elegans* (Li et al., 2004). In addition, our screening shows a new physical interactor of TACC3: KIF1C, a plus-end MT motor that promotes podosome dynamics (Kopp et al., 2006) and has a homolog (KLP-1) that interacts with TAC-1. These findings not only support the fidelity of the TACC3-interactome but also suggest the identification of a functional module conserved across species. Phylogenetic analysis performed in this study indicates that human *TACC* genes are the product of two consecutive genomic duplications that occur after the divergence of vertebrates and uro-chordates (**Figure 13-14**). Our results support the idea that *TACC1* and *2* evolve from the most recent duplications and are more evolutionarily related to each other than to *TACC3*. Thus, we hypothesize that this evolutionary condition of *TACC3* and possible technical limitations of the technology used are the main reasons why no additional interologs were detected in our screening.

Some of the interactions described in this work also provide novel mechanistic hypotheses on the role of TACCs in MT-network organization and centrosome or basal body biology. Consistent with the centrosomal localization of TACC3, we have identified an interaction with TUBGCP6, which is a member of the γ-TURC required for MT nucleation at the centrosome (Murphy et al., 2001). A second centrosomal protein found in our interactome is the putative tumor suppressor LZTS2 (also named LAPSER1). The *LZTS2* gene was previously mapped to a region with frequent loss of heterozygosity (LOH) in patients with epithelial cancer types (Cabeza-Arvelaiz et al., 2001). Moreover, recent studies demonstrate the involvement of LZTS2 in cytokinesis by co-localizing and interacting with the essential mitotic regulators in the centrosome and midbody (Sudo and Maru, 2007). TACC1 and TACC2 have also been identified in our screening as interacting partners of TACC3. Notably, TACC1 has been found to form a complex with the major regulator of cytokinesis AURKB (Delaval et al., 2004), which further supports the predicted roles of TACC3 in centrosomal biology and suggests novel functions in cell division.

Three relevant interactors found in our Y2H screen and corroborated by co-IP assays are ARHGEF2 (also known as GEF-H1/Lfc), CGN and TSC2 (**Figures 15-17**). Since TACCs are deregulated in many epithelial neoplasias (Still et al., 1999a; Still et al., 1999b), TACC3 may be involved in cell migration and differentiation through its interaction with ARHGEF2 and CGN. ARHGEF2 is a guanine nucleotide exchange factor for RHOA and CGN is a cell-to-cell tight junction adaptor (Citi et al., 1988; Ren et al., 1998). The RHO family of small GTPases—RHOA, RAC1 and CDC42—are key regulators of actin cytoskeletal remodeling, cell adhesion, and migration (Etienne-Manneville and Hall, 2002; Ridley, 2001). Thus, reciprocal activation of RHOA, RAC and CDC42 is critical for the regulation of these processes, and deregulation of this balance may promote cell transformation and metastasis (Sahai and Marshall, 2002). In this context, CGN binding to ARHGEF2 inhibits RHOA activation, promoting polarized epithelial formation (Aijaz et al., 2005). The specific role of TACCs in this process is unknown but TSC1-TSC2 complex has been shown to regulate RHO GTPases (Astrinidis et al., 2002; Goncharova et al., 2004; Lamb et al., 2000). This function of TSC proteins may explain the metastatic phenotype of benign smooth muscle-like cells in LAM caused by *TSC1* and *TSC2* mutations (Hohman et al., 2008). Binding of TSC2 to TSC1 causes activation of RAC1 and, consequently, inhibition of RHOA activity, leading to stress fiber disassembly and focal adhesion remodeling (Goncharova et al., 2004). Intriguingly, TSC2 binds to TSC1 through TSC2-HBD (Hodges et al., 2001; van Slegtenhorst et al., 1998), and this domain seems to be both necessary and sufficient for TSC2 regulation of the

actin cytoskeleton and focal adhesion (Goncharova et al., 2004). Since TACC3 might interact with TSC2 through the TSC2-HBD domain (as shown in **Figure 18**) it could have a role in promoting cytoskeletal remodeling and the metastatic LAM phenotype. Alternatively, RHOA and the actin cytoskeleton can potentially be regulated by the TACC3-TSC2-mTORC2 axis (Jacinto et al., 2004; Sarbassov et al., 2004). Indeed, mTORC2 positively regulates the actin cytoskeleton through RHO GTPases signaling (Jacinto et al., 2004). Similar regulation may also occur during cell division. Once ARHGEF2 has been released from its phospho-dependent inhibition by AURKA, it activates RHOA to promote cytokinesis (Birkenfeld et al., 2007). ARHGEF2 and TSC2 may then compete for TACC3 binding in a similar manner to the transition from epithelial proliferation to differentiation. The role of TACC3 in these processes may be common or converge on other TACCs, as our data suggest heterodimer formations. In further support of the potential associations of TSC/mTOR pathway components with centrosome biology, a recent integration of physical interactions has revealed associations between the glycogen synthase kinase 3 beta (GSK3B), AMPK, KIF1C and LZTS2 (Pilot-Storck et al., 2010). Intriguingly, GSK3B co-immunoprecipitates and phosphorylates TSC1 and TSC2 and, probably, plays a role in regulation of cell growth and proliferation through the mTOR pathway (Inoki et al., 2006; Mak et al., 2005; Mak et al., 2003).

With regard to the process mediating epithelial polarity, the TACC3 interactome may also provide additional hypotheses on the development of renal cysts in TSC patients. Renal cysts appear more frequently in patients with *TSC2* mutations (Dabora et al., 2001; Sancak et al., 2005), probably caused by large deletions involving the adjacent gene *PKD1* (Sampson et al., 1997). Tsc1- and Tsc2-deficent MEFs show enhanced primary cilium development, and the corresponding genes interact with *Pkd1* in this process (Bonnet et al., 2009; Hartman et al., 2009). As corroborated by co-AP and co-IP assays, the physical interaction of TACC3 with key players in primary cilium development, where CEP164 is a promoter (Graser et al., 2007) and CP110 a suppressor (Spektor et al., 2007; Tsang et al., 2008), suggests that TSC2 function in this process can be mediated through regulation of these interactions. Similarly to processes of epithelial polarity and mitotic exit, inactivation of AURKA, the master regulator of TACCs, is necessary for cilium formation (Pugacheva et al., 2007), which in turn might be coordinated with regulation of the novel TACC3 interactions with TSC2 and CEP164/CP110.

This study also reveals a novel role of TSC2 in the maintenance of the nuclear envelope structure. Consistent with the findings of previous reports showing purification of TSC2 with nuclear fraction (Rosner et al., 2007; York et al., 2006), we illustrate through immunofluorescence, co-immunoprecipitation and cellular fractionation that TSC2/Tsc2 localizes to the nuclear envelope in interphase cells (**Figures 20-22**). Moreover, TACC3/Tacc3 also localizes to the nuclear envelope in unsynchronized cultures (**Figure 21**). Thus, both Tacc3 and Tsc2 co-purify with the major structural component of the inner nuclear membrane, Lmna (**Figure 22**). In agreement with these observations, Tsc2 and Tacc3 but not Tsc1 deficiency results in morphological alterations of the nuclear envelope detected by Nup62 immunostaining, suggesting a combined role for TACC3 and TSC2 in maintaining proper nuclear envelope structure (**Figure 23**). These observations suggest a specific role for TSC2 relative to TSC1. Individuals with a *TSC1* mutation present less severe phenotypes than those with a *TSC2* mutation in multiple clinical features that relate to brain (e.g. seizures, mental retardation, number of tubers), kidney (e.g. renal angiomyolipomas and cists), dermatologic (e.g. facial agiofibromas), and retinal (e.g. retinal hamartomas) involvement of TSC (Dabora et al., 2001; Jones et al., 1999; Sancak et al., 2005). At least two hypotheses may explain these observations: first, second-hit events (Knudson, 1971) may occur more often in *TSC2* than in *TSC1*; second, loss of specific functions of TSC1 or TSC2 such as deregulation of nuclear envelope structure may have different effects in cells (Dabora et al., 2001). Mutations in genes encoding nuclear envelope proteins cause a wide variety of diseases termed "nuclear envelopathies" or "laminopathies", which are commonly associated with muscle-related anomalies and, in some cases, accompanied by neurological abnormalities (Dauer and Worman, 2009; Elcock and Bridger, 2008). In this context, besides the known disease caused by mutations in *LMNA* (Worman et al., 2009), new studies have identified novel functions of nuclear pore proteins (nucleoporins), including roles in cell division, transcriptional regulation, and signaling, providing new insights into disease (Chakraborty et al., 2008; Hetzer and Wente, 2009; Lupu et al., 2008). In particular, a recessively inherited missense mutation in the nucleoporin gene *NUP62* leads to infantile bilateral striatal necrosis, a neurological disorder caused by progressive damage to a part of the brain called the striatum (Basel-Vanagaite et al., 2006). However, although no clear overlap has been reported between clinical manifestations in "nuclear envelopathies" and TSC, abnormal neuronal migration may be a common link. In this scenario, TACCs are critical in interkinetic nuclear migration in neuronal progenitors: concomitant to altered MT organization, perturbation of TACCs affects nuclear position and mode of division (Xie et al., 2007). Neuronal defects in TSC

patients have been considered to be caused by disorders of cell migration (Crino and Henske, 1999; Gomez, 1999; Vinters et al., 1999) and, in fact, cells lacking TSC1 or TSC2 have an altered capacity for motility and migration (Crino et al., 2006). Together with the involvement of TSC1-TSC2 complex in regulation of the actin cytoskeleton described above, our findings revealing a possible coordinated role of TACC3 and TSC2 in maintaining nuclear envelope structure may give novel insights into the neuronal migration defect in TSC disease.

Subcellular localization analyses performed in this work suggest a role for TACC3-TSC2 in regulation of cell division (**Figure 26**). In metaphase, both TACC3 and total-TSC2 localize to the spindle MTs and poles, whereas pS939-TSC2 specifically localizes to the poles. In telophase and cytokinesis, total- and pS939-TSC2 concentrate at the cleavage furrow, with TACC3 more concentrated in the pericentrosomal region and at the remaining polar spindle MTs in the midbody. Notably, depletion of TACC3 results in loss of pS939-TSC2, but this depletion does not affect pS2448-mTOR localization to mitotic and cytokinetic structures, which suggests a specific function for TSC2 relative to TACC3 (**Figures 28-29**). Consistent with pS939-TSC2 mislocalization in cytokinetic structures after TACC3 depletion, Tsc2 deficiency results in abnormally elongated abscission, cytokinetic delay and elevated proportions of binucleated cells (**Figures 30-32**). In agreement, studies in angiofibroma stroma cells from TSC patients report increased cytokinetic figures associated with binucleated cells (Toyoshima et al., 1999). Abnormally elongated abscission and binucleated cells are also observed in Tacc3-deficient MEFs, sustaining the hypothesis that TACC3 and TSC2 work together in the regulation of cell division and, in particular, cytokinesis. Surprisingly, Tsc1-deficient MEFs present a slower completion of cytokinesis and an increased incidence of binucleated cells, but not elongated abscission, suggesting that TSC1 may play a non-redundant role in cell division (**Figures 33-34**). Given these observations, we propose that localization of pS939-TSC2 mediated by TACC3 may be necessary for proper completion of cytokinesis.

Since TACC3 and TSC2 seem to play a coordinated role in cell division, they may also be involved in cell proliferation. In this context, previous studies report that TACC3 depletion induces postmitotic arrest (Schneider et al., 2008). In contrast, it is well known that the TSC1-TSC2 complex regulates the mTOR pathway and, consequently, depletion of TSC2 results in enhanced activation of mTOR and its downstream targets leading to cell proliferation (El-Hashemite et al., 2003; Goncharova et al., 2002). Accordingly, our study shows that shRNA-mediated depletion of TACC3 decreases viability of MCF7 cells compared to controls, whereas loss of TSC2 has the opposite effect (**Figure 36**). Intriguingly,

simultaneous depletion of TACC3 and TSC2 rescues the reduced viability observed in single depletion of TACC3 to a level comparable to that observed in TSC2-depletion. Given these observations, we suggest the existence of a genetic interaction between *TACC3* and *TSC2*, where *TSC2* acts epistatically to *TACC3*. Moreover, depletion of either TACC3 or TSC2 leads to increased levels of CHFR and the mitotic regulator CCNB1 (**Figure 37**). CHFR senses the structure of the nuclear envelope and probably that of the MT network (Scolnick and Halazonetis, 2000; Summers et al., 2005). When cells are exposed to mitotic stress, CHFR leads to a delay in chromosome condensation and, therefore, impairs progression to metaphase (Scolnick and Halazonetis, 2000). However, CHFR-induced cell cycle delay is likely to be transient, and CCNB1 targeting to the nucleus overcomes this delay (Summers et al., 2005). Accumulation of CCNB1 is consistent with previous observations of cell cycle-dependent regulation and depletion studies of TACC3 (Jeng et al., 2009; Schneider et al., 2007a; Yao et al., 2007). In addition, studies in *X. laevis* report the involvement of maskin in cyclin B1 translation, where this regulation is necessary for the integrity of the mitotic apparatus and for cell division (Groisman et al., 2000). Thus, considering the results of viability assays after TACC3 and TSC2 depletion, we propose that TACC3-TSC2 regulation of the cell cycle could be initially mediated by CHFR at the early mitotic checkpoint. Progression to metaphase may then be mediated by increased levels of CCNB1 (Lindqvist et al., 2009), but subsequent TACC3 depletion would impair spindle assembly and mislocalization of pS939-TSC2 and, in turn leading to abnormal/delayed cytokinesis (**Figure 43**). Mitotic defects caused by TACC3 depletion would likely evoke prolonged activation of the SAC, which prevents degradation of CCNB1 and anaphase transition (Bharadwaj and Yu, 2004). In contrast, a recent study reports that SAC is not permanent due to slow but continuous degradation of CCNB1 and allows mitotic slippage of cells with relatively minor defects into a tetraploid G1 state (Brito and Rieder, 2006). In accordance with our observations in *Tacc3*$^{-/-}$ MEFs, these cells are typically characterized by the appearance of interphase micronuclei resulting from lagging chromosomes (Brito and Rieder, 2006). Thus, we hypothesize that the reduced viability observed in our study after TACC3 depletion may be caused by post-mitotic G1/S arrest (Roland Piekorz personal communication). In the case of single depletion of TSC2, we observe high levels of CHFR/CCNB1 together with increased cell viability, where the elevated proliferation is probably due to the accompanying increase in mTOR signaling and translation. In contrast, we do not observe an increase in CHFR and CCNB1 levels after simultaneous depletion of TACC3 and TSC2, which is consistent with the epistatic relationship.

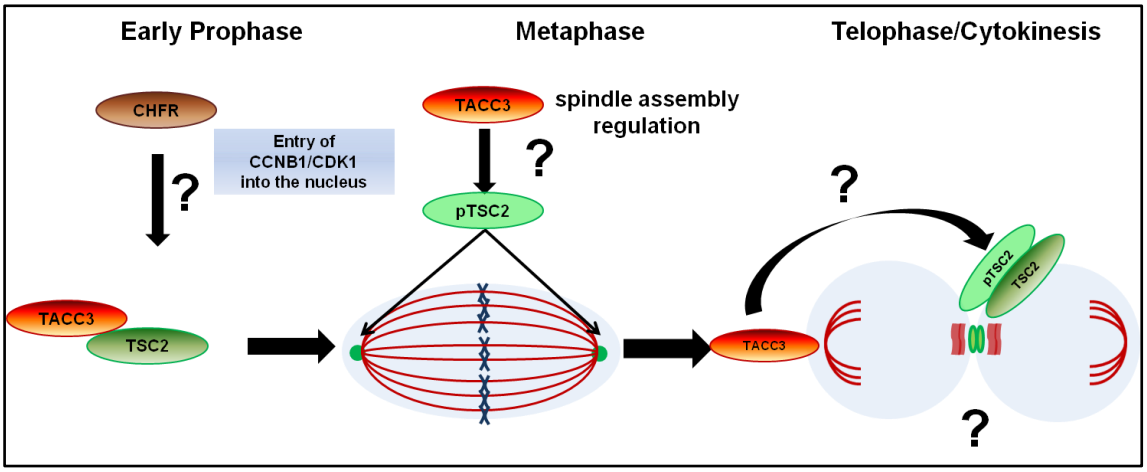

Figure 43: Model for TACC3-TSC2 associations in cell division

TACC3-TSC2 may have coordinated MT stabilization roles in early phases of mitosis, being sensed by CHFR. In metaphase, TACC3 regulates pS939-TSC2 localization to the spindle poles, which is necessary for correct spindle assembly. Finally, cytokinesis is also regulated by TACC3 and by total- and pS939-TSC2, and is essential for proper completion of cytokinesis.

Although there is extensive knowledge on the role of the TSC/mTOR pathway in nutrient and cell growth signaling, less is known about the function of these proteins in regulating tissue architecture, which is commonly disrupted in TSC patients (Napolioni and Curatolo, 2008). Epithelial tissues must be able to integrate signals controlling cell-cell junction remodeling, cell division and tissue architecture in order to avoid uncontrolled proliferation and tumor formation (Gibson and Gibson, 2009). Therefore, control of epithelial cell polarity is a fundamental step in the development of multicellular organisms. Importantly, there are more and more examples of links between complexes involved in cell proliferation and survival and complexes involved in cell polarity and cell-cell junction formation. Similarly to TSC disease, mutations in the *serine/threonine kinase 11 (LKB1)* gene lead to the Peutz-Jegher syndrome (PJS), which is a cancer predisposition disorder typically characterized by hamartomatous polyps in the gastrointestinal tract (Hearle et al., 2006; Hemminki et al., 1998; Katajisto et al., 2007). Another disease associated with hamartomas is Cowden syndrome (CS), which originates from mutations in the *phosphatase and tensin homolog (PTEN)* gene that regulates the PKB/AKT pathway upstream of TSC (Pilarski, 2009). Interestingly, LKB1, PTEN and TSC1-TSC2 are all related to the mTOR pathway (Tee and Blenis, 2005). LKB1, the human homolog of D-LKB1, is certainly involved in the determination of cell polarity (Baas et al., 2004a; Baas et al., 2004b), whereas PTEN has been shown to interact with D-PAR3

(Pinal et al., 2006; von Stein et al., 2005), another essential protein for establishing of cell polarity and epithelial junctions (Suzuki and Ohno, 2006). Moreover, a physical interaction has been described between TSC2 and PALS1-associated tight junction protein (PATJ) (Massey-Harroche et al., 2007), a known regulator of tight junction formation and epithelial polarity (Shin et al., 2005).

To evaluate whether TSC2 and TACC3 are involved in the regulation of tissue architecture we performed gene expression depletion(s) in a model of three-dimensional (3D) MCF10A cell culture. 3D culture can be used for the study of epithelial cell arrangement into tissue structures and the investigation of critical pathways in establishing and maintaining structural and functional aspects of differentiation (Plachot et al., 2009). A proper basoapical tissue polarity axis is a critical feature of normal epithelial differentiation. Indeed, apical polarity loss, characterized by the formation of a multilayer of cells or the lack of basal positioning of nuclei, has been used as a parameter for the characterization of early lesions in cancer (Konska et al., 1998). Apical polarity can be assessed by immunostaining for the core tight junction protein ZO-1 (Fogg et al., 2005; Plachot and Lelievre, 2004), while basal polarity can be assessed by immunostaining for α6-integrin (Koukoulis et al., 1991). Here we show how depletion of either TACC3 or TSC2, but not TSC1, in MCF10A leads to overgrowth of the acinar structures, distorted morphology and disruption of apical polarity compared to controls (**Figures 39-40**). In addition, we illustrate that simultaneous depletion of TACC3/TSC2 and TACC3/TSC1 results in a similar, but milder, phenotype to the one observed in single TACC3 or TSC2-depletion (**Figures 41-42**). We hypothesize that TACC3 plays a role in maintaining cell polarity through its functional roles in centrosome biology, which in turn is strongly related to polarity (Buendia et al., 1990; Cowan and Hyman, 2004; Lingle et al., 1998; Rindler et al., 1987). In the case of TSC2, such functions may be related to the actin cytoskeleton through mTORC2 regulation (Jacinto et al., 2004; Sarbassov et al., 2004). Since TSC2 actively regulates mTORC1 (Castro et al., 2003; Garami et al., 2003; Inoki et al., 2003a; Kwiatkowski, 2003b; Manning and Cantley, 2003), which is firmly linked to cell cycle progression and cell growth (Inoki et al., 2003b; Kim et al., 2002), and together with our findings that implicate TSC2 in cell division, we propose a coordinated role in maintaining cell polarity and cell proliferation. In recent years, emerging evidence suggests a relationship between cell polarity and cell cycle machineries (Bilder, 2004; Brenman, 2007; Partanen et al., 2009; Williams and Brenman, 2008). Interestingly, the metabolic sensor AMPK and its upstream regulator LKB1 have been related to both cell polarity and cell division roles in *D. melanogaster* (Brenman, 2007; Williams and Brenman, 2008). These reports

support our findings implicating TACC3 and TSC2 in cell division and cell polarity, although further experiments would be required to elucidate the exact mechanism of these functions. Together, the novel associations with the centrosomal protein TACC3 and the key role of the TACC3/TSC2 module in apicobasal differentiation described here may lead to increased understanding of the tumor suppressor function of TSC2 and its involvement in cyst formation and pathogenesis.

CONCLUSIONS

Conclusions

1. TACC3 physically interacts with key proteins involved in centrosome biology, including important regulators of cytokinesis and/or cilia formation, proposing novel roles for TACC proteins.

2. TACC3 also physically interacts with TSC2, mostly through mitosis, suggesting a coordinated role in cell division.

3. In interphase, TACC3 and TSC2 localize to the nuclear envelope and their defficency causes morphological alterations of this structure.

4. During cell division, TACC3 mediates pS939-TSC2 localization to cytokinetic structures and deficiency of TACC3 or TSC2 causes abnormalities in cytokinesis.

5. In cell proliferation and/or viability, *TSC2* acts epistatically to *TACC3*.

6. TACC3/TSC2 cell cycle regulation is mediated, in part, by the early mitotic checkpoint, CHFR.

7. Depletion of TACC3 and/or TSC2 affects apicobasal polarity, suggesting a possible role in epithelial differentiation and tissue architecture.

RESUM EN CATALÀ

Sumari

La major part dels estudis realitzats per tal d'esbrinar les funcions de les proteïnes TSC1 i TSC2 causants de l'Esclerosi Tuberosa (TSC) s'han centrat en la seva capacitat de regular la transcripció i el creixement cel·lular, però la seva relació amb alteracions d'estructures cel·lulars i el cicle cel·lular no estan ben determinades. Les proteïnes TACC tenen un paper primordial en estructures i processos relacionats amb les xarxes de microtúbuls (MTs). En aquest estudi hem realitzat un mapatge d'interaccions centrat en TACC3 i hem identificat TSC2 i 15 proteïnes més, com són els homo- i heterodímers de TACC, i dues proteïnes (ch-TOG/CKAP5 i FAM161B), la interacció de les quals està conservada entre espècies. TACC3 i TSC2 co-localitzen i co-purifiquen amb components de l'embolcall nuclear i la seva deficiència dóna lloc a alteracions d'aquesta estructura. Al llarg de la divisió cel·lular, TACC3 és necessària per a la localització de phospho-Ser939-TSC2 als pols del fus mitòtic i al punt de divisió de citocinesi. En concordança, cèl·lules deficients en Tacc3 i Tsc2 presenten un retràs en la citocinesi i una elevada freqüència de cèl·lules binucleades. Pel que fa a la regulació del cicle cel·lular, *TSC2* actua de forma epistàtica sobre *TACC3* i, a més de la seva funció de senyalització en la via TSC/mTOR i les associacions amb la citocinesi, convergeix amb el punt de regulació temprà de mitosi mediat per CHFR. Els nostres resultats relacionen TACC3 amb noves funcions estructurals i de divisió cel·lular per part de TSC2, la qual cosa podria proporcionar noves explicacions a les manifestacions clíniques i patològiques de la limfangioleiomiomatosi (LAM) i TSC.

El centrosoma

Visió general

El centrosoma és el centre organitzador de microtúbuls (de l'anglès MTOC, *microtubule organizing center*) present en totes les cèl·lules animals. Es tracta de una estructura exclusiva de cèl·lules eucariotes que fou descoberta per Theodor Boveri (Boveri, 1914). La seva funció està directament relacionada amb procesos dependents de microtúbuls (MT) com són la mobilitat cel·lular, l'adhesió i la polaritat en interfase, així com la organització del fus mitòtic al llarg de la mitosi (Bettencourt-Dias and Glover, 2007). Aberracions en el nombre de centrosomes poden interferir en la correcta formació del fus mitòtic i, per tant, en la segregació dels cromosomes, donant lloc a inestabilitat cromosómica (Sankaran and Parvin, 2006).

El centrosoma és un orgànul petit (1-2 μm de diàmetre) que es localitza al centre de la cèl·lula (Wilson, 1925). Està constituït per dos cilindres disposats perpendicularment anomenats centríols, envoltats per una massa amorfa de material pericentriolar (de l'anglès PCM, *pericentriolar material*) (Bettencourt-Dias and Glover, 2007). El PCM conté un complex de proteïnes (γ-TURC, de l'anglès, *γ-tubulin ring complex*) que permet la nucleació i l'ancoratge dels microtúbuls (Sankaran and Parvin, 2006). Cada centríol està constituït per nou grups de tres MT fusionats (triplets de MT) disposats conformant una estructura de molí.

El cicle de divisió del centrosoma comença en la fase G1/S i cap al final de la fase G2 cada cèl·lula té dos centrosomes. S'han descrit cinc punts consecutius que defineixen aquest procés: 1er/ desorientació dels centríols; 2^{on}/ nucleació dels centríols; 3er/ elongació dels procentríols; 4^{t}/ maduració del centrosoma; i 5^{è}/ separació dels centrosomes (revisat per (Lukasiewicz and Lingle, 2009)).

La duplicació del centrosoma es dóna un sol cop per cada cicle cel·lular i està sotmesa a un estricte control. Per tal que es doni una correcta divisió cel·lular, el cicle del centrosoma ha d'estar coordinat amb la duplicació del contingut genètic. De fet, s'ha demostrat que un augment en la activitat de la quinasa depenent de ciclina 2 (CDK2) podria estar implicat en la progressió del cicle cel·lular cap a la fase S, així com en la regulació de la duplicació del centrosoma (Hinchcliffe et al., 1999; Lacey et al., 1999; Matsumoto et al., 1999; Meraldi et al., 1999). Diferents estudis han descrit que la fosforilació i la proteòlisi són els principals mecanismes de regulació del cicle centrosomal (revisat per (Fry et al., 2000; Hansen et al., 2002; Meraldi and Nigg, 2002)). S'ha vist que els nivells de fosforilació al centrosoma augmenten substancialment durant el procés de maduració (Rusan and

Rogers, 2009). Tot i que s'han identificat un gran nombre de proteïnes implicades en aquest procés, les dues quinases PLK1 (de l'anglès, *polo-like kinase 1*) i AURKA (de l'anglès, *aurora kinase A*) són les que tenen un paper més important en la maduració del centrosoma. La separació dels centrosomes està també regulada per una gran varietat de quinases entre les quals hi figuren PLK1, AURKA i NEK2 (de l'anglès, *NIMA (never in mitosis)-related kinase*) (revisat per (Lukasiewicz and Lingle, 2009)). La proteïna quinasa que juga un paper més important en el procés de separació dels centrosomes és NEK2, mitjançant la fosforilació i subseqüent desplaçament de les proteïnes encarregades de mantenir la cohesió entre els dos centríols (Fry et al., 1998; Mayor et al., 2000). Pel que fa als processos de proteòlisi, les ubiquitina lligases principalment implicades en la regulació del cicle del centrosoma són les del complex SCF (SKIP, Cullin i F-box) i de l'APC/C (de l'anglès, *anaphase promoting complex*) (Freed et al., 1999; Gstaiger et al., 1999; Wigley et al., 1999).

Centrosomes, polaritat i càncer

Per la major part dels tipus cel·lulars, la posició del centrosoma en relació al nucli defineix un "eix cel·lular" que determina la polaritat funcional de la cèl·lula (Buendia et al., 1990). Aquesta polaritat es manté, en part, per la organització del fus de MTs originat al centrosoma i pel tràfic vesicular que hi ha al llarg d'aquests MTs (Rindler et al., 1987). Un nombre anormal de centrosomes pot afectar directament a la polaritat de la cèl·lula, així com a l'herència del material genètic (revisat per (Zyss and Gergely, 2009)). Defectes en la organització i la polaritat cel·lular entre cèl·lules adjacents (en conjunt, definit com anaplàsia) (Lingle et al., 1998), així com un nombre anormal de cromosomes (definit com aneuploïdia) són característiques de les cèl·lules canceroses. Les principals aberracions del centrosoma són l'amplificació (parells de centrosomes que contenen més de quatre centríols i/o la presència de més de dos centrosomes dins d'una cèl·lula) o la hiperplàsia (centrosomes que són més grans del normal) (Salisbury et al., 2004). Avui en dia, està ben establert que tant les aberracions numèriques del centrosoma com les estructurals són comuns en molts tipus de processos neoplàsics humans i de fet, estan associats amb l'aneuploïdia (Nigg, 2002).

La família de proteïnes TACC

Visió general

L'anàlisi proteòmic dels centrosomes humans va revelar que una elevada porció de les proteïnes centrosomals (~75%) contenen regions *coiled-coil* (Andersen et al., 2003). El motiu proteic *coiled-coil* és una estructura conservada evolutivament i adaptada per intervenir en les interaccions proteïna-proteïna (Salisbury, 2003). Així, algunes d'aquestes proteïnes *coiled-coil* actuen com a àncores per a altres proteïnes essencials i reguladores del centrosoma (Salisbury et al., 2004). El domini TACC (de l'anglès, *transforming acidic coiled-coil*) cobreix una regió d'aproximadament 200 aminoàcids (aa) a l'extrem carboxil (C-term) i és essencial per a la localització de les proteïnes en el centrosoma i el fus mitòtic (Gergely, 2002).

Les proteïnes TACC van ser inicialment descrites en *D. melanogaster* com a necessàries per a l'activitat centrosomal i per a l'encadellat dels microtúbuls durant la divisió cel·lular (Gergely et al., 2000a; Gergely et al., 2000b). Un sol membre de la família TACC s'ha descrit en *C. elegans* (TAC-1) (Bellanger and Gonczy, 2003; Le Bot et al., 2003; Srayko et al., 2003), *D. melanogaster* (D-TACC) (Gergely et al., 2000b), *X. laevis* (tacc3) (Stebbins-Boaz et al., 1999) i *S. pombe* (alp7) (Sato et al., 2004). En mamífers, la família TACC consta de tres membres: TACC1 (Still et al., 1999a), TACC2 (Chen et al., 2000; Pu et al., 2001) i TACC3 (McKeveney et al., 2001; Sadek et al., 2003; Still et al., 1999b). D'acord amb un paper clau en la biologia del centrosoma, la localització de les TACCs als centrosomes depèn de la seva fosforilació per AURKA en cèl·lules humanes, així com en els seus ortòlegs a *C. elegans*, *X. laevis* i *D. melanogaster* i, a més, s'ha proposat que aquesta modificació es requereix per la regulació de la dinàmica i la organització del fus mitòtic (Barros et al., 2005; Giet et al., 2002; Kinoshita et al., 2005; LeRoy et al., 2007; Peset et al., 2005).

Principalment, les proteïnes TACC realitzen les seves funcions al llarg de la mitosi (Gergely et al., 2000a). TACC1 podria ser necessària per la progressió cel·lular cap al final de la fase M (Delaval et al., 2004). Pel que fa a TACC2 no es coneix gaire la seva implicació en aquests processos, però TACC3 sembla ser essencial en la progressió de la mitosi, així com en l'alineació i separació dels cromosomes i la citoquinesi (Gergely, 2002; Schneider et al., 2007a; Yao et al., 2007).

TACCs *i càncer*

Els tres gens que codifiquen les proteïnes TACC es troben en regions cromosòmiques reorganitzades en certs tipus de càncer (Adnane et al., 1991; Still et al., 1999a; Still et al., 1999b). *TACC1*, que es troba en el cromosoma 8p11, va ser identificat per estar sobreexpressat en càncer de mama (Still et al., 1999a), mentre que altres estudis reporten la seva reduïda expressió en teixits cancerosos d'ovari i mama (Conte et al., 2002; Lauffart et al., 2005). La variant de *TACC2*, *AZU-1*, va ser aïllada per primera vegada en una cerca de gens supressors de tumors en càncer de mama (Chen et al., 2000), encara que estudis posteriors no donen gaire suport a aquesta idea (Schuendeln et al., 2004). Recentment, TACC3 també s'ha pogut relacionar amb alguns tipus de càncers humans (Chen et al., 2000; Lauffart et al., 2005; Still et al., 1999b; Ulisse et al., 2007). Juntament amb TACC1, nivells baixos de TACC3 s'han associat amb la tumorogènesi ovàrica (Lauffart et al., 2005). El càncer de tiroides també presenta alteracions en la expressió de TACC3 (Ulisse et al., 2007). Per contra, TACC3 s'ha vist sobreexpressada en el càncer de pulmó de cèl·lula petita (Jung et al., 2006). En conjunt, aquestes observacions suggereixen una relació entre la desregulació de les proteïnes TACC i la susceptibilitat al càncer i/o d'altres patologies associades a alteracions en la divisió cel·lular.

EL complex d'esclerosi tuberosa

Visió general

L'esclerosi tuberosa (de l'anglès, *tuberous sclerosis complex, TSC*) és un trastorn genètic amb un patró d'herència autosòmica dominant, penetrància variable, i una prevalença de 1-9/100,000 en la població total (identificadors de la malaltia Orphanet 805 i OMIM 191100/191092). La TSC és causada per mutacions de pèrdua de funció en els gens supressors de tumors *TSC1* o *TSC2* (European Chromosome 16 Tuberous Sclerosis Consortium, 1993; van Slegtenhorst et al., 1997) i es caracteritza per la presència de hamartomes, que consisteixen en tumors benignes, displàsics i desorganitzats que creixen en diferents òrgans i teixits (revisat per (Kwiatkowski, 2003b; Pan et al., 2004)). Els pacients de TSC poden desenvolupar anormalitats neurològiques com atacs d'epilèpsia, retard mental i autisme. En alguns casos apareixen quists renals i els individus amb delecions genòmiques de *PKD1* i *TSC2* a la línia germinal desenvolupen la malaltia renal policística infantil (Brook-Carter et al., 1994; Harris et al., 1995).

Els dos gens directament relacionats amb aquesta malaltia són: *TSC1*, situat al cromosoma 9q34 el qual codifica una proteïna de 130 kDa, anomenada *hamartin* (van Slegtenhorst et al., 1997) i *TSC2*, situat al cromosoma 16p13.3 el qual codifica una proteïna de 200 kDa, anomenada *tuberin* (European Chromosome 16 Tuberous Sclerosis Consortium, 1993). *Hamartin* i *tuberin* s'associen físicament *in vitro* i *in vivo* en forma d'heterodímers. La regió d'*hamartin* d'unió a *tuberin* es troba entre els aa 302-430 i en el cas de *tuberin*, la regió d'unió a *hamartin* es troba en els primers 418 aa dins el primer dels dos motius *coiled-coil* de la proteïna (Crino et al., 2006; van Slegtenhorst et al., 1998).

Pel que fa a la seva funció, *hamartin* i *tuberin* formen un complex dins de la via de senyalització PI3K-AKT1-mTOR encarregada de la regulació de nutrients i el creixement cel·lular (revisat per (Crino et al., 2006; Kwiatkowski, 2003b; Pan et al., 2004)). *Tuberin* conté un domini d'activació de proteïna GTPasa (de l'anglès, *GAP domain*) que augmenta l'activitat GTPasa de RHEB, que al seu torn és un regulador positiu del complex sensible a rapamicina mTOR/RAPTOR anomenat mTORC1 (Castro et al., 2003; Garami et al., 2003; Inoki et al., 2003a; Kwiatkowski, 2003a; Manning and Cantley, 2003; Saucedo et al., 2003; Tee et al., 2003; Zhang et al., 2003). El complex mTORC1 regula positivament múltiples processos, que inclouen la traducció del ARNm a través de p70-S6K/S6 i 4E-BP1/eIF4E, la biogènesi dels ribosomes, l'autofàgia, l'angiogènesi i l'apoptosi (Lazaris-Karatzas et al., 1990; Raught et al., 2004; Richardson et al., 2004;

Wendel et al., 2004). A més, mTOR forma un segon complex no sensible a la rapamicina quan s'uneix a RICTOR, anomenat mTORC2 (Jacinto et al., 2004; Sarbassov et al., 2004). El complex mTORC2 regula positivament el citoesquelet d'actina i influencia l'apoptosi a través de la fosforilació d'AKT en el residu Ser473 i d'activitats PKC1/RHO (Jacinto et al., 2004; Peterson et al., 2009; Sarbassov et al., 2004; Sarbassov et al., 2005).

Noves funcions de TSC1/TSC2*: el centrosoma i la polaritat cel·lular*

Els pacients de TSC acostumen a tenir defectes neuronals que poden estar provocats per migracions i posicionaments anormals de les neurones (Crino and Henske, 1999; Gutmann et al., 2000; Sparagana and Roach, 2000; Vinters et al., 1999). Recentment, s'ha estudiat en models de ratolí que *hamartin* i *tuberin* podrien estar jugant un paper important en la regulació de la polaritat neuronal (Choi et al., 2008). De fet, les proteïnes TACC també semblen ser crítiques en la migració nuclear interquinètica necessària pel manteniment del reservori de cèl·lules progenitores neurals (Xie et al., 2007). Per altra banda, les malalties cístiques renals estan associades amb l'absència o la disfunció dels cilis primaris i, per tant, la pèrdua de la polaritat i la correcta disposició dels teixits (Nauli et al., 2003; Yoder et al., 2002a; Yoder et al., 2002b).

Hipòtesi

El manteniment de la integritat estructural, el nombre i la funció del centrosoma són factors crítics per tota una sèrie de propietats cel·lulars que inclouen la motilitat, l'adhesió i la polaritat en interfase, així com la divisió al llarg de la mitosi i citoquinesi (revisat per (Bettencourt-Dias and Glover, 2007)). Alteracions en el centrosoma són comuns en diferents tipus de neoplàsies (revisat per (Nigg, 2002)), algunes malalties neurològiques (revisat per (Badano et al., 2005)) i estan relacionades amb la pèrdua de la polaritat en diferents models cel·lulars (revisat per (Sankaran and Parvin, 2006)). Diferents estudis han demostrat un paper important de les proteïnes TACC en la funció del centrosoma i la dinàmica de MTs al llarg de la divisió cel·lular (revisat per (Peset and Vernos, 2008)). S'han descrit tres gens humans que codifiquen per proteïnes TACC i la seva expressió s'ha vist alterada en cèl·lules canceroses, encara que no existeixen evidències específiques pel que fa a la seva localització cel·lular (Gergely et al., 2000a) o les seves interaccions amb proteïnes relacionades amb la regulació de la expressió gènica (Angrisano et al., 2006; Gangisetty et al., 2004; Garriga-Canut and Orkin, 2004; Lauffart et al., 2002; Sadek et al., 2000; Still et al., 2004). Fins al moment, no s'han descrit altres associacions que puguin aclarir el paper de les TACCs en estructures o processos cel·lulars en relació a malalties humanes. Per tal d'obtenir més informació en aquests aspectes, nosaltres hem mapat l'interactoma de TACC3 (és a dir, interaccions físiques entre proteïnes i TACC3). Els resultats d'aquest anàlisi han revelat la interacció física amb TSC2 i la possible funció conjunta de les dues proteïnes en el manteniment de la estructura nuclear i el control de diferents fases de la divisió cel·lular.

Objectius

Els principals objectius d'aquest estudi van ser:

Objectiu #1: Estudiar les característiques funcionals i les associacions genètiques i moleculars dels gens *TACC* humans i els seus productes en relació amb la biologia del centrosoma.

Objectiu #2: Avaluar les possibles implicacions en malalties humanes de les noves associacions genètiques i proteòmiques identificades en l'Objectiu #1.

Materials i Mètodes

Sistema del doble híbrid (de l'anglès, yeast two hybrid, Y2H)

L'assaig del doble híbrid en llevats es va realitzar en base a dues estratègies diferents, la transformació o l'aparellament, seguint la metodologia prèviament descrita (Vidalain et al., 2004; Walhout and Vidal, 2001) i l'ús de dues llibreries de cDNA, de cervell fetal humà o de melsa (ProQuest, Invitrogen). Tres esquers de TACC3 es van definir d'acord als seus dominis proteics (Gergely et al., 2000a; Piekorz et al., 2002; Still et al., 2004) i es van clonar en el vector pDONR201 de *Gateway* (Invitrogen) seguint la metodologia descrita per la companyia subministradora.

Els constructes es van transformar en soques de llevat MaV203 (Invitrogen) o AH109 (Clontech) i l'anàlisi es va realitzar utilitzant medi selectiu sense histidina i suplementat amb 10 mM (protocol d'aparellament) o 20 mM (protocol de transformació) de 3-amino-1,2,4-triazol (3-AT, Sigma-Aldrich) per tal de provar la activació del reporter HIS3 depenent de la interacció. Prèviament, els esquers van ser examinats per l'auto-activació en el rang de 10-18 mM de concentració de 3-AT. Amb aquestes condicions, es van poder examinar més de 10 milions de transformants per l'esquer. Les colònies positives es van créixer en medi selectiu durant 3 cicles (10-15 dies) per evitar la aparició de cDNAs contaminants i després es va procedir a la amplificació per PCR i la identificació de les seqüències de les possibles preses (Vidalain et al., 2004).

Anàlisi dels perfils d'expressió

La similitud dels perfils d'expressió es va avaluar amb el càlcul del coeficient de correlació de Pearson (CCP) mitjançant els nivells d'expressió normalitzats (gcRMA) del conjunt de dades GeneAtlas U133A humans (http://biogps.gnf.org) (Su et al., 2004). Les comparacions es van realitzar per a totes les sondes possibles de *microarray* i els *p* valors van ser ajustats per la correcció de Bonferroni.

Anàlisi fil·logenètic

Les recerques Psi-Blast (Altschul et al., 1997) es van realitzar contra genomes dipositats en Ensembl des de Gener de 2008 (Flicek et al., 2008) i fent servir les proteïnes TACC humanes. Els paràmetres es van establir a un màxim de cinc

interaccions i un *e*-valor amb llindar de 0.0001. La metodologia emprada en aquest treball està adaptada de Huerta-Cepas *et al.* (Huerta-Cepas et al., 2007).

Cultius cel·lulars

En aquest treball s'han emprat les següents línies cel·lulars:

HeLa; MCF7; HEK293; BT474; HME/TERT (cèl·lules epitelials humans immortalitzades amb telomerasa); MCF10A; fibroblasts embrionaris de ratolí (MEFs) *Tsc2*$^{+/+}$ *p53*$^{-/-}$ i *Tsc2*$^{-/-}$ *p53*$^{-/-}$; MEFs *Tacc3*$^{+/-}$ i *Tacc3*$^{-/-}$; cèl·lules derivades de leiomioma uterí de rates Eker (ELT3) deficients en tuberina (Howe et al., 1995); MEFs *Tsc1*$^{-/-}$ van ser transduïdes retroviralment amb *TSC1*/pMSCVneo humà com s'ha descrit prèviament (Astrinidis et al., 2002).

Tècniques moleculars

Les tècniques moleculars emprades en aquest treball són les següents:

- Doble sincronització amb Timidina
- Assaig d'unió a microtúbuls
- Assaig de citoquinesi
- Fraccionament cel·lular
- Assaig de viabilitat/proliferació
- Cultiu cel·lular de MCF10A en 3D sobre membranes basals reconstituïdes
- Assaig de co-purificació per afinitat
- Assaig de co-immunoprecipitació
- Western blot
- Anàlisi cel·lular per immunofluorescència
- Disseny de *shRNAs* i preparació viral

Resultats

L'interactoma de TACC3

Aquest treball es va iniciar amb el mapatge d'interaccions físiques amb TACC3 mitjançant la tècnica del doble híbrid (Y2H) i fent servir el domini TACC com a esquer (**Figura 12**). Tota una sèrie de proves moleculars i funcionals recolzen l'alta qualitat d'aquest interactoma. Dues interaccions conservades entre espècies, o interòlogs, van ser identificades: chTOG/CKAP5, interòlog en *C. elegans*, *D. melanogaster* i *X. laevis (Peset and Vernos, 2008)*, i FAM161B, interòlog en *C. elegans* (Li et al., 2004). El mapa d'interaccions proteïna-proteïna centrat en TACC3 inclou funcions relacionades amb estructures microtubulars ja conegudes prèviament per altres TACCs com són la regulació de citocinesi i/o la formació de cilis (ARHGEF2 (Birkenfeld et al., 2007), CP110 (Tsang et al., 2008), LZTS2 (Sudo and Maru, 2007) i TACC1 (Delaval et al., 2004)).

Algunes de les interaccions identificades en el Y2H van ser confirmades mitjançant l'assaig de co-purificació per afinitat (co-AP) en cèl·lules HEK293, com és el cas de CP110, KIF1C, i HMMR (**Figura 15**). D'altres com les interaccions amb ARHGEF2, CGN i TSC2 van ser confirmades per co-immunoprecipitació (co-IP) endògena (**Figures 16-17**). Cal destacar que prèviament s'ha descrit que ARHGEF2 i CGN interactuen físicament (Aijaz et al., 2005), la qual cosa dóna suport a la detecció d'associacions biològicament rellevants per TACC3. La associació entre TACC3 i TSC2 es va detectar mitjançant assajos de co-IP de manera recíproca i fent ús de diferents línies cel·lulars i anticossos (**Figura 17**). A més, assajos de co-AP amb fragments predefinits de TSC2 (Goncharova et al., 2004) ens van permetre acotar la regió d'interacció amb TACC3 (**Figura 18**). Els nostres resultats suggereixen que la regió N-terminal de TSC2 (TSC2-HBD), que conté el domini d'interacció amb TSC1 i un motiu *coiled-coil*, és probablement la responsable de la interacció amb TACC3. D'acord amb els processos biològics associats a l'interactoma de TACC3, aquest fragment està relacionat amb la regulació del citoesquelet i l'adhesió cel·lular (Astrinidis et al., 2002; Goncharova et al., 2004).

TACC3-TSC2 *localitzen a l'embolcall nuclear i la seva deficiència condueix a alteracions morfològiques d'aquesta estructura*

Un assaig d'unió a microtúbuls fent l'ús de taxol i nocodazol va mostrar que TSC2 i el seu company TSC1 estan associats amb els microtúbuls (**Figura 19**). Estudis de localització cel·lular en cèl·lules HeLa i fibroblasts embrionaris murins (MEF) amb el genotip $Tsc2^{-/-}Tp53^{-/-}$ o controls amb el genotip $Tsc2^{+/+}Tp53^{+/+}$ ens van suggerir que TSC2 es localitzava a l'embolcall nuclear (**Figura 20A**), la qual cosa va ser corroborada per co-IP amb la subunitat del porus nuclear NUP62 (**Figura 20B**). A més, es va poder comprovar mitjançant assajos de fraccionament cel·lular que TACC3 i TSC2 co-purificaven amb el component estructural de la membrana nuclear interna làmina A (LMNA) (**Figura 22**). Aquestes observacions ens indicaven que TSC2 és un component de l'embolcall i d'alguna manera predeien la possible presència d'anomalies estructurals causades per la deficiència de TSC2 o TACC3. Per tal d'avaluar aquesta hipòtesi, es van realitzar immunofluorescències en MEFs deficients en Tsc2 o Tacc3 fent servir com a marcador de l'embolcall nuclear un anticòs contra Nup62. Així, vam poder observar com les cèl·lules deficients en una de les dues proteïnes presentaven anormalitats morfològiques a l'embolcall nuclear (**Figura 23**). Aquestes alteracions no es van observar en MEFs deficients en Tsc1, així com TSC1 tampoc co-purificava amb Lmna, la qual cosa ens suggereix que TSC2 té una funció específica, possiblement en relació a TACC3.

La localització de pS939-TSC2 en citocinesi és depenent de TACC3

Donada la interacció física entre TACC3 i TSC2, i la coneguda implicació de TACC3 en el control de la divisió cel·lular (Albee and Wiese, 2008; Gergely et al., 2003; Kinoshita et al., 2005; Schneider et al., 2007a; Yao et al., 2007), vam voler analitzar la localització subcel·lular d'ambdues proteïnes al llarg del cicle cel·lular. En metafase, TACC3 i TSC2 es van localitzar als fusos microtubulars i als pols, mentre que la forma fosforilada de TSC2 al residu Ser939 es trobava exclusivament als pols (**Figura 26A**). En telofase i citocinesi, tant TSC2 total com pS939-TSC2 es trobaven particularment concentrades en el punt de divisió en citocinesi, mentre que TACC3 es va veure localitzada en la regió pericentrosomal i als fusos microtubulars restants en la meitat del cos de divisió de les dues cèl·lules (**Figura 26B**). Assajos de co-IP en cèl·lules sincronitzades per doble bloqueig amb timidina ens van demostrar que existia una forta associació entre TACC3 i TSC2 en mitosi, la qual cosa ens fa pensar que les dues proteïnes podrien estar jugant algun paper conjunt en la regulació de la divisió cel·lular (**Figura 27**). D'altra banda, la depleció total de TACC3 en cèl·lules HeLa va resultar en una pèrdua de pS939-TSC2 als pols

i en el punt de divisió de citocinesi, fet que donava suport a la possible funció d'ambdues proteïnes en la divisió cel·lular (**Figura 28**).

La deficiència de TACC3 i TSC2 dóna lloc a un retràs en citocinesi i a la formació de cèl·lules binucleades

D'acord amb la localització de TSC2 en estructures citocinètiques, en el nostre estudi vam poder observar com les MEFs deficients en *Tsc2* presentaven separacions anormalment allargades en citocinesi comparant-les amb les MEFs control (**Figura 29**). A més, aquestes MEFs deficients en *Tsc2* presentaven un alt percentatge de cèl·lules binucleades (**Figura 31**). Els mateixos fenotips van ser observats en MEFs deficients en *Tacc3*. Per tal d'examinar més a fons l'efecte de TSC2 sobre la progressió del cicle cel·lular, vam realitzar un assaig de sincronització amb *nocodazole* de cèl·lules ELT3 (de l'anglès, *eker rat leiomyoma tumor cell*) deficients en *Tsc2* i reconstituïdes amb TSC2 humana en que detectàvem el nombre de cèl·lules en citocinesi al llarg del temps (**Figura 32**). Així, 90 minuts després de l'alliberament de les cèl·lules del *nocodazole*, les cèl·lules deficients en *Tsc2* presentaven fins a set cops més figures citocinètiques que les reconstituïdes. D'acord amb aquestes observacions, els cultius deficients en Tsc1 també presentaven un retard en citocinesi després de l'alliberament del *nocodazole* (**Figura 33**), així com una major incidència en cèl·lules binucleades (**Figura 34**). No obstant, els cultius deficients *Tsc1* no presentaven figures aberrants en citocinesi, el que suggereix que TSC1 podria tenir alguna funció en citocinesi, però que aquesta no és fonamental en la regulació del procés.

TSC2 actua de manera epistàtica sobre TACC3 en el control de la viabilitat cel·lular

Per tal de profunditzar en el paper que juga la interacció TACC3-TSC2 en la proliferació cel·lular vam examinar l'efecte de la depleció de cadascuna de les proteïnes i les dues simultàniament sobre la viabilitat. Cèl·lules MCF7 van ser infectades amb constructes de shRNAs lentivirals i es va realitzar un assaig de proliferació amb MTT. La depleció de TSC2 va resultar en un augment de la proliferació, mentre que en el cas de la depleció de TACC3 observàvem el contrari (**Figura 36**). A més, análisis en els nivells de proteïnes van revelar un increment de CHFR (**Figura 37**), suggerint algún tipus de implicació per part del punt de control temprà de mitosi en la proliferació d'aquestes cèl·lules deplecionades amb TACC3 i TSC2. Sorprenentment, quan vam realitzar la depleció simultània de les

dues proteïnes, vam recuperar la viabilitat reduïda observada en les cèl·lules que no expressaven TACC3. D'aquesta manera, nosaltres suggerim que *TSC2* actua de manera epistàtica sobre *TACC3* en la regulació de la viabilitat cel·lular.

La deficiència de TACC3 i TSC2 dona lloc a anormalitats en la arquitectura cel·lular i a una pèrdua de polaritat cel·lular

Donada la interacció genètica existent entre TACC3 i TSC2 i la seva implicació en divisió cel·lular i proliferació, el nostre següent objectiu va ser determinar el paper d'aquesta relació en la regulació de l'arquitectura cel·lular, que està freqüentment alterada en pacients de TSC (revisat per (Napolioni and Curatolo, 2008)). Per tal d'analitzar-ho vam realitzar la depleció simple i combinada de TACC3, TSC2 i TSC1 i vam mesurar la dinàmica de creixement durant la diferenciació apicobasal de cèl·lules MCF10A cultivades en una membrana basal reconstituïda (Debnath et al., 2003). La manca de TACC3 i TSC2 de manera individual i/o la depleció simultània de les dues va resultar en alteracions morfològiques dels complexes acinars comparant-los amb els controls (**Figures 39-41**). Per altra banda, la depleció de TSC1 no va causar cap canvi fenotípic en vers als controls, mentre que la depleció simultània de TSC1 i TACC3 va resultar en fenotips aberrants, similars als observats en el cas de les deplecions amb TACC3 i TSC2. Les anormalitats observades en aquests complexos cel·lulars van ser analitzades a partir d'imatges en camp clar (mesurant la mida i circularitat de cada complex) i mitjançant tècniques d'immunofluorescència analitzades per microscòpia confocal. En conjunt, aquests resultats ens van suggerir una possible implicació de TACC3 i TSC2 en processos de diferenciació apicobasal.

Discussió

En aquest estudi es descriu la participació de *TSC2*/TSC2 en el manteniment estructural de l'embolcall nuclear i en el control de les diferents fases de la divisió cel·lular, probablement mitjançant la interacció amb *TACC3*/TACC3. En primer lloc, l'interactoma centrat en TACC3 descriu interaccions en concordança amb associacions moleculars i funcionals ja conegudes i conservades entre diferents espècies amb les TACCs (Peset and Vernos, 2008). A més, aquest interactoma també ens mostra noves possibles funcions d'aquesta família de proteïnes en la organització de xarxes de MT i la biologia del centrosoma. Donat que els membres de la família de proteïnes TACC s'han vist alterats en diferents neoplàsies epitelials (Raff, 2002), TACC3 podria estar implicada en processos de migració i diferenciació cel·lular mitjançant la seva interacció amb ARHGEF2 i CGN, ambdues confirmades per assajos de co-IP. ARHGEF2 és un factor activador de RhoA i CGN és un adaptador d'unions estretes cèl·lula-cèl·lula (de l'anglès, *cell-to-cell tight junction adaptor*) (Citi et al., 1988; Ren et al., 1998). CGN s'uneix a ARHGEF2 i inhibeix l'activació de RhoA, promovent la formació d'estructures epitelials polaritzades (Aijaz et al., 2005). La funció de les TACCs en aquests processos és desconeguda, però s'ha vist que TSC1/TSC2 juguen un paper important en la regulació de les Rho GTPases (Astrinidis et al., 2002; Goncharova et al., 2004; Lamb et al., 2000). Així, aquesta funció de les proteïnes TSC podria explicar el fenotip metastàtic que presenten les cèl·lules llises del múscul en la linfangioleiomiomatosi (LAM), causada per mutacions en *TSC2* (revisat per (Hohman et al., 2008)). La unió de TSC2 a TSC1 causa l'activació de RAC1 i, conseqüentment, la inhibició de l'activitat de RhoA (Goncharova et al., 2004). Donat que TACC3 podria estar interaccionant amb TSC2 a través del domini TSC2-HBD, hipotetitzem un possible paper en la remodelació del citoesquelet i el fenotip metastàtic observat en LAM. Alternativament, l'eix TACC3-TSC2-mTORC2 també podria estar regulant RhoA i el citoesquelet d'actina (Jacinto et al., 2004; Sarbassov et al., 2004). Pensem que la divisió cel·lular podria estar regulada de la mateixa manera. ARHGEF2, un cop s'ha alliberat de la inhibició fosfo-depenent per part d'ARUKA, activa RhoA per tal de promoure la citoquinesi (Birkenfeld et al., 2007). Així, ARHGEF2 i TSC2 podrien estar competint per la unió a TACC3 d'una manera similar a la transició de la proliferació cel·lular cap a la diferenciació.

En relació als processos que regulen la polaritat epitelial, l'interactoma centrat en TACC3 pot donar lloc a noves hipòtesis en el desenvolupament de cists renals en pacients TSC. Els cists renals apareixen més freqüentment en pacients amb mutacions en *TSC2* (Dabora et al., 2001; Sancak et al., 2005). Les MEFs

deficients en Tsc1 i Tsc2 presenten un augment en el desenvolupament de cilis primaris i els seus productes gènics corresponents interaccionen amb Pkd1 en aquest procés (Bonnet et al., 2009; Hartman et al., 2009). El fet de que en aquest treball s'hagi identificat la interacció de proteïnes involucrades en funcions relacionades amb el desenvolupament de cilis com són CEP164 (Graser et al., 2007) i CP110 (Spektor et al., 2007; Tsang et al., 2008) amb TACC3, suggereix que la funció de TSC2 en aquest procés podria dependre de la regulació d'aquestes interaccions. De la mateixa manera que en processos de polaritat epitelial i mitosi, la inactivació d'AURKA (Pugacheva et al., 2007), el principal regulador de les TACCs, és necessària per a la formació de cilis, que a l'hora podria estar coordinada amb la regulació de les noves interaccions descrites per TACC3 amb TSC2 i CEP164/CP110.

Un altre punt important que podem destacar d'aquest treball és la nova funció de *TSC2*/TSC2 en la estructura de l'embolcall nuclear i el punt de regulació de mitosi mediat per CHFR. Els nostres resultats suggereixen que aquesta funció és específica de *TSC2*/TSC2 en relació a *TSC1*/TSC1, la qual cosa podria explicar l'augment de severitat clínica associada a mutacions en *TSC2* (Dabora et al., 2001; Sancak et al., 2005). L'alteració de l'embolcall nuclear s'acostuma a associar amb malalties genètiques amb anomalies musculars, en alguns casos acompanyades per alteracions neurològiques (revisat per (Elcock and Bridger, 2008)). A més, les TACCs són crítiques en la migració nuclear intercinètica en progenitors neuronals: al mateix temps que s'observen alteracions en la organització de microtúbuls, la pertorbació de les TACCs afecta a la posició nuclear i la divisió (Xie et al., 2007). Aquestes observacions poden estar relacionades amb els defectes en migració neuronal que presenta la TSC (Crino and Henske, 1999; Vinters et al., 1999). Per altra banda, la interacció genètica en el punt de regulació de mitosi i les associacions moleculars depenents de la localització en citocinesi suggereixen un control global en processos de divisió cel·lular per part de *TACC3*/TACC3-*TSC2*/TSC2. Els nostres resultats proposen que quan la divisió cel·lular comença, CHFR detecta l'estructura de l'embolcall nuclear i probablement la xarxa de microtúbuls (Scolnick and Halazonetis, 2000; Summers et al., 2005) mitjançant un mecanisme en que intervenen TACC3 i TSC2. A més, TACC3 sembla que també regula la localització de pS939-TSC2 i possiblement també regula la citocinesi, donat que hem observat alteracions d'aquest procés en MEFs de Tacc3- i Tsc2-deficient. Aquest treball també suggereix que TSC1 podria tenir un paper complementari en citocinesi, encara que aquest seria independent de TACC3, donades les diferències en la localització cel·lular i la implicació de la forma fosforilada de TSC2, que es considerava "inactiva" (pS939). Cal destacar que

l'augment en la freqüència de cèl·lules binucleades observat en els nostres resultats és concordant amb estudis previs en que s'observaven tetraploïdies en cèl·lules derivades de rates Eker amb una mutació germinal en *Tsc2* (Gui et al., 2007). En conjunt, aquest estudi evidencia que les noves interaccions i funcions de *TACC3*/TACC3 i *TSC2*/TSC2 poden estar relacionades amb la biologia del centrosoma i la malaltia TSC.

Conclusions

1. El mapatge d'interaccions centrat en TACC3 identifica proteïnes involucrades en la biologia del centrosoma i inclou reguladors importants de la citocinesi i la formació de cilis, la qual cosa proposa noves funcions per les TACCs.

2. TACC3 i TSC2 s'associen principalment en mitosi, la qual cosa suggereix una funció coordinada en la divisió cel·lular.

3. En interfase, TACC3 i TSC2 localitza a l'embolcall nuclear i la seva deficiència provoca alteracions morfològiques d'aquesta estructura.

4. En divisió cel·lular, la localització de pS939-TSC2 està mediada per TACC3 i la deficiència de TACC3 o TSC2 provoca anormalitats en citocinesi.

5. En proliferació cel·lular, *TSC2* és epistàtic sobre *TACC3*.

6. La regulació del cicle cel·lular per part de TACC3/TSC2 està mediada, en part, pel punt de regulació temprà de mitosi, CHFR.

7. La depleció de TACC3 i/o TSC2 afecta la polaritat apicobasal en cultius en 3D, la qual cosa suggereix posibles funcions en la diferenciació cel·lular i l'arquitectura tisular.

BIBLIOGRAPHY

Adnane, J., Gaudray, P., Dionne, C.A., Crumley, G., Jaye, M., Schlessinger, J., Jeanteur, P., Birnbaum, D., and Theillet, C. (1991). BEK and FLG, two receptors to members of the FGF family, are amplified in subsets of human breast cancers. Oncogene *6*, 659-663.

Aicher, L.D., Campbell, J.S., and Yeung, R.S. (2001). Tuberin phosphorylation regulates its interaction with hamartin. Two proteins involved in tuberous sclerosis. J Biol Chem *276*, 21017-21021.

Aijaz, S., D'Atri, F., Citi, S., Balda, M.S., and Matter, K. (2005). Binding of GEF-H1 to the tight junction-associated adaptor cingulin results in inhibition of Rho signaling and G1/S phase transition. Dev Cell *8*, 777-786.

Akaike, H. (1973). Information theory and extension of the maximum likelihood principle. Proceedings of the 2nd international symposium on information theory, 267-281.

Albee, A.J., and Wiese, C. (2008). Xenopus TACC3/maskin is not required for microtubule stability but is required for anchoring microtubules at the centrosome. Mol Biol Cell *19*, 3347-3356.

Altschul, S.F., Madden, T.L., Schaffer, A.A., Zhang, J., Zhang, Z., Miller, W., and Lipman, D.J. (1997). Gapped BLAST and PSI-BLAST: a new generation of protein database search programs. Nucleic Acids Res *25*, 3389-3402.

Andersen, J.S., Wilkinson, C.J., Mayor, T., Mortensen, P., Nigg, E.A., and Mann, M. (2003). Proteomic characterization of the human centrosome by protein correlation profiling. Nature *426*, 570-574.

Andreassen, P.R., Lohez, O.D., Lacroix, F.B., and Margolis, R.L. (2001). Tetraploid state induces p53-dependent arrest of nontransformed mammalian cells in G1. Mol Biol Cell *12*, 1315-1328.

Angrisano, T., Lembo, F., Pero, R., Natale, F., Fusco, A., Avvedimento, V.E., Bruni, C.B., and Chiariotti, L. (2006). TACC3 mediates the association of MBD2 with histone acetyltransferases and relieves transcriptional repression of methylated promoters. Nucleic Acids Res *34*, 364-372.

Astrinidis, A., Cash, T.P., Hunter, D.S., Walker, C.L., Chernoff, J., and Henske, E.P. (2002). Tuberin, the tuberous sclerosis complex 2 tumor suppressor gene product, regulates Rho activation, cell adhesion and migration. Oncogene *21*, 8470-8476.

Astrinidis, A., Senapedis, W., Coleman, T.R., and Henske, E.P. (2003). Cell cycle-regulated phosphorylation of hamartin, the product of the tuberous sclerosis complex 1 gene, by cyclin-dependent kinase 1/cyclin B. J Biol Chem *278*, 51372-51379.

Astrinidis, A., Senapedis, W., and Henske, E.P. (2006). Hamartin, the tuberous sclerosis complex 1 gene product, interacts with polo-like kinase 1 in a phosphorylation-dependent manner. Hum Mol Genet *15*, 287-297.

Ault, J.G., and Rieder, C.L. (1994). Centrosome and kinetochore movement during mitosis. Curr Opin Cell Biol *6*, 41-49.

Baas, A.F., Kuipers, J., van der Wel, N.N., Batlle, E., Koerten, H.K., Peters, P.J., and Clevers, H.C. (2004a). Complete polarization of single intestinal epithelial cells upon activation of LKB1 by STRAD. Cell *116*, 457-466.

Baas, A.F., Smit, L., and Clevers, H. (2004b). LKB1 tumor suppressor protein: PARtaker in cell polarity. Trends Cell Biol *14*, 312-319.

Babu, J.R., Jeganathan, K.B., Baker, D.J., Wu, X., Kang-Decker, N., and van Deursen, J.M. (2003). Rae1 is an essential mitotic checkpoint regulator that cooperates with Bub3 to prevent chromosome missegregation. J Cell Biol *160*, 341-353.

Badano, J.L., Teslovich, T.M., and Katsanis, N. (2005). The centrosome in human genetic disease. Nat Rev Genet *6*, 194-205.

Bahe, S., Stierhof, Y.D., Wilkinson, C.J., Leiss, F., and Nigg, E.A. (2005). Rootletin forms centriole-associated filaments and functions in centrosome cohesion. J Cell Biol *171*, 27-33.

Bakal, C.J., Finan, D., LaRose, J., Wells, C.D., Gish, G., Kulkarni, S., DeSepulveda, P., Wilde, A., and Rottapel, R. (2005). The Rho GTP exchange factor Lfc promotes spindle assembly in early mitosis. Proc Natl Acad Sci U S A *102*, 9529-9534.

Baker, D.J., Jeganathan, K.B., Cameron, J.D., Thompson, M., Juneja, S., Kopecka, A., Kumar, R., Jenkins, R.B., de Groen, P.C., Roche, P., and van Deursen, J.M. (2004). BubR1 insufficiency causes early onset of aging-associated phenotypes and infertility in mice. Nat Genet *36*, 744-749.

Barros, T.P., Kinoshita, K., Hyman, A.A., and Raff, J.W. (2005). Aurora A activates D-TACC-Msps complexes exclusively at centrosomes to stabilize centrosomal microtubules. J Cell Biol *170*, 1039-1046.

Basel-Vanagaite, L., Muncher, L., Straussberg, R., Pasmanik-Chor, M., Yahav, M., Rainshtein, L., Walsh, C.A., Magal, N., Taub, E., Drasinover, V.*, et al.* (2006). Mutated nup62 causes autosomal recessive infantile bilateral striatal necrosis. Ann Neurol *60*, 214-222.

Bellanger, J.M., and Gonczy, P. (2003). TAC-1 and ZYG-9 form a complex that promotes microtubule assembly in C. elegans embryos. Curr Biol *13*, 1488-1498.

Bellion, A., Baudoin, J.P., Alvarez, C., Bornens, M., and Metin, C. (2005). Nucleokinesis in tangentially migrating neurons comprises two alternating phases: forward migration of the Golgi/centrosome associated with centrosome splitting and myosin contraction at the rear. J Neurosci *25*, 5691-5699.

Bement, W.M., Benink, H.A., and von Dassow, G. (2005). A microtubule-dependent zone of active RhoA during cleavage plane specification. J Cell Biol *170*, 91-101.

Bettencourt-Dias, M., and Glover, D.M. (2007). Centrosome biogenesis and function: centrosomics brings new understanding. Nat Rev Mol Cell Biol.

Bharadwaj, R., and Yu, H. (2004). The spindle checkpoint, aneuploidy, and cancer. Oncogene *23*, 2016-2027.

Bilder, D. (2004). Epithelial polarity and proliferation control: links from the Drosophila neoplastic tumor suppressors. Genes Dev *18*, 1909-1925.

Birkenfeld, J., Nalbant, P., Bohl, B.P., Pertz, O., Hahn, K.M., and Bokoch, G.M. (2007). GEF-H1 modulates localized RhoA activation during cytokinesis under the control of mitotic kinases. Dev Cell *12*, 699-712.

Bischoff, J.R., Anderson, L., Zhu, Y., Mossie, K., Ng, L., Souza, B., Schryver, B., Flanagan, P., Clairvoyant, F., Ginther, C.*, et al.* (1998). A homologue of Drosophila aurora kinase is oncogenic and amplified in human colorectal cancers. EMBO J *17*, 3052-3065.

Bissler, J.J., McCormack, F.X., Young, L.R., Elwing, J.M., Chuck, G., Leonard, J.M., Schmithorst, V.J., Laor, T., Brody, A.S., Bean, J.*, et al.* (2008). Sirolimus for angiomyolipoma in tuberous sclerosis complex or lymphangioleiomyomatosis. N Engl J Med *358*, 140-151.

Blower, M.D., Feric, E., Weis, K., and Heald, R. (2007). Genome-wide analysis demonstrates conserved localization of messenger RNAs to mitotic microtubules. J Cell Biol *179*, 1365-1373.

Blower, M.D., Nachury, M., Heald, R., and Weis, K. (2005). A Rae1-containing ribonucleoprotein complex is required for mitotic spindle assembly. Cell *121*, 223-234.

Bolton, P.F., Park, R.J., Higgins, J.N., Griffiths, P.D., and Pickles, A. (2002). Neuro-epileptic determinants of autism spectrum disorders in tuberous sclerosis complex. Brain *125*, 1247-1255.

Bonne, G., Di Barletta, M.R., Varnous, S., Becane, H.M., Hammouda, E.H., Merlini, L., Muntoni, F., Greenberg, C.R., Gary, F., Urtizberea, J.A.*, et al.* (1999). Mutations in the gene encoding lamin A/C cause autosomal dominant Emery-Dreifuss muscular dystrophy. Nat Genet *21*, 285-288.

Bonnet, C.S., Aldred, M., von Ruhland, C., Harris, R., Sandford, R., and Cheadle, J.P. (2009). Defects in cell polarity underlie TSC and ADPKD-associated cystogenesis. Hum Mol Genet *18*, 2166-2176.

Bourne, H.R., Sanders, D.A., and McCormick, F. (1991). The GTPase superfamily: conserved structure and molecular mechanism. Nature *349*, 117-127.

Bouton, A.H., Riggins, R.B., and Bruce-Staskal, P.J. (2001). Functions of the adapter protein Cas: signal convergence and the determination of cellular responses. Oncogene *20*, 6448-6458.

Boveri, T. (1914). Zur Frage der Entstehung maligner Tumoren. Gustav Fischer Verlag.

Boxem, M., Maliga, Z., Klitgord, N., Li, N., Lemmens, I., Mana, M., de Lichtervelde, L., Mul, J.D., van de Peut, D., Devos, M.*, et al.* (2008). A protein domain-based interactome network for C. elegans early embryogenesis. Cell *134*, 534-545.

Brenman, J.E. (2007). AMPK/LKB1 signaling in epithelial cell polarity and cell division. Cell Cycle *6*, 2755-2759.

Brito, D.A., and Rieder, C.L. (2006). Mitotic checkpoint slippage in humans occurs via cyclin B destruction in the presence of an active checkpoint. Curr Biol *16*, 1194-1200.

Brittle, A.L., and Ohkura, H. (2005). Centrosome maturation: Aurora lights the way to the poles. Curr Biol *15*, R880-882.

Brook-Carter, P.T., Peral, B., Ward, C.J., Thompson, P., Hughes, J., Maheshwar, M.M., Nellist, M., Gamble, V., Harris, P.C., and Sampson, J.R. (1994). Deletion of the TSC2 and PKD1 genes associated with severe infantile polycystic kidney disease--a contiguous gene syndrome. Nat Genet *8*, 328-332.

Brown, N., and Costanzo, V. (2009). An ATM and ATR dependent pathway targeting centrosome dependent spindle assembly. Cell Cycle *8*, 1997-2001.

Buendia, B., Bre, M.H., Griffiths, G., and Karsenti, E. (1990). Cytoskeletal control of centrioles movement during the establishment of polarity in Madin-Darby canine kidney cells. J Cell Biol *110*, 1123-1135.

Cabeza-Arvelaiz, Y., Thompson, T.C., Sepulveda, J.L., and Chinault, A.C. (2001). LAPSER1: a novel candidate tumor suppressor gene from 10q24.3. Oncogene *20*, 6707-6717.

Capell, B.C., and Collins, F.S. (2006). Human laminopathies: nuclei gone genetically awry. Nat Rev Genet *7*, 940-952.

Carroll, P.E., Okuda, M., Horn, H.F., Biddinger, P., Stambrook, P.J., Gleich, L.L., Li, Y.Q., Tarapore, P., and Fukasawa, K. (1999). Centrosome hyperamplification in human cancer: chromosome instability induced by p53 mutation and/or Mdm2 overexpression. Oncogene *18*, 1935-1944.

Carter, S.B. (1967). Effects of cytochalasins on mammalian cells. Nature *213*, 261-264.

Casper, K.A., Donnelly, L.F., Chen, B., and Bissler, J.J. (2002). Tuberous sclerosis complex: renal imaging findings. Radiology *225*, 451-456.

Castro, A.F., Rebhun, J.F., Clark, G.J., and Quilliam, L.A. (2003). Rheb binds tuberous sclerosis complex 2 (TSC2) and promotes S6 kinase activation in a rapamycin- and farnesylation-dependent manner. J Biol Chem *278*, 32493-32496.

Caviness, V.S., Jr., and Takahashi, T. (1991). Cerebral lesions of tuberous sclerosis in relation to normal histogenesis. Ann N Y Acad Sci *615*, 187-195.

Citi, S., Sabanay, H., Jakes, R., Geiger, B., and Kendrick-Jones, J. (1988). Cingulin, a new peripheral component of tight junctions. Nature *333*, 272-276.

Conte, N., Charafe-Jauffret, E., Delaval, B., Adelaide, J., Ginestier, C., Geneix, J., Isnardon, D., Jacquemier, J., and Birnbaum, D. (2002). Carcinogenesis and translational controls: TACC1 is down-regulated in human cancers and associates with mRNA regulators. Oncogene *21*, 5619-5630.

Conte, N., Delaval, B., Ginestier, C., Ferrand, A., Isnardon, D., Larroque, C., Prigent, C., Seraphin, B., Jacquemier, J., and Birnbaum, D. (2003). TACC1-chTOG-Aurora A protein complex in breast cancer. Oncogene *22*, 8102-8116.

Costello, L.C., Hartman, T.E., and Ryu, J.H. (2000). High frequency of pulmonary lymphangioleiomyomatosis in women with tuberous sclerosis complex. Mayo Clin Proc *75*, 591-594.

Cowan, C.R., and Hyman, A.A. (2004). Centrosomes direct cell polarity independently of microtubule assembly in C. elegans embryos. Nature *431*, 92-96.

Crino, P.B., and Henske, E.P. (1999). New developments in the neurobiology of the tuberous sclerosis complex. Neurology *53*, 1384-1390.

Crino, P.B., Nathanson, K.L., and Henske, E.P. (2006). The tuberous sclerosis complex. N Engl J Med *355*, 1345-1356.

Cuenca, A.A., Schetter, A., Aceto, D., Kemphues, K., and Seydoux, G. (2003). Polarization of the C. elegans zygote proceeds via distinct establishment and maintenance phases. Development *130*, 1255-1265.

Cullen, C.F., and Ohkura, H. (2001). Msps protein is localized to acentrosomal poles to ensure bipolarity of Drosophila meiotic spindles. Nat Cell Biol *3*, 637-642.

Curatolo, P., Seri, S., Verdecchia, M., and Bombardieri, R. (2001). Infantile spasms in tuberous sclerosis complex. Brain Dev *23*, 502-507.

Chakraborty, P., Wang, Y., Wei, J.H., van Deursen, J., Yu, H., Malureanu, L., Dasso, M., Forbes, D.J., Levy, D.E., Seemann, J., and Fontoura, B.M. (2008). Nucleoporin levels regulate cell cycle progression and phase-specific gene expression. Dev Cell *15*, 657-667.

Chen, H.M., Schmeichel, K.L., Mian, I.S., Lelievre, S., Petersen, O.W., and Bissell, M.J. (2000). AZU-1: a candidate breast tumor suppressor and biomarker for tumor progression. Mol Biol Cell *11*, 1357-1367.

Chen, Z., Indjeian, V.B., McManus, M., Wang, L., and Dynlacht, B.D. (2002). CP110, a cell cycle-dependent CDK substrate, regulates centrosome duplication in human cells. Dev Cell *3*, 339-350.

Chng, W.J., Ahmann, G.J., Henderson, K., Santana-Davila, R., Greipp, P.R., Gertz, M.A., Lacy, M.Q., Dispenzieri, A., Kumar, S., Rajkumar, S.V.*, et al.* (2006). Clinical implication of centrosome amplification in plasma cell neoplasm. Blood *107*, 3669-3675.

Choi, Y.J., Di Nardo, A., Kramvis, I., Meikle, L., Kwiatkowski, D.J., Sahin, M., and He, X. (2008). Tuberous sclerosis complex proteins control axon formation. Genes Dev *22*, 2485-2495.

Chong-Kopera, H., Inoki, K., Li, Y., Zhu, T., Garcia-Gonzalo, F.R., Rosa, J.L., and Guan, K.L. (2006). TSC1 stabilizes TSC2 by inhibiting the interaction between TSC2 and the HERC1 ubiquitin ligase. J Biol Chem *281*, 8313-8316.

Chorianopoulos, D., and Stratakos, G. (2008). Lymphangioleiomyomatosis and tuberous sclerosis complex. Lung *186*, 197-207.

D'Avino, P.P. (2009). How to scaffold the contractile ring for a safe cytokinesis - lessons from Anillin-related proteins. J Cell Sci *122*, 1071-1079.

Dabora, S.L., Jozwiak, S., Franz, D.N., Roberts, P.S., Nieto, A., Chung, J., Choy, Y.S., Reeve, M.P., Thiele, E., Egelhoff, J.C.*, et al.* (2001). Mutational analysis in a cohort of 224 tuberous sclerosis patients indicates increased severity of TSC2, compared with TSC1, disease in multiple organs. Am J Hum Genet *68*, 64-80.

Dan, H.C., Sun, M., Yang, L., Feldman, R.I., Sui, X.M., Ou, C.C., Nellist, M., Yeung, R.S., Halley, D.J., Nicosia, S.V.*, et al.* (2002). Phosphatidylinositol 3-kinase/Akt pathway regulates tuberous sclerosis tumor suppressor complex by phosphorylation of tuberin. J Biol Chem *277*, 35364-35370.

Daniels, M.J., Wang, Y., Lee, M., and Venkitaraman, A.R. (2004). Abnormal cytokinesis in cells deficient in the breast cancer susceptibility protein BRCA2. Science *306*, 876-879.

Dauer, W.T., and Worman, H.J. (2009). The nuclear envelope as a signaling node in development and disease. Dev Cell *17*, 626-638.

Dawe, H.R., Adams, M., Wheway, G., Szymanska, K., Logan, C.V., Noegel, A.A., Gull, K., and Johnson, C.A. (2009). Nesprin-2 interacts with meckelin and mediates ciliogenesis via remodelling of the actin cytoskeleton. J Cell Sci *122*, 2716-2726.

de Anda, F.C., Pollarolo, G., Da Silva, J.S., Camoletto, P.G., Feiguin, F., and Dotti, C.G. (2005). Centrosome localization determines neuronal polarity. Nature *436*, 704-708.

De Brabander, M. (1982). A model for the microtubule organizing activity of the centrosomes and kinetochores in mammalian cells. Cell Biol Int Rep *6*, 901-915.

De Luca, M., Lavia, P., and Guarguaglini, G. (2006). A functional interplay between Aurora-A, Plk1 and TPX2 at spindle poles: Plk1 controls centrosomal localization of Aurora-A and TPX2 spindle association. Cell Cycle *5*, 296-303.

Debnath, J., Muthuswamy, S.K., and Brugge, J.S. (2003). Morphogenesis and oncogenesis of MCF-10A mammary epithelial acini grown in three-dimensional basement membrane cultures. Methods *30*, 256-268.

Delaval, B., Ferrand, A., Conte, N., Larroque, C., Hernandez-Verdun, D., Prigent, C., and Birnbaum, D. (2004). Aurora B -TACC1 protein complex in cytokinesis. Oncogene *23*, 4516-4522.

Didier, C., Merdes, A., Gairin, J.E., and Jabrane-Ferrat, N. (2008). Inhibition of proteasome activity impairs centrosome-dependent microtubule nucleation and organization. Mol Biol Cell *19*, 1220-1229.

Doxsey, S. (2002). Duplicating dangerously: linking centrosome duplication and aneuploidy. Mol Cell *10*, 439-440.

Drechsel, D.N., Hyman, A.A., Hall, A., and Glotzer, M. (1997). A requirement for Rho and Cdc42 during cytokinesis in Xenopus embryos. Curr Biol *7*, 12-23.

Edgar, R.C. (2004). MUSCLE: a multiple sequence alignment method with reduced time and space complexity. BMC Bioinformatics *5*, 113.

Ehrhardt, A.G., and Sluder, G. (2005). Spindle pole fragmentation due to proteasome inhibition. J Cell Physiol *204*, 808-818.

El-Hashemite, N., Zhang, H., Henske, E.P., and Kwiatkowski, D.J. (2003). Mutation in TSC2 and activation of mammalian target of rapamycin signalling pathway in renal angiomyolipoma. Lancet *361*, 1348-1349.

Elcock, L.S., and Bridger, J.M. (2008). Exploring the effects of a dysfunctional nuclear matrix. Biochem Soc Trans *36*, 1378-1383.

Erickson, H.P., and Stoffler, D. (1996). Protofilaments and rings, two conformations of the tubulin family conserved from bacterial FtsZ to alpha/beta and gamma tubulin. J Cell Biol *135*, 5-8.

Etienne-Manneville, S., and Hall, A. (2002). Rho GTPases in cell biology. Nature *420*, 629-635.

European Chromosome 16 Tuberous Sclerosis Consortium (1993). Identification and characterization of the tuberous sclerosis gene on chromosome 16. Cell *75*, 1305-1315.

Ferguson, R.L., and Maller, J.L. (2010). Centrosomal localization of cyclin E-Cdk2 is required for initiation of DNA synthesis. Curr Biol *20*, 856-860.

Fields, S., and Song, O. (1989). A novel genetic system to detect protein-protein interactions. Nature *340*, 245-246.

Flicek, P., Aken, B.L., Beal, K., Ballester, B., Caccamo, M., Chen, Y., Clarke, L., Coates, G., Cunningham, F., Cutts, T.*, et al.* (2008). Ensembl 2008. Nucleic Acids Res *36*, D707-714.

Fogg, V.C., Liu, C.J., and Margolis, B. (2005). Multiple regions of Crumbs3 are required for tight junction formation in MCF10A cells. J Cell Sci *118*, 2859-2869.

Franz, D.N., Brody, A., Meyer, C., Leonard, J., Chuck, G., Dabora, S., Sethuraman, G., Colby, T.V., Kwiatkowski, D.J., and McCormack, F.X. (2001). Mutational and radiographic analysis of pulmonary disease consistent with lymphangioleiomyomatosis and micronodular pneumocyte hyperplasia in women with tuberous sclerosis. Am J Respir Crit Care Med *164*, 661-668.

Freed, E., Lacey, K.R., Huie, P., Lyapina, S.A., Deshaies, R.J., Stearns, T., and Jackson, P.K. (1999). Components of an SCF ubiquitin ligase localize to the centrosome and regulate the centrosome duplication cycle. Genes Dev *13*, 2242-2257.

Fry, A.M., Mayor, T., Meraldi, P., Stierhof, Y.D., Tanaka, K., and Nigg, E.A. (1998). C-Nap1, a novel centrosomal coiled-coil protein and candidate substrate of the cell cycle-regulated protein kinase Nek2. J Cell Biol *141*, 1563-1574.

Fry, A.M., Mayor, T., and Nigg, E.A. (2000). Regulating centrosomes by protein phosphorylation. Curr Top Dev Biol *49*, 291-312.

Fukasawa, K. (2007). Oncogenes and tumour suppressors take on centrosomes. Nat Rev Cancer *7*, 911-924.

Fukasawa, K., Choi, T., Kuriyama, R., Rulong, S., and Vande Woude, G.F. (1996). Abnormal centrosome amplification in the absence of p53. Science *271*, 1744-1747.

Fukasawa, K., Wiener, F., Vande Woude, G.F., and Mai, S. (1997). Genomic instability and apoptosis are frequent in p53 deficient young mice. Oncogene *15*, 1295-1302.

Fygenson, D.K., Braun, E., and Libchaber, A. (1994). Phase diagram of microtubules. Phys Rev E Stat Phys Plasmas Fluids Relat Interdiscip Topics *50*, 1579-1588.

Gangisetty, O., Lauffart, B., Sondarva, G.V., Chelsea, D.M., and Still, I.H. (2004). The transforming acidic coiled coil proteins interact with nuclear histone acetyltransferases. Oncogene *23*, 2559-2563.

Gao, X., and Pan, D. (2001). TSC1 and TSC2 tumor suppressors antagonize insulin signaling in cell growth. Genes Dev *15*, 1383-1392.

Garami, A., Zwartkruis, F.J., Nobukuni, T., Joaquin, M., Roccio, M., Stocker, H., Kozma, S.C., Hafen, E., Bos, J.L., and Thomas, G. (2003). Insulin activation of Rheb, a mediator of mTOR/S6K/4E-BP signaling, is inhibited by TSC1 and 2. Mol Cell *11*, 1457-1466.

Garriga-Canut, M., and Orkin, S.H. (2004). Transforming acidic coiled-coil protein 3 (TACC3) controls friend of GATA-1 (FOG-1) subcellular localization and regulates the association between GATA-1 and FOG-1 during hematopoiesis. J Biol Chem *279*, 23597-23605.

Gergely, F. (2002). Centrosomal TACCtics. Bioessays *24*, 915-925.

Gergely, F., Draviam, V.M., and Raff, J.W. (2003). The ch-TOG/XMAP215 protein is essential for spindle pole organization in human somatic cells. Genes Dev *17*, 336-341.

Gergely, F., Karlsson, C., Still, I., Cowell, J., Kilmartin, J., and Raff, J.W. (2000a). The TACC domain identifies a family of centrosomal proteins that can interact with microtubules. Proc Natl Acad Sci U S A *97*, 14352-14357.

Gergely, F., Kidd, D., Jeffers, K., Wakefield, J.G., and Raff, J.W. (2000b). D-TACC: a novel centrosomal protein required for normal spindle function in the early Drosophila embryo. Embo J *19*, 241-252.

Gibson, W.T., and Gibson, M.C. (2009). Cell topology, geometry, and morphogenesis in proliferating epithelia. Curr Top Dev Biol *89*, 87-114.

Giet, R., McLean, D., Descamps, S., Lee, M.J., Raff, J.W., Prigent, C., and Glover, D.M. (2002). Drosophila Aurora A kinase is required to localize D-TACC to centrosomes and to regulate astral microtubules. J Cell Biol *156*, 437-451.

Gillberg, I.C., Gillberg, C., and Ahlsen, G. (1994). Autistic behaviour and attention deficits in tuberous sclerosis: a population-based study. Dev Med Child Neurol *36*, 50-56.

Gingras, A.C., Raught, B., and Sonenberg, N. (1999). eIF4 initiation factors: effectors of mRNA recruitment to ribosomes and regulators of translation. Annu Rev Biochem *68*, 913-963.

Gisselsson, D., Bjork, J., Hoglund, M., Mertens, F., Dal Cin, P., Akerman, M., and Mandahl, N. (2001). Abnormal nuclear shape in solid tumors reflects mitotic instability. Am J Pathol *158*, 199-206.

Glotzer, M. (2005). The molecular requirements for cytokinesis. Science *307*, 1735-1739.

Glover, D.M., Leibowitz, M.H., McLean, D.A., and Parry, H. (1995). Mutations in aurora prevent centrosome separation leading to the formation of monopolar spindles. Cell *81*, 95-105.

Goldstein, B., and Hird, S.N. (1996). Specification of the anteroposterior axis in Caenorhabditis elegans. Development *122*, 1467-1474.

Gomez, M.R., Sampson, J.R, Whittemore, V.H. (1999). Tuberous Sclerosis Complex. Oxford University Press.

Goncharova, E., Goncharov, D., Noonan, D., and Krymskaya, V.P. (2004). TSC2 modulates actin cytoskeleton and focal adhesion through TSC1-binding domain and the Rac1 GTPase. J Cell Biol *167*, 1171-1182.

Goncharova, E.A., Goncharov, D.A., Eszterhas, A., Hunter, D.S., Glassberg, M.K., Yeung, R.S., Walker, C.L., Noonan, D., Kwiatkowski, D.J., Chou, M.M.*, et al.* (2002). Tuberin regulates p70 S6 kinase activation and ribosomal protein S6 phosphorylation. A role for the TSC2 tumor suppressor gene in pulmonary lymphangioleiomyomatosis (LAM). J Biol Chem *277*, 30958-30967.

Goncharova, E.A., Goncharov, D.A., Lim, P.N., Noonan, D., and Krymskaya, V.P. (2006). Modulation of cell migration and invasiveness by tumor suppressor TSC2 in lymphangioleiomyomatosis. Am J Respir Cell Mol Biol *34*, 473-480.

Gorgidze, L.A., and Vorobjev, I.A. (1995). Centrosome and microtubules behavior in the cytoplasts. J Submicrosc Cytol Pathol *27*, 381-389.

Graser, S., Stierhof, Y.D., Lavoie, S.B., Gassner, O.S., Lamla, S., Le Clech, M., and Nigg, E.A. (2007). Cep164, a novel centriole appendage protein required for primary cilium formation. J Cell Biol *179*, 321-330.

Groisman, I., Huang, Y.S., Mendez, R., Cao, Q., Theurkauf, W., and Richter, J.D. (2000). CPEB, maskin, and cyclin B1 mRNA at the mitotic apparatus: implications for local translational control of cell division. Cell *103*, 435-447.

Gstaiger, M., Marti, A., and Krek, W. (1999). Association of human SCF(SKP2) subunit p19(SKP1) with interphase centrosomes and mitotic spindle poles. Exp Cell Res *247*, 554-562.

Gui, Y., He, G.H., Walsh, M.P., and Zheng, X.L. (2007). Predisposition to tetraploidy in pulmonary vascular smooth muscle cells derived from the Eker rats. Am J Physiol Lung Cell Mol Physiol *293*, L702-711.

Guidotti, J.E., Bregerie, O., Robert, A., Debey, P., Brechot, C., and Desdouets, C. (2003). Liver cell polyploidization: a pivotal role for binuclear hepatocytes. J Biol Chem *278*, 19095-19101.

Guindon, S., and Gascuel, O. (2003). A simple, fast, and accurate algorithm to estimate large phylogenies by maximum likelihood. Syst Biol *52*, 696-704.

Gunsalus, K.C., Bonaccorsi, S., Williams, E., Verni, F., Gatti, M., and Goldberg, M.L. (1995). Mutations in twinstar, a Drosophila gene encoding a cofilin/ADF homologue, result in defects in centrosome migration and cytokinesis. J Cell Biol *131*, 1243-1259.

Gutmann, D.H., Zhang, Y., Hasbani, M.J., Goldberg, M.P., Plank, T.L., and Petri Henske, E. (2000). Expression of the tuberous sclerosis complex gene products, hamartin and tuberin, in central nervous system tissues. Acta Neuropathol *99*, 223-230.

Hannan, K.M., Brandenburger, Y., Jenkins, A., Sharkey, K., Cavanaugh, A., Rothblum, L., Moss, T., Poortinga, G., McArthur, G.A., Pearson, R.B., and Hannan, R.D. (2003). mTOR-dependent regulation of ribosomal gene transcription requires S6K1 and is mediated by phosphorylation of the carboxy-terminal activation domain of the nucleolar transcription factor UBF. Mol Cell Biol *23*, 8862-8877.

Hansen, D.V., Hsu, J.Y., Kaiser, B.K., Jackson, P.K., and Eldridge, A.G. (2002). Control of the centriole and centrosome cycles by ubiquitination enzymes. Oncogene *21*, 6209-6221.

Hara, K., Yonezawa, K., Weng, Q.P., Kozlowski, M.T., Belham, C., and Avruch, J. (1998). Amino acid sufficiency and mTOR regulate p70 S6 kinase and eIF-4E BP1 through a common effector mechanism. J Biol Chem *273*, 14484-14494.

Harris, P.C., Ward, C.J., Peral, B., and Hughes, J. (1995). Autosomal dominant polycystic kidney disease: molecular analysis. Hum Mol Genet *4 Spec No*, 1745-1749.

Hartman, T.R., Liu, D., Zilfou, J.T., Robb, V., Morrison, T., Watnick, T., and Henske, E.P. (2009). The tuberous sclerosis proteins regulate formation of the primary cilium via a rapamycin-insensitive and polycystin 1-independent pathway. Hum Mol Genet *18*, 151-163.

Haviv, L., Gillo, D., Backouche, F., and Bernheim-Groswasser, A. (2008). A cytoskeletal demolition worker: myosin II acts as an actin depolymerization agent. J Mol Biol *375*, 325-330.

Hearle, N., Schumacher, V., Menko, F.H., Olschwang, S., Boardman, L.A., Gille, J.J., Keller, J.J., Westerman, A.M., Scott, R.J., Lim, W.*, et al.* (2006). Frequency and spectrum of cancers in the Peutz-Jeghers syndrome. Clin Cancer Res *12*, 3209-3215.

Hemminki, A., Markie, D., Tomlinson, I., Avizienyte, E., Roth, S., Loukola, A., Bignell, G., Warren, W., Aminoff, M., Hoglund, P.*, et al.* (1998). A serine/threonine kinase gene defective in Peutz-Jeghers syndrome. Nature *391*, 184-187.

Hetzer, M.W., and Wente, S.R. (2009). Border control at the nucleus: biogenesis and organization of the nuclear membrane and pore complexes. Dev Cell *17*, 606-616.

Hinchcliffe, E.H., Li, C., Thompson, E.A., Maller, J.L., and Sluder, G. (1999). Requirement of Cdk2-cyclin E activity for repeated centrosome reproduction in Xenopus egg extracts. Science *283*, 851-854.

Hinchcliffe, E.H., Miller, F.J., Cham, M., Khodjakov, A., and Sluder, G. (2001). Requirement of a centrosomal activity for cell cycle progression through G1 into S phase. Science *291*, 1547-1550.

Hirano, A., and Kurimura, T. (1974). Virally transformed cells and cytochalasin B. I. The effect of cytochalasin B on cytokinesis, karyokinesis and DNA synthesis in cells. Exp Cell Res *89*, 111-120.

Hodges, A.K., Li, S., Maynard, J., Parry, L., Braverman, R., Cheadle, J.P., DeClue, J.E., and Sampson, J.R. (2001). Pathological mutations in TSC1 and TSC2 disrupt the interaction between hamartin and tuberin. Hum Mol Genet *10*, 2899-2905.

Hohman, D.W., Noghrehkar, D., and Ratnayake, S. (2008). Lymphangioleiomyomatosis: A review. Eur J Intern Med *19*, 319-324.

Hollander, M.C., Sheikh, M.S., Bulavin, D.V., Lundgren, K., Augeri-Henmueller, L., Shehee, R., Molinaro, T.A., Kim, K.E., Tolosa, E., Ashwell, J.D.*, et al.* (1999). Genomic instability in Gadd45a-deficient mice. Nat Genet *23*, 176-184.

Howe, S.R., Gottardis, M.M., Everitt, J.I., Goldsworthy, T.L., Wolf, D.C., and Walker, C. (1995). Rodent model of reproductive tract leiomyomata. Establishment and characterization of tumor-derived cell lines. Am J Pathol *146*, 1568-1579.

Huang, J., Dibble, C.C., Matsuzaki, M., and Manning, B.D. (2008). The TSC1-TSC2 complex is required for proper activation of mTOR complex 2. Mol Cell Biol *28*, 4104-4115.

Huerta-Cepas, J., Dopazo, H., Dopazo, J., and Gabaldon, T. (2007). The human phylome. Genome Biol *8*, R109.

Huttenlocher, P.R., and Heydemann, P.T. (1984). Fine structure of cortical tubers in tuberous sclerosis: a Golgi study. Ann Neurol *16*, 595-602.

Huttenlocher, P.R., and Wollmann, R.L. (1991). Cellular neuropathology of tuberous sclerosis. Ann N Y Acad Sci *615*, 140-148.

Hwang, L.H., Lau, L.F., Smith, D.L., Mistrot, C.A., Hardwick, K.G., Hwang, E.S., Amon, A., and Murray, A.W. (1998). Budding yeast Cdc20: a target of the spindle checkpoint. Science *279*, 1041-1044.

Inoki, K., Li, Y., Xu, T., and Guan, K.L. (2003a). Rheb GTPase is a direct target of TSC2 GAP activity and regulates mTOR signaling. Genes Dev *17*, 1829-1834.

Inoki, K., Ouyang, H., Zhu, T., Lindvall, C., Wang, Y., Zhang, X., Yang, Q., Bennett, C., Harada, Y., Stankunas, K.*, et al.* (2006). TSC2 integrates Wnt and energy signals via a coordinated phosphorylation by AMPK and GSK3 to regulate cell growth. Cell *126*, 955-968.

Inoki, K., Zhu, T., and Guan, K.L. (2003b). TSC2 mediates cellular energy response to control cell growth and survival. Cell *115*, 577-590.

Jacinto, E., Loewith, R., Schmidt, A., Lin, S., Ruegg, M.A., Hall, A., and Hall, M.N. (2004). Mammalian TOR complex 2 controls the actin cytoskeleton and is rapamycin insensitive. Nat Cell Biol *6*, 1122-1128.

Jantsch-Plunger, V., Gonczy, P., Romano, A., Schnabel, H., Hamill, D., Schnabel, R., Hyman, A.A., and Glotzer, M. (2000). CYK-4: A Rho family gtpase activating protein (GAP) required for central spindle formation and cytokinesis. J Cell Biol *149*, 1391-1404.

Jeng, J.C., Lin, Y.M., Lin, C.H., and Shih, H.M. (2009). Cdh1 controls the stability of TACC3. Cell Cycle *8*, 3529-3536.

Jiang, X., and Yeung, R.S. (2006). Regulation of microtubule-dependent protein transport by the TSC2/mammalian target of rapamycin pathway. Cancer Res *66*, 5258-5269.

Joinson, C., O'Callaghan, F.J., Osborne, J.P., Martyn, C., Harris, T., and Bolton, P.F. (2003). Learning disability and epilepsy in an epidemiological sample of individuals with tuberous sclerosis complex. Psychol Med *33*, 335-344.

Jones, A.C., Shyamsundar, M.M., Thomas, M.W., Maynard, J., Idziaszczyk, S., Tomkins, S., Sampson, J.R., and Cheadle, J.P. (1999). Comprehensive mutation analysis of TSC1 and TSC2-and phenotypic correlations in 150 families with tuberous sclerosis. Am J Hum Genet *64*, 1305-1315.

Ju, X., Katiyar, S., Wang, C., Liu, M., Jiao, X., Li, S., Zhou, J., Turner, J., Lisanti, M.P., Russell, R.G.*, et al.* (2007). Akt1 governs breast cancer progression in vivo. Proc Natl Acad Sci U S A *104*, 7438-7443.

Jung, C.K., Jung, J.H., Park, G.S., Lee, A., Kang, C.S., and Lee, K.Y. (2006). Expression of transforming acidic coiled-coil containing protein 3 is a novel independent prognostic marker in non-small cell lung cancer. Pathol Int *56*, 503-509.

Kalitsis, P., Earle, E., Fowler, K.J., and Choo, K.H. (2000). Bub3 gene disruption in mice reveals essential mitotic spindle checkpoint function during early embryogenesis. Genes Dev *14*, 2277-2282.

Kamijo, K., Ohara, N., Abe, M., Uchimura, T., Hosoya, H., Lee, J.S., and Miki, T. (2006). Dissecting the role of Rho-mediated signaling in contractile ring formation. Mol Biol Cell *17*, 43-55.

Katajisto, P., Vallenius, T., Vaahtomeri, K., Ekman, N., Udd, L., Tiainen, M., and Makela, T.P. (2007). The LKB1 tumor suppressor kinase in human disease. Biochim Biophys Acta *1775*, 63-75.

Kenerson, H., Dundon, T.A., and Yeung, R.S. (2005). Effects of rapamycin in the Eker rat model of tuberous sclerosis complex. Pediatr Res *57*, 67-75.

Khodjakov, A., and Rieder, C.L. (1999). The sudden recruitment of gamma-tubulin to the centrosome at the onset of mitosis and its dynamic exchange throughout the cell cycle, do not require microtubules. J Cell Biol *146*, 585-596.

Khodjakov, A., and Rieder, C.L. (2001). Centrosomes enhance the fidelity of cytokinesis in vertebrates and are required for cell cycle progression. J Cell Biol *153*, 237-242.

Kiemeney, L.A., Sulem, P., Besenbacher, S., Vermeulen, S.H., Sigurdsson, A., Thorleifsson, G., Gudbjartsson, D.F., Stacey, S.N., Gudmundsson, J., Zanon, C.*, et al.* (2010). A sequence variant at 4p16.3 confers susceptibility to urinary bladder cancer. Nat Genet.

Kim, D.H., Sarbassov, D.D., Ali, S.M., King, J.E., Latek, R.R., Erdjument-Bromage, H., Tempst, P., and Sabatini, D.M. (2002). mTOR interacts with raptor to form a nutrient-sensitive complex that signals to the cell growth machinery. Cell *110*, 163-175.

Kim, J., Lee, J.E., Heynen-Genel, S., Suyama, E., Ono, K., Lee, K., Ideker, T., Aza-Blanc, P., and Gleeson, J.G. Functional genomic screen for modulators of ciliogenesis and cilium length. Nature *464*, 1048-1051.

Kinoshita, K., Habermann, B., and Hyman, A.A. (2002). XMAP215: a key component of the dynamic microtubule cytoskeleton. Trends Cell Biol *12*, 267-273.

Kinoshita, K., Noetzel, T.L., Pelletier, L., Mechtler, K., Drechsel, D.N., Schwager, A., Lee, M., Raff, J.W., and Hyman, A.A. (2005). Aurora A phosphorylation of TACC3/maskin is required for centrosome-dependent microtubule assembly in mitosis. J Cell Biol *170*, 1047-1055.

Kishi, K., Sasaki, T., Kuroda, S., Itoh, T., and Takai, Y. (1993). Regulation of cytoplasmic division of Xenopus embryo by rho p21 and its inhibitory GDP/GTP exchange protein (rho GDI). J Cell Biol *120*, 1187-1195.

Knudson, A.G., Jr. (1971). Mutation and cancer: statistical study of retinoblastoma. Proc Natl Acad Sci U S A *68*, 820-823.

Kochanski, R.S., and Borisy, G.G. (1990). Mode of centriole duplication and distribution. J Cell Biol *110*, 1599-1605.

Konska, G., Guillot, J., De Latour, M., and Fonck, Y. (1998). Expression of Tn antigen and N-acetyllactosamine residues in malignant and benign human breast tumors detected by lectins and monoclonal antibody 83D4. Int J Oncol *12*, 361-367.

Kopp, P., Lammers, R., Aepfelbacher, M., Woehlke, G., Rudel, T., Machuy, N., Steffen, W., and Linder, S. (2006). The kinesin KIF1C and microtubule plus ends regulate podosome dynamics in macrophages. Mol Biol Cell *17*, 2811-2823.

Koukoulis, G.K., Virtanen, I., Korhonen, M., Laitinen, L., Quaranta, V., and Gould, V.E. (1991). Immunohistochemical localization of integrins in the normal, hyperplastic, and neoplastic breast. Correlations with their functions as receptors and cell adhesion molecules. Am J Pathol *139*, 787-799.

Kudryavtsev, B.N., Kudryavtseva, M.V., Sakuta, G.A., and Stein, G.I. (1993). Human hepatocyte polyploidization kinetics in the course of life cycle. Virchows Arch B Cell Pathol Incl Mol Pathol *64*, 387-393.

Kwiatkowski, D.J. (2003a). Rhebbing up mTOR: new insights on TSC1 and TSC2, and the pathogenesis of tuberous sclerosis. Cancer Biol Ther *2*, 471-476.

Kwiatkowski, D.J. (2003b). Tuberous sclerosis: from tubers to mTOR. Ann Hum Genet *67*, 87-96.

Kwiatkowski, D.J., and Manning, B.D. (2005). Tuberous sclerosis: a GAP at the crossroads of multiple signaling pathways. Hum Mol Genet *14 Spec No. 2*, R251-258.

Lacey, K.R., Jackson, P.K., and Stearns, T. (1999). Cyclin-dependent kinase control of centrosome duplication. Proc Natl Acad Sci U S A *96*, 2817-2822.

Lamb, R.F., Roy, C., Diefenbach, T.J., Vinters, H.V., Johnson, M.W., Jay, D.G., and Hall, A. (2000). The TSC1 tumour suppressor hamartin regulates cell adhesion through ERM proteins and the GTPase Rho. Nat Cell Biol *2*, 281-287.

Lane, H.A., and Nigg, E.A. (1996). Antibody microinjection reveals an essential role for human polo-like kinase 1 (Plk1) in the functional maturation of mitotic centrosomes. J Cell Biol *135*, 1701-1713.

Lanni, J.S., and Jacks, T. (1998). Characterization of the p53-dependent postmitotic checkpoint following spindle disruption. Mol Cell Biol *18*, 1055-1064.

Lauffart, B., Gangisetty, O., and Still, I.H. (2003). Molecular cloning, genomic structure and interactions of the putative breast tumor suppressor TACC2. Genomics *81*, 192-201.

Lauffart, B., Howell, S.J., Tasch, J.E., Cowell, J.K., and Still, I.H. (2002). Interaction of the transforming acidic coiled-coil 1 (TACC1) protein with ch-TOG and GAS41/NuBI1 suggests multiple TACC1-containing protein complexes in human cells. Biochem J *363*, 195-200.

Lauffart, B., Vaughan, M.M., Eddy, R., Chervinsky, D., DiCioccio, R.A., Black, J.D., and Still, I.H. (2005). Aberrations of TACC1 and TACC3 are associated with ovarian cancer. BMC Womens Health *5*, 8.

Lazaris-Karatzas, A., Montine, K.S., and Sonenberg, N. (1990). Malignant transformation by a eukaryotic initiation factor subunit that binds to mRNA 5' cap. Nature *345*, 544-547.

Le Bot, N., Tsai, M.C., Andrews, R.K., and Ahringer, J. (2003). TAC-1, a regulator of microtubule length in the C. elegans embryo. Curr Biol *13*, 1499-1505.

Lee, M.J., Gergely, F., Jeffers, K., Peak-Chew, S.Y., and Raff, J.W. (2001). Msps/XMAP215 interacts with the centrosomal protein D-TACC to regulate microtubule behaviour. Nat Cell Biol *3*, 643-649.

LeRoy, P.J., Hunter, J.J., Hoar, K.M., Burke, K.E., Shinde, V., Ruan, J., Bowman, D., Galvin, K., and Ecsedy, J.A. (2007). Localization of human TACC3 to mitotic spindles is mediated by phosphorylation on Ser558 by Aurora A: a novel pharmacodynamic method for measuring Aurora A activity. Cancer Res *67*, 5362-5370.

Li, F., Ackermann, E.J., Bennett, C.F., Rothermel, A.L., Plescia, J., Tognin, S., Villa, A., Marchisio, P.C., and Altieri, D.C. (1999). Pleiotropic cell-division defects and apoptosis induced by interference with survivin function. Nat Cell Biol *1*, 461-466.

Li, J., Wang, J., Jiao, H., Liao, J., and Xu, X. (2010). Cytokinesis and cancer: Polo loves ROCK'n' Rho(A). J Genet Genomics *37*, 159-172.

Li, S., Armstrong, C.M., Bertin, N., Ge, H., Milstein, S., Boxem, M., Vidalain, P.O., Han, J.D., Chesneau, A., Hao, T.*, et al.* (2004). A map of the interactome network of the metazoan C. elegans. Science *303*, 540-543.

Lindqvist, A., Rodriguez-Bravo, V., and Medema, R.H. (2009). The decision to enter mitosis: feedback and redundancy in the mitotic entry network. J Cell Biol *185*, 193-202.

Lingle, W.L., Barrett, S.L., Negron, V.C., D'Assoro, A.B., Boeneman, K., Liu, W., Whitehead, C.M., Reynolds, C., and Salisbury, J.L. (2002). Centrosome amplification drives chromosomal instability in breast tumor development. Proc Natl Acad Sci U S A *99*, 1978-1983.

Lingle, W.L., Lutz, W.H., Ingle, J.N., Maihle, N.J., and Salisbury, J.L. (1998). Centrosome hypertrophy in human breast tumors: implications for genomic stability and cell polarity. Proc Natl Acad Sci U S A *95*, 2950-2955.

Lingle, W.L., and Salisbury, J.L. (1999). Altered centrosome structure is associated with abnormal mitoses in human breast tumors. Am J Pathol *155*, 1941-1951.

Lodish, H.B., A; Zipursky, SL; Matsudaira, P; Baltimore, D and Darnell, J (1999). Molecular Cell Biology. W. H. Freeman and Company, New York.

Lukasiewicz, K.B., and Lingle, W.L. (2009). Aurora A, centrosome structure, and the centrosome cycle. Environ Mol Mutagen *50*, 602-619.

Luke, Y., Zaim, H., Karakesisoglou, I., Jaeger, V.M., Sellin, L., Lu, W., Schneider, M., Neumann, S., Beijer, A., Munck, M.*, et al.* (2008). Nesprin-2 Giant (NUANCE) maintains nuclear envelope architecture and composition in skin. J Cell Sci *121*, 1887-1898.

Lupu, F., Alves, A., Anderson, K., Doye, V., and Lacy, E. (2008). Nuclear pore composition regulates neural stem/progenitor cell differentiation in the mouse embryo. Dev Cell *14*, 831-842.

Macurek, L., Lindqvist, A., Lim, D., Lampson, M.A., Klompmaker, R., Freire, R., Clouin, C., Taylor, S.S., Yaffe, M.B., and Medema, R.H. (2008). Polo-like kinase-1 is activated by aurora A to promote checkpoint recovery. Nature *455*, 119-123.

Maheshwar, M.M., Cheadle, J.P., Jones, A.C., Myring, J., Fryer, A.E., Harris, P.C., and Sampson, J.R. (1997). The GAP-related domain of tuberin, the product of the TSC2 gene, is a target for missense mutations in tuberous sclerosis. Hum Mol Genet *6*, 1991-1996.

Mak, B.C., Kenerson, H.L., Aicher, L.D., Barnes, E.A., and Yeung, R.S. (2005). Aberrant beta-catenin signaling in tuberous sclerosis. Am J Pathol *167*, 107-116.

Mak, B.C., Takemaru, K., Kenerson, H.L., Moon, R.T., and Yeung, R.S. (2003). The tuberin-hamartin complex negatively regulates beta-catenin signaling activity. J Biol Chem *278*, 5947-5951.

Malone, C.J., Misner, L., Le Bot, N., Tsai, M.C., Campbell, J.M., Ahringer, J., and White, J.G. (2003). The C. elegans hook protein, ZYG-12, mediates the essential attachment between the centrosome and nucleus. Cell *115*, 825-836.

Manning, B.D., and Cantley, L.C. (2003). Rheb fills a GAP between TSC and TOR. Trends Biochem Sci *28*, 573-576.

Manning, B.D., Tee, A.R., Logsdon, M.N., Blenis, J., and Cantley, L.C. (2002). Identification of the tuberous sclerosis complex-2 tumor suppressor gene product tuberin as a target of the phosphoinositide 3-kinase/akt pathway. Mol Cell *10*, 151-162.

Mantel, C., Braun, S.E., Reid, S., Henegariu, O., Liu, L., Hangoc, G., and Broxmeyer, H.E. (1999). p21(cip-1/waf-1) deficiency causes deformed nuclear architecture, centriole overduplication, polyploidy, and relaxed microtubule damage checkpoints in human hematopoietic cells. Blood *93*, 1390-1398.

Mao, Y., Abrieu, A., and Cleveland, D.W. (2003). Activating and silencing the mitotic checkpoint through CENP-E-dependent activation/inactivation of BubR1. Cell *114*, 87-98.

Margall-Ducos, G., Celton-Morizur, S., Couton, D., Bregerie, O., and Desdouets, C. (2007). Liver tetraploidization is controlled by a new process of incomplete cytokinesis. J Cell Sci *120*, 3633-3639.

Margolis, R.L., and Andreassen, P.R. (1993). The telophase disc: its possible role in mammalian cell cleavage. Bioessays *15*, 201-207.

Massey-Harroche, D., Delgrossi, M.H., Lane-Guermonprez, L., Arsanto, J.P., Borg, J.P., Billaud, M., and Le Bivic, A. (2007). Evidence for a molecular link between the tuberous sclerosis complex and the Crumbs complex. Hum Mol Genet *16*, 529-536.

Matsumoto, Y., Hayashi, K., and Nishida, E. (1999). Cyclin-dependent kinase 2 (Cdk2) is required for centrosome duplication in mammalian cells. Curr Biol *9*, 429-432.

Matsumura, F. (2005). Regulation of myosin II during cytokinesis in higher eukaryotes. Trends Cell Biol *15*, 371-377.

Matthews, L.R., Vaglio, P., Reboul, J., Ge, H., Davis, B.P., Garrels, J., Vincent, S., and Vidal, M. (2001). Identification of potential interaction networks using sequence-based searches for conserved protein-protein interactions or "interologs". Genome Res *11*, 2120-2126.

Matuliene, J., and Kuriyama, R. (2002). Kinesin-like protein CHO1 is required for the formation of midbody matrix and the completion of cytokinesis in mammalian cells. Mol Biol Cell *13*, 1832-1845.

Matuliene, J., and Kuriyama, R. (2004). Role of the midbody matrix in cytokinesis: RNAi and genetic rescue analysis of the mammalian motor protein CHO1. Mol Biol Cell *15*, 3083-3094.

Maxwell, C.A., Keats, J.J., Crainie, M., Sun, X., Yen, T., Shibuya, E., Hendzel, M., Chan, G., and Pilarski, L.M. (2003). RHAMM is a centrosomal protein that interacts with dynein and maintains spindle pole stability. Mol Biol Cell *14*, 2262-2276.

Mayor, T., Stierhof, Y.D., Tanaka, K., Fry, A.M., and Nigg, E.A. (2000). The centrosomal protein C-Nap1 is required for cell cycle-regulated centrosome cohesion. J Cell Biol *151*, 837-846.

McIntosh, J.R. (1991). Structural and mechanical control of mitotic progression. Cold Spring Harb Symp Quant Biol *56*, 613-619.

McKeveney, P.J., Hodges, V.M., Mullan, R.N., Maxwell, P., Simpson, D., Thompson, A., Winter, P.C., Lappin, T.R., and Maxwell, A.P. (2001). Characterization and localization of expression of an erythropoietin-induced gene, ERIC-1/TACC3, identified in erythroid precursor cells. Br J Haematol *112*, 1016-1024.

Meraldi, P., Honda, R., and Nigg, E.A. (2002). Aurora-A overexpression reveals tetraploidization as a major route to centrosome amplification in p53-/- cells. EMBO J *21*, 483-492.

Meraldi, P., Lukas, J., Fry, A.M., Bartek, J., and Nigg, E.A. (1999). Centrosome duplication in mammalian somatic cells requires E2F and Cdk2-cyclin A. Nat Cell Biol *1*, 88-93.

Meraldi, P., and Nigg, E.A. (2002). The centrosome cycle. FEBS Lett *521*, 9-13.

Michel, L.S., Liberal, V., Chatterjee, A., Kirchwegger, R., Pasche, B., Gerald, W., Dobles, M., Sorger, P.K., Murty, V.V., and Benezra, R. (2001). MAD2 haplo-insufficiency causes premature anaphase and chromosome instability in mammalian cells. Nature *409*, 355-359.

Miloloza, A., Kubista, M., Rosner, M., and Hengstschlager, M. (2002). Evidence for separable functions of tuberous sclerosis gene products in mammalian cell cycle regulation. J Neuropathol Exp Neurol *61*, 154-163.

Minn, A.J., Boise, L.H., and Thompson, C.B. (1996). Expression of Bcl-xL and loss of p53 can cooperate to overcome a cell cycle checkpoint induced by mitotic spindle damage. Genes Dev *10*, 2621-2631.

Mitchison, T., and Kirschner, M. (1984a). Dynamic instability of microtubule growth. Nature *312*, 237-242.

Mitchison, T., and Kirschner, M. (1984b). Microtubule assembly nucleated by isolated centrosomes. Nature *312*, 232-237.

Miyoshi, Y., Iwao, K., Egawa, C., and Noguchi, S. (2001). Association of centrosomal kinase STK15/BTAK mRNA expression with chromosomal instability in human breast cancers. Int J Cancer *92*, 370-373.

Moritz, M., Braunfeld, M.B., Fung, J.C., Sedat, J.W., Alberts, B.M., and Agard, D.A. (1995). Three-dimensional structural characterization of centrosomes from early Drosophila embryos. J Cell Biol *130*, 1149-1159.

Murphy, S.M., Preble, A.M., Patel, U.K., O'Connell, K.L., Dias, D.P., Moritz, M., Agard, D., Stults, J.T., and Stearns, T. (2001). GCP5 and GCP6: two new members of the human gamma-tubulin complex. Mol Biol Cell *12*, 3340-3352.

Nakayama, K., Nagahama, H., Minamishima, Y.A., Matsumoto, M., Nakamichi, I., Kitagawa, K., Shirane, M., Tsunematsu, R., Tsukiyama, T., Ishida, N.*, et al.* (2000). Targeted disruption of Skp2 results in accumulation of cyclin E and p27(Kip1), polyploidy and centrosome overduplication. EMBO J *19*, 2069-2081.

Nakayama, K.I., and Nakayama, K. (2006). Ubiquitin ligases: cell-cycle control and cancer. Nat Rev Cancer *6*, 369-381.

Napolioni, V., and Curatolo, P. (2008). Genetics and molecular biology of tuberous sclerosis complex. Curr Genomics *9*, 475-487.

Nauli, S.M., Alenghat, F.J., Luo, Y., Williams, E., Vassilev, P., Li, X., Elia, A.E., Lu, W., Brown, E.M., Quinn, S.J., *et al.* (2003). Polycystins 1 and 2 mediate mechanosensation in the primary cilium of kidney cells. Nat Genet *33*, 129-137.

Nellist, M., Sancak, O., Goedbloed, M.A., Rohe, C., van Netten, D., Mayer, K., Tucker-Williams, A., van den Ouweland, A.M., and Halley, D.J. (2005). Distinct effects of single amino-acid changes to tuberin on the function of the tuberin-hamartin complex. Eur J Hum Genet *13*, 59-68.

Nicklas, R.B., and Ward, S.C. (1994). Elements of error correction in mitosis: microtubule capture, release, and tension. J Cell Biol *126*, 1241-1253.

Nigg, E.A. (2002). Centrosome aberrations: cause or consequence of cancer progression? Nat Rev Cancer *2*, 815-825.

Nigg, E.A. (2006). Origins and consequences of centrosome aberrations in human cancers. Int J Cancer *119*, 2717-2723.

Nigg, E.A., and Raff, J.W. (2009). Centrioles, centrosomes, and cilia in health and disease. Cell *139*, 663-678.

Nishimura, Y., and Yonemura, S. (2006). Centralspindlin regulates ECT2 and RhoA accumulation at the equatorial cortex during cytokinesis. J Cell Sci *119*, 104-114.

O'Brien, L.L., Albee, A.J., Liu, L., Tao, W., Dobrzyn, P., Lizarraga, S.B., and Wiese, C. (2005). The Xenopus TACC homologue, maskin, functions in mitotic spindle assembly. Mol Biol Cell *16*, 2836-2847.

O'Callaghan, F.J., Noakes, M.J., Martyn, C.N., and Osborne, J.P. (2004). An epidemiological study of renal pathology in tuberous sclerosis complex. BJU Int *94*, 853-857.

O'Connell, K.F., Maxwell, K.N., and White, J.G. (2000). The spd-2 gene is required for polarization of the anteroposterior axis and formation of the sperm asters in the Caenorhabditis elegans zygote. Dev Biol *222*, 55-70.

Olson, J.E., Wang, X., Pankratz, V.S., Fredericksen, Z.S., Vachon, C.M., Vierkant, R.A., Cerhan, J.R., and Couch, F.J. (2010). Centrosome-related genes, genetic variation, and risk of breast cancer. Breast Cancer Res Treat.

Pan, D., Dong, J., Zhang, Y., and Gao, X. (2004). Tuberous sclerosis complex: from Drosophila to human disease. Trends Cell Biol *14*, 78-85.

Partanen, J.I., Nieminen, A.I., and Klefstrom, J. (2009). 3D view to tumor suppression: Lkb1, polarity and the arrest of oncogenic c-Myc. Cell Cycle *8*, 716-724.

Peset, I., Seiler, J., Sardon, T., Bejarano, L.A., Rybina, S., and Vernos, I. (2005). Function and regulation of Maskin, a TACC family protein, in microtubule growth during mitosis. J Cell Biol *170*, 1057-1066.

Peset, I., and Vernos, I. (2008). The TACC proteins: TACC-ling microtubule dynamics and centrosome function. Trends Cell Biol *18*, 379-388.

Peters, D.G., Kudla, D.M., Deloia, J.A., Chu, T.J., Fairfull, L., Edwards, R.P., and Ferrell, R.E. (2005). Comparative gene expression analysis of ovarian carcinoma and normal ovarian epithelium by serial analysis of gene expression. Cancer Epidemiol Biomarkers Prev *14*, 1717-1723.

Peterson, T.R., Laplante, M., Thoreen, C.C., Sancak, Y., Kang, S.A., Kuehl, W.M., Gray, N.S., and Sabatini, D.M. (2009). DEPTOR is an mTOR inhibitor frequently overexpressed in multiple myeloma cells and required for their survival. Cell *137*, 873-886.

Piekorz, R.P., Hoffmeyer, A., Duntsch, C.D., McKay, C., Nakajima, H., Sexl, V., Snyder, L., Rehg, J., and Ihle, J.N. (2002). The centrosomal protein TACC3 is essential for hematopoietic stem cell function and genetically interfaces with p53-regulated apoptosis. Embo J *21*, 653-664.

Piel, M., Meyer, P., Khodjakov, A., Rieder, C.L., and Bornens, M. (2000). The respective contributions of the mother and daughter centrioles to centrosome activity and behavior in vertebrate cells. J Cell Biol *149*, 317-330.

Piel, M., Nordberg, J., Euteneuer, U., and Bornens, M. (2001). Centrosome-dependent exit of cytokinesis in animal cells. Science *291*, 1550-1553.

Pihan, G.A., Purohit, A., Wallace, J., Knecht, H., Woda, B., Quesenberry, P., and Doxsey, S.J. (1998). Centrosome defects and genetic instability in malignant tumors. Cancer Res *58*, 3974-3985.

Pihan, G.A., Purohit, A., Wallace, J., Malhotra, R., Liotta, L., and Doxsey, S.J. (2001). Centrosome defects can account for cellular and genetic changes that characterize prostate cancer progression. Cancer Res *61*, 2212-2219.

Pihan, G.A., Wallace, J., Zhou, Y., and Doxsey, S.J. (2003). Centrosome abnormalities and chromosome instability occur together in pre-invasive carcinomas. Cancer Res *63*, 1398-1404.

Pilarski, R. (2009). Cowden syndrome: a critical review of the clinical literature. J Genet Couns *18*, 13-27.

Pilot-Storck, F., Chopin, E., Rual, J.F., Baudot, A., Dobrokhotov, P., Robinson-Rechavi, M., Brun, C., Cusick, M.E., Hill, D.E., Schaeffer, L.*, et al.* (2010). Interactome mapping of the phosphatidylinositol 3-kinase-mammalian target of rapamycin pathway identifies deformed epidermal autoregulatory factor-1 as a new glycogen synthase kinase-3 interactor. Mol Cell Proteomics.

Pinal, N., Goberdhan, D.C., Collinson, L., Fujita, Y., Cox, I.M., Wilson, C., and Pichaud, F. (2006). Regulated and polarized PtdIns(3,4,5)P3 accumulation is essential for apical membrane morphogenesis in photoreceptor epithelial cells. Curr Biol *16*, 140-149.

Plachot, C., Chaboub, L.S., Adissu, H.A., Wang, L., Urazaev, A., Sturgis, J., Asem, E.K., and Lelievre, S.A. (2009). Factors necessary to produce basoapical polarity in human glandular epithelium formed in conventional and high-throughput three-dimensional culture: example of the breast epithelium. BMC Biol *7*, 77.

Plachot, C., and Lelievre, S.A. (2004). DNA methylation control of tissue polarity and cellular differentiation in the mammary epithelium. Exp Cell Res *298*, 122-132.

Plank, T.L., Yeung, R.S., and Henske, E.P. (1998). Hamartin, the product of the tuberous sclerosis 1 (TSC1) gene, interacts with tuberin and appears to be localized to cytoplasmic vesicles. Cancer Res *58*, 4766-4770.

Potter, C.J., Huang, H., and Xu, T. (2001). Drosophila Tsc1 functions with Tsc2 to antagonize insulin signaling in regulating cell growth, cell proliferation, and organ size. Cell *105*, 357-368.

Pu, J.J., Li, C., Rodriguez, M., and Banerjee, D. (2001). Cloning and structural characterization of ECTACC, a new member of the transforming acidic coiled coil (TACC) gene family: cDNA sequence and expression analysis in human microvascular endothelial cells. Cytokine *13*, 129-137.

Pugacheva, E.N., and Golemis, E.A. (2005). The focal adhesion scaffolding protein HEF1 regulates activation of the Aurora-A and Nek2 kinases at the centrosome. Nat Cell Biol *7*, 937-946.

Pugacheva, E.N., Jablonski, S.A., Hartman, T.R., Henske, E.P., and Golemis, E.A. (2007). HEF1-dependent Aurora A activation induces disassembly of the primary cilium. Cell *129*, 1351-1363.

Pujana, M.A., Han, J.D., Starita, L.M., Stevens, K.N., Tewari, M., Ahn, J.S., Rennert, G., Moreno, V., Kirchhoff, T., Gold, B.*, et al.* (2007). Network modeling links breast cancer susceptibility and centrosome dysfunction. Nat Genet *39*, 1338-1349.

Raff, J.W. (2002). Centrosomes and cancer: lessons from a TACC. Trends Cell Biol *12*, 222-225.

Raught, B., Peiretti, F., Gingras, A.C., Livingstone, M., Shahbazian, D., Mayeur, G.L., Polakiewicz, R.D., Sonenberg, N., and Hershey, J.W. (2004). Phosphorylation of eucaryotic translation initiation factor 4B Ser422 is modulated by S6 kinases. EMBO J *23*, 1761-1769.

Ren, Y., Li, R., Zheng, Y., and Busch, H. (1998). Cloning and characterization of GEF-H1, a microtubule-associated guanine nucleotide exchange factor for Rac and Rho GTPases. J Biol Chem *273*, 34954-34960.

Richardson, C.J., Broenstrup, M., Fingar, D.C., Julich, K., Ballif, B.A., Gygi, S., and Blenis, J. (2004). SKAR is a specific target of S6 kinase 1 in cell growth control. Curr Biol *14*, 1540-1549.

Ridley, A.J. (2001). Rho GTPases and cell migration. J Cell Sci *114*, 2713-2722.

Rindler, M.J., Ivanov, I.E., and Sabatini, D.D. (1987). Microtubule-acting drugs lead to the nonpolarized delivery of the influenza hemagglutinin to the cell surface of polarized Madin-Darby canine kidney cells. J Cell Biol *104*, 231-241.

Rosner, M., Freilinger, A., and Hengstschlager, M. (2007). Akt regulates nuclear/cytoplasmic localization of tuberin. Oncogene *26*, 521-531.

Rusan, N.M., and Rogers, G.C. (2009). Centrosome function: sometimes less is more. Traffic *10*, 472-481.

Ryu, J.H., Moss, J., Beck, G.J., Lee, J.C., Brown, K.K., Chapman, J.T., Finlay, G.A., Olson, E.J., Ruoss, S.J., Maurer, J.R.*, et al.* (2006). The NHLBI lymphangioleiomyomatosis registry: characteristics of 230 patients at enrollment. Am J Respir Crit Care Med *173*, 105-111.

Sadek, C.M., Jalaguier, S., Feeney, E.P., Aitola, M., Damdimopoulos, A.E., Pelto-Huikko, M., and Gustafsson, J.A. (2000). Isolation and characterization of AINT: a novel ARNT interacting protein expressed during murine embryonic development. Mech Dev *97*, 13-26.

Sadek, C.M., Pelto-Huikko, M., Tujague, M., Steffensen, K.R., Wennerholm, M., and Gustafsson, J.A. (2003). TACC3 expression is tightly regulated during early differentiation. Gene Expr Patterns *3*, 203-211.

Sadler, P.L., and Shakes, D.C. (2000). Anucleate Caenorhabditis elegans sperm can crawl, fertilize oocytes and direct anterior-posterior polarization of the 1-cell embryo. Development *127*, 355-366.

Sahai, E., and Marshall, C.J. (2002). RHO-GTPases and cancer. Nat Rev Cancer *2*, 133-142.

Salisbury, J.L. (2003). Centrosomes: coiled-coils organize the cell center. Curr Biol *13*, R88-90.

Salisbury, J.L., D'Assoro, A.B., and Lingle, W.L. (2004). Centrosome amplification and the origin of chromosomal instability in breast cancer. J Mammary Gland Biol Neoplasia *9*, 275-283.

Sampson, J.R., Maheshwar, M.M., Aspinwall, R., Thompson, P., Cheadle, J.P., Ravine, D., Roy, S., Haan, E., Bernstein, J., and Harris, P.C. (1997). Renal cystic disease in tuberous sclerosis: role of the polycystic kidney disease 1 gene. Am J Hum Genet *61*, 843-851.

Sancak, O., Nellist, M., Goedbloed, M., Elfferich, P., Wouters, C., Maat-Kievit, A., Zonnenberg, B., Verhoef, S., Halley, D., and van den Ouweland, A. (2005). Mutational analysis of the TSC1 and TSC2 genes in a diagnostic setting: genotype--phenotype correlations and comparison of diagnostic DNA techniques in Tuberous Sclerosis Complex. Eur J Hum Genet *13*, 731-741.

Sankaran, S., and Parvin, J.D. (2006). Centrosome function in normal and tumor cells. J Cell Biochem *99*, 1240-1250.

Sarbassov, D.D., Ali, S.M., Kim, D.H., Guertin, D.A., Latek, R.R., Erdjument-Bromage, H., Tempst, P., and Sabatini, D.M. (2004). Rictor, a novel binding partner of mTOR, defines a rapamycin-insensitive and raptor-independent pathway that regulates the cytoskeleton. Curr Biol *14*, 1296-1302.

Sarbassov, D.D., Guertin, D.A., Ali, S.M., and Sabatini, D.M. (2005). Phosphorylation and regulation of Akt/PKB by the rictor-mTOR complex. Science *307*, 1098-1101.

Sato, M., Vardy, L., Angel Garcia, M., Koonrugsa, N., and Toda, T. (2004). Interdependency of fission yeast Alp14/TOG and coiled coil protein Alp7 in microtubule localization and bipolar spindle formation. Mol Biol Cell *15*, 1609-1622.

Saucedo, L.J., Gao, X., Chiarelli, D.A., Li, L., Pan, D., and Edgar, B.A. (2003). Rheb promotes cell growth as a component of the insulin/TOR signalling network. Nat Cell Biol *5*, 566-571.

Scolnick, D.M., and Halazonetis, T.D. (2000). Chfr defines a mitotic stress checkpoint that delays entry into metaphase. Nature *406*, 430-435.

Schneider, L., Essman, F., Kletke, A., Rio, P., Hanenberg, H., Wetzel, W., Schulze-Osthoff, K., Nurnberg, B., and Piekorz, R.P. (2007a). The transforming acidic coiled coil 3 protein is essential for spindle-dependent chromosome alignment and mitotic survival. J Biol Chem.

Schneider, L., Essmann, F., Kletke, A., Rio, P., Hanenberg, H., Schulze-Osthoff, K., Nurnberg, B., and Piekorz, R.P. (2008). TACC3 depletion sensitizes to paclitaxel-induced cell death and overrides p21WAF-mediated cell cycle arrest. Oncogene *27*, 116-125.

Schneider, L., Essmann, F., Kletke, A., Rio, P., Hanenberg, H., Wetzel, W., Schulze-Osthoff, K., Nurnberg, B., and Piekorz, R.P. (2007b). The transforming acidic coiled coil 3 protein is essential for spindle-dependent chromosome alignment and mitotic survival. J Biol Chem *282*, 29273-29283.

Schuendeln, M.M., Piekorz, R.P., Wichmann, C., Lee, Y., McKinnon, P.J., Boyd, K., Takahashi, Y., and Ihle, J.N. (2004). The centrosomal, putative tumor suppressor protein TACC2 is dispensable for normal development, and deficiency does not lead to cancer. Mol Cell Biol *24*, 6403-6409.

Seki, A., Coppinger, J.A., Du, H., Jang, C.Y., Yates, J.R., 3rd, and Fang, G. (2008a). Plk1- and beta-TrCP-dependent degradation of Bora controls mitotic progression. J Cell Biol *181*, 65-78.

Seki, A., Coppinger, J.A., Jang, C.Y., Yates, J.R., and Fang, G. (2008b). Bora and the kinase Aurora a cooperatively activate the kinase Plk1 and control mitotic entry. Science *320*, 1655-1658.

Sen, S., Zhou, H., and White, R.A. (1997). A putative serine/threonine kinase encoding gene BTAK on chromosome 20q13 is amplified and overexpressed in human breast cancer cell lines. Oncogene *14*, 2195-2200.

Sen, S., Zhou, H., Zhang, R.D., Yoon, D.S., Vakar-Lopez, F., Ito, S., Jiang, F., Johnston, D., Grossman, H.B., Ruifrok, A.C.*, et al.* (2002). Amplification/overexpression of a mitotic kinase gene in human bladder cancer. J Natl Cancer Inst *94*, 1320-1329.

Shepherd, C.W., Houser, O.W., and Gomez, M.R. (1995). MR findings in tuberous sclerosis complex and correlation with seizure development and mental impairment. AJNR Am J Neuroradiol *16*, 149-155.

Shillingford, J.M., Murcia, N.S., Larson, C.H., Low, S.H., Hedgepeth, R., Brown, N., Flask, C.A., Novick, A.C., Goldfarb, D.A., Kramer-Zucker, A.*, et al.* (2006). The mTOR pathway is regulated by polycystin-1, and its inhibition reverses renal cystogenesis in polycystic kidney disease. Proc Natl Acad Sci U S A *103*, 5466-5471.

Shin, K., Straight, S., and Margolis, B. (2005). PATJ regulates tight junction formation and polarity in mammalian epithelial cells. J Cell Biol *168*, 705-711.

Sluder, G. (2005). Two-way traffic: centrosomes and the cell cycle. Nat Rev Mol Cell Biol *6*, 743-748.

Sluder, G., and Hinchcliffe, E.H. (2000). The coordination of centrosome reproduction with nuclear events during the cell cycle. Curr Top Dev Biol *49*, 267-289.

Song, L., and Rape, M. (2010). Regulated degradation of spindle assembly factors by the anaphase-promoting complex. Mol Cell *38*, 369-382.

Sotillo, R., Schvartzman, J.M., Socci, N.D., and Benezra, R. (2010). Mad2-induced chromosome instability leads to lung tumour relapse after oncogene withdrawal. Nature *464*, 436-440.

Soucek, T., Pusch, O., Wienecke, R., DeClue, J.E., and Hengstschlager, M. (1997). Role of the tuberous sclerosis gene-2 product in cell cycle control. Loss of the tuberous sclerosis gene-2 induces quiescent cells to enter S phase. J Biol Chem *272*, 29301-29308.

Soucek, T., Yeung, R.S., and Hengstschlager, M. (1998). Inactivation of the cyclin-dependent kinase inhibitor p27 upon loss of the tuberous sclerosis complex gene-2. Proc Natl Acad Sci U S A *95*, 15653-15658.

Sparagana, S.P., and Roach, E.S. (2000). Tuberous sclerosis complex. Curr Opin Neurol *13*, 115-119.

Spektor, A., Tsang, W.Y., Khoo, D., and Dynlacht, B.D. (2007). Cep97 and CP110 suppress a cilia assembly program. Cell *130*, 678-690.

Srayko, M., Quintin, S., Schwager, A., and Hyman, A.A. (2003). Caenorhabditis elegans TAC-1 and ZYG-9 form a complex that is essential for long astral and spindle microtubules. Curr Biol *13*, 1506-1511.

Steadman, B.T., Schmidt, P.H., Shanks, R.A., Lapierre, L.A., and Goldenring, J.R. (2002). Transforming acidic coiled-coil-containing protein 4 interacts with centrosomal AKAP350 and the mitotic spindle apparatus. J Biol Chem *277*, 30165-30176.

Stebbins-Boaz, B., Cao, Q., de Moor, C.H., Mendez, R., and Richter, J.D. (1999). Maskin is a CPEB-associated factor that transiently interacts with elF-4E. Mol Cell *4*, 1017-1027.

Stemmer, K., Ellinger-Ziegelbauer, H., Ahr, H.J., and Dietrich, D.R. (2007). Carcinogen-specific gene expression profiles in short-term treated Eker and wild-type rats indicative of pathways involved in renal tumorigenesis. Cancer Res *67*, 4052-4068.

Still, I.H., Hamilton, M., Vince, P., Wolfman, A., and Cowell, J.K. (1999a). Cloning of TACC1, an embryonically expressed, potentially transforming coiled coil containing gene, from the 8p11 breast cancer amplicon. Oncogene *18*, 4032-4038.

Still, I.H., Vettaikkorumakankauv, A.K., DiMatteo, A., and Liang, P. (2004). Structure-function evolution of the transforming acidic coiled coil genes revealed by analysis of phylogenetically diverse organisms. BMC Evol Biol *4*, 16.

Still, I.H., Vince, P., and Cowell, J.K. (1999b). The third member of the transforming acidic coiled coil-containing gene family, TACC3, maps in 4p16, close to translocation breakpoints in multiple myeloma, and is upregulated in various cancer cell lines. Genomics *58*, 165-170.

Stocker, H., Radimerski, T., Schindelholz, B., Wittwer, F., Belawat, P., Daram, P., Breuer, S., Thomas, G., and Hafen, E. (2003). Rheb is an essential regulator of S6K in controlling cell growth in Drosophila. Nat Cell Biol *5*, 559-565.

Straight, A.F., Cheung, A., Limouze, J., Chen, I., Westwood, N.J., Sellers, J.R., and Mitchison, T.J. (2003). Dissecting temporal and spatial control of cytokinesis with a myosin II Inhibitor. Science *299*, 1743-1747.

Su, A.I., Wiltshire, T., Batalov, S., Lapp, H., Ching, K.A., Block, D., Zhang, J., Soden, R., Hayakawa, M., Kreiman, G.*, et al.* (2004). A gene atlas of the mouse and human protein-encoding transcriptomes. Proc Natl Acad Sci U S A *101*, 6062-6067.

Subramanian, A., Tamayo, P., Mootha, V.K., Mukherjee, S., Ebert, B.L., Gillette, M.A., Paulovich, A., Pomeroy, S.L., Golub, T.R., Lander, E.S., and Mesirov, J.P. (2005). Gene set enrichment analysis: a knowledge-based approach for interpreting genome-wide expression profiles. Proc Natl Acad Sci U S A *102*, 15545-15550.

Sudakin, V., Chan, G.K., and Yen, T.J. (2001). Checkpoint inhibition of the APC/C in HeLa cells is mediated by a complex of BUBR1, BUB3, CDC20, and MAD2. J Cell Biol *154*, 925-936.

Sudo, H., and Maru, Y. (2007). LAPSER1 is a putative cytokinetic tumor suppressor that shows the same centrosome and midbody subcellular localization pattern as p80 katanin. Faseb J *21*, 2086-2100.

Summers, M.K., Bothos, J., and Halazonetis, T.D. (2005). The CHFR mitotic checkpoint protein delays cell cycle progression by excluding Cyclin B1 from the nucleus. Oncogene *24*, 2589-2598.

Suzuki, A., and Ohno, S. (2006). The PAR-aPKC system: lessons in polarity. J Cell Sci *119*, 979-987.

Tanaka, T., Kimura, M., Matsunaga, K., Fukada, D., Mori, H., and Okano, Y. (1999). Centrosomal kinase AIK1 is overexpressed in invasive ductal carcinoma of the breast. Cancer Res *59*, 2041-2044.

Tapon, N., Ito, N., Dickson, B.J., Treisman, J.E., and Hariharan, I.K. (2001). The Drosophila tuberous sclerosis complex gene homologs restrict cell growth and cell proliferation. Cell *105*, 345-355.

Tatsuka, M., Katayama, H., Ota, T., Tanaka, T., Odashima, S., Suzuki, F., and Terada, Y. (1998). Multinuclearity and increased ploidy caused by overexpression of the aurora- and Ipl1-like midbody-associated protein mitotic kinase in human cancer cells. Cancer Res *58*, 4811-4816.

Taveira-DaSilva, A.M., Pacheco-Rodriguez, G., and Moss, J. The natural history of lymphangioleiomyomatosis: markers of severity, rate of progression and prognosis. Lymphat Res Biol *8*, 9-19.

Tee, A.R., and Blenis, J. (2005). mTOR, translational control and human disease. Semin Cell Dev Biol *16*, 29-37.

Tee, A.R., Manning, B.D., Roux, P.P., Cantley, L.C., and Blenis, J. (2003). Tuberous sclerosis complex gene products, Tuberin and Hamartin, control mTOR signaling by acting as a GTPase-activating protein complex toward Rheb. Curr Biol *13*, 1259-1268.

Terada, Y., Tatsuka, M., Suzuki, F., Yasuda, Y., Fujita, S., and Otsu, M. (1998). AIM-1: a mammalian midbody-associated protein required for cytokinesis. EMBO J *17*, 667-676.

Theodoropoulos, P.A., Polioudaki, H., Kostaki, O., Derdas, S.P., Georgoulias, V., Dargemont, C., and Georgatos, S.D. (1999). Taxol affects nuclear lamina and pore complex organization and inhibits import of karyophilic proteins into the cell nucleus. Cancer Res *59*, 4625-4633.

Toji, S., Yabuta, N., Hosomi, T., Nishihara, S., Kobayashi, T., Suzuki, S., Tamai, K., and Nojima, H. (2004). The centrosomal protein Lats2 is a phosphorylation target of Aurora-A kinase. Genes Cells *9*, 383-397.

Toyoda, H., Bregerie, O., Vallet, A., Nalpas, B., Pivert, G., Brechot, C., and Desdouets, C. (2005). Changes to hepatocyte ploidy and binuclearity profiles during human chronic viral hepatitis. Gut *54*, 297-302.

Toyoshima, M., Ohno, K., Katsumoto, T., Maki, H., and Takeshita, K. (1999). Cellular senescence of angiofibroma stroma cells from patients with tuberous sclerosis. Brain Dev *21*, 184-191.

Tsai, L.H., and Gleeson, J.G. (2005). Nucleokinesis in neuronal migration. Neuron *46*, 383-388.

Tsang, W.Y., Bossard, C., Khanna, H., Peranen, J., Swaroop, A., Malhotra, V., and Dynlacht, B.D. (2008). CP110 suppresses primary cilia formation through its interaction with CEP290, a protein deficient in human ciliary disease. Dev Cell *15*, 187-197.

Tutt, A., Gabriel, A., Bertwistle, D., Connor, F., Paterson, H., Peacock, J., Ross, G., and Ashworth, A. (1999). Absence of Brca2 causes genome instability by chromosome breakage and loss associated with centrosome amplification. Curr Biol *9*, 1107-1110.

Uetake, Y., and Sluder, G. (2004). Cell cycle progression after cleavage failure: mammalian somatic cells do not possess a "tetraploidy checkpoint". J Cell Biol *165*, 609-615.

Ulisse, S., Baldini, E., Toller, M., Delcros, J.G., Gueho, A., Curcio, F., De Antoni, E., Giacomelli, L., Ambesi-Impiombato, F.S., Bocchini, S.*, et al.* (2007). Transforming acidic coiled-coil 3 and Aurora-A interact in human thyrocytes and their expression is deregulated in thyroid cancer tissues. Endocr Relat Cancer *14*, 827-837.

van Slegtenhorst, M., de Hoogt, R., Hermans, C., Nellist, M., Janssen, B., Verhoef, S., Lindhout, D., van den Ouweland, A., Halley, D., Young, J.*, et al.* (1997). Identification of the tuberous sclerosis gene TSC1 on chromosome 9q34. Science *277*, 805-808.

van Slegtenhorst, M., Nellist, M., Nagelkerken, B., Cheadle, J., Snell, R., van den Ouweland, A., Reuser, A., Sampson, J., Halley, D., and van der Sluijs, P. (1998). Interaction between hamartin and tuberin, the TSC1 and TSC2 gene products. Hum Mol Genet *7*, 1053-1057.

Vazquez-Martin, A., Oliveras-Ferraros, C., Bernado, L., Lopez-Bonet, E., and Menendez, J.A. (2009a). The serine 2481-autophosphorylated form of mammalian Target Of Rapamycin (mTOR) is localized to midzone and midbody in dividing cancer cells. Biochem Biophys Res Commun *380*, 638-643.

Vazquez-Martin, A., Oliveras-Ferraros, C., Lopez-Bonet, E., and Menendez, J.A. (2009b). AMPK: Evidence for an energy-sensing cytokinetic tumor suppressor. Cell Cycle *8*, 3679-3683.

Vazquez-Martin, A., Oliveras-Ferraros, C., and Menendez, J.A. (2009c). The active form of the metabolic sensor: AMP-activated protein kinase (AMPK) directly binds the mitotic apparatus and travels from centrosomes to the spindle midzone during mitosis and cytokinesis. Cell Cycle *8*, 2385-2398.

Verbrugge, J., Choudhary, A.K., and Ladda, R. (2009). Tethered cord, corpus callosum abnormalities, and periventricular cysts in Wolf-Hirschhorn syndrome. Report of two cases and review of the literature. Am J Med Genet A *149A*, 2280-2284.

Vidal, M., Brachmann, R.K., Fattaey, A., Harlow, E., and Boeke, J.D. (1996a). Reverse two-hybrid and one-hybrid systems to detect dissociation of protein-protein and DNA-protein interactions. Proc Natl Acad Sci U S A *93*, 10315-10320.

Vidal, M., Braun, P., Chen, E., Boeke, J.D., and Harlow, E. (1996b). Genetic characterization of a mammalian protein-protein interaction domain by using a yeast reverse two-hybrid system. Proc Natl Acad Sci U S A *93*, 10321-10326.

Vidalain, P.O., Boxem, M., Ge, H., Li, S., and Vidal, M. (2004). Increasing specificity in high-throughput yeast two-hybrid experiments. Methods *32*, 363-370.

Vinters, H.V., Park, S.H., Johnson, M.W., Mischel, P.S., Catania, M., and Kerfoot, C. (1999). Cortical dysplasia, genetic abnormalities and neurocutaneous syndromes. Dev Neurosci *21*, 248-259.

Visintin, R., Prinz, S., and Amon, A. (1997). CDC20 and CDH1: a family of substrate-specific activators of APC-dependent proteolysis. Science *278*, 460-463.

von Stein, W., Ramrath, A., Grimm, A., Muller-Borg, M., and Wodarz, A. (2005). Direct association of Bazooka/PAR-3 with the lipid phosphatase PTEN reveals a link between the PAR/aPKC complex and phosphoinositide signaling. Development *132*, 1675-1686.

Vorobjev, I.A., and Chentsov Yu, S. (1982). Centrioles in the cell cycle. I. Epithelial cells. J Cell Biol *93*, 938-949.

Walhout, A.J., and Vidal, M. (2001). High-throughput yeast two-hybrid assays for large-scale protein interaction mapping. Methods *24*, 297-306.

Wallenfang, M.R., and Seydoux, G. (2000). Polarization of the anterior-posterior axis of C. elegans is a microtubule-directed process. Nature *408*, 89-92.

Wassmann, K., Liberal, V., and Benezra, R. (2003). Mad2 phosphorylation regulates its association with Mad1 and the APC/C. EMBO J *22*, 797-806.

Watson, G.H. (1991). Cardiac rhabdomyomas in tuberous sclerosis. Ann N Y Acad Sci *615*, 50-57.

Weaver, V.M., Howlett, A.R., Langton-Webster, B., Petersen, O.W., and Bissell, M.J. (1995). The development of a functionally relevant cell culture model of progressive human breast cancer. Semin Cancer Biol *6*, 175-184.

Weisenberg, R.C., Borisy, G.G., and Taylor, E.W. (1968). The colchicine-binding protein of mammalian brain and its relation to microtubules. Biochemistry *7*, 4466-4479.

Weisenberg, R.C., Deery, W.J., and Dickinson, P.J. (1976). Tubulin-nucleotide interactions during the polymerization and depolymerization of microtubules. Biochemistry *15*, 4248-4254.

Wendel, H.G., De Stanchina, E., Fridman, J.S., Malina, A., Ray, S., Kogan, S., Cordon-Cardo, C., Pelletier, J., and Lowe, S.W. (2004). Survival signalling by Akt and eIF4E in oncogenesis and cancer therapy. Nature *428*, 332-337.

Whitfield, M.L., Sherlock, G., Saldanha, A.J., Murray, J.I., Ball, C.A., Alexander, K.E., Matese, J.C., Perou, C.M., Hurt, M.M., Brown, P.O., and Botstein, D. (2002). Identification of genes periodically expressed in the human cell cycle and their expression in tumors. Mol Biol Cell *13*, 1977-2000.

Wigley, W.C., Fabunmi, R.P., Lee, M.G., Marino, C.R., Muallem, S., DeMartino, G.N., and Thomas, P.J. (1999). Dynamic association of proteasomal machinery with the centrosome. J Cell Biol *145*, 481-490.

Wilson, E.B. (1925). The cell in development and inheritance. Macmillan Company, New York.

Williams, T., and Brenman, J.E. (2008). LKB1 and AMPK in cell polarity and division. Trends Cell Biol *18*, 193-198.

Worman, H.J., Fong, L.G., Muchir, A., and Young, S.G. (2009). Laminopathies and the long strange trip from basic cell biology to therapy. J Clin Invest *119*, 1825-1836.

Wright, W.E., and Hayflick, L. (1972). Formation of anucleate and multinucleate cells in normal and SV 40 transformed WI-38 by cytochalasin B. Exp Cell Res *74*, 187-194.

Xie, W., Li, L., and Cohen, S.N. (1998). Cell cycle-dependent subcellular localization of the TSG101 protein and mitotic and nuclear abnormalities associated with TSG101 deficiency. Proc Natl Acad Sci U S A *95*, 1595-1600.

Xie, Z., Moy, L.Y., Sanada, K., Zhou, Y., Buchman, J.J., and Tsai, L.H. (2007). Cep120 and TACCs control interkinetic nuclear migration and the neural progenitor pool. Neuron *56*, 79-93.

Xu, X., Weaver, Z., Linke, S.P., Li, C., Gotay, J., Wang, X.W., Harris, C.C., Ried, T., and Deng, C.X. (1999). Centrosome amplification and a defective G2-M cell cycle checkpoint induce genetic instability in BRCA1 exon 11 isoform-deficient cells. Mol Cell *3*, 389-395.

Yaba, A., Bianchi, V., Borini, A., and Johnson, J. (2008). A putative mitotic checkpoint dependent on mTOR function controls cell proliferation and survival in ovarian granulosa cells. Reprod Sci *15*, 128-138.

Yang, Q., Inoki, K., Kim, E., and Guan, K.L. (2006). TSC1/TSC2 and Rheb have different effects on TORC1 and TORC2 activity. Proc Natl Acad Sci U S A *103*, 6811-6816.

Yao, R., Natsume, Y., and Noda, T. (2007). TACC3 is required for the proper mitosis of sclerotome mesenchymal cells during formation of the axial skeleton. Cancer Sci *98*, 555-562.

Yoder, B.K., Hou, X., and Guay-Woodford, L.M. (2002a). The polycystic kidney disease proteins, polycystin-1, polycystin-2, polaris, and cystin, are co-localized in renal cilia. J Am Soc Nephrol *13*, 2508-2516.

Yoder, B.K., Tousson, A., Millican, L., Wu, J.H., Bugg, C.E., Jr., Schafer, J.A., and Balkovetz, D.F. (2002b). Polaris, a protein disrupted in orpk mutant mice, is required for assembly of renal cilium. Am J Physiol Renal Physiol *282*, F541-552.

Yonemura, S., Hirao-Minakuchi, K., and Nishimura, Y. (2004). Rho localization in cells and tissues. Exp Cell Res *295*, 300-314.

York, B., Lou, D., and Noonan, D.J. (2006). Tuberin nuclear localization can be regulated by phosphorylation of its carboxyl terminus. Mol Cancer Res *4*, 885-897.

York, B., Lou, D., Panettieri, R.A., Jr., Krymskaya, V.P., Vanaman, T.C., and Noonan, D.J. (2005). Cross-talk between tuberin, calmodulin, and estrogen signaling pathways. FASEB J *19*, 1202-1204.

Yoshizaki, H., Ohba, Y., Kurokawa, K., Itoh, R.E., Nakamura, T., Mochizuki, N., Nagashima, K., and Matsuda, M. (2003). Activity of Rho-family GTPases during cell division as visualized with FRET-based probes. J Cell Biol *162*, 223-232.

Yu, X., Minter-Dykhouse, K., Malureanu, L., Zhao, W.M., Zhang, D., Merkle, C.J., Ward, I.M., Saya, H., Fang, G., van Deursen, J., and Chen, J. (2005). Chfr is required for tumor suppression and Aurora A regulation. Nat Genet *37*, 401-406.

Yuce, O., Piekny, A., and Glotzer, M. (2005). An ECT2-centralspindlin complex regulates the localization and function of RhoA. J Cell Biol *170*, 571-582.

Zhai, Y., Kronebusch, P.J., Simon, P.M., and Borisy, G.G. (1996). Microtubule dynamics at the G2/M transition: abrupt breakdown of cytoplasmic microtubules at nuclear envelope breakdown and implications for spindle morphogenesis. J Cell Biol *135*, 201-214.

Zhang, Y., Gao, X., Saucedo, L.J., Ru, B., Edgar, B.A., and Pan, D. (2003). Rheb is a direct target of the tuberous sclerosis tumour suppressor proteins. Nat Cell Biol *5*, 578-581.

Zhao, J., Ren, Y., Jiang, Q., and Feng, J. (2003). Parkin is recruited to the centrosome in response to inhibition of proteasomes. J Cell Sci *116*, 4011-4019.

Zhao, W.M., Seki, A., and Fang, G. (2006). Cep55, a microtubule-bundling protein, associates with centralspindlin to control the midbody integrity and cell abscission during cytokinesis. Mol Biol Cell *17*, 3881-3896.

Zheng, Y., Wong, M.L., Alberts, B., and Mitchison, T. (1995). Nucleation of microtubule assembly by a gamma-tubulin-containing ring complex. Nature *378*, 578-583.

Zhou, H., Kuang, J., Zhong, L., Kuo, W.L., Gray, J.W., Sahin, A., Brinkley, B.R., and Sen, S. (1998). Tumour amplified kinase STK15/BTAK induces centrosome amplification, aneuploidy and transformation. Nat Genet *20*, 189-193.

Zhu, C., Bossy-Wetzel, E., and Jiang, W. (2005). Recruitment of MKLP1 to the spindle midzone/midbody by INCENP is essential for midbody formation and completion of cytokinesis in human cells. Biochem J *389*, 373-381.

Zollino, M., Lecce, R., Fischetto, R., Murdolo, M., Faravelli, F., Selicorni, A., Butte, C., Memo, L., Capovilla, G., and Neri, G. (2003). Mapping the Wolf-Hirschhorn syndrome phenotype outside the currently accepted WHS critical region and defining a new critical region, WHSCR-2. Am J Hum Genet *72*, 590-597.

Zyss, D., and Gergely, F. (2009). Centrosome function in cancer: guilty or innocent? Trends Cell Biol *19*, 334-346.

PUBLICATIONS

Gómez-Baldó L, Schmidt S, Maxwell CA, Bonifaci N, Gabaldón T, Vidalain PO, Senapedis W, Kletke A, Rosing M, Barnekow A, Rottapel R, Capellá G**,** Vidal M, Astrinidis A, Piekorz RP and Pujana MA (2010). **TACC3-TSC2 maintain nuclear envelope structure and control cell division.** Cell Cycle

Maxwell CA, Moreno V, Sole X, **Gómez L**, Hernandez P, Urruticoechea A and Pujana MA (2008). **Genetic interactions: the missing links for a better understanding of cancer susceptibility, progression and treatment.** *Molecular Cancer*

Sole X, Hernandez P, Lopez de Heredia M, Armengol L, Rodriguez-Santiago B, **Gómez L**, Maxwell CA, Abril J, Perez-Jurado L, Estivill X, Nunes V, Capella G, Gruber SB, Moreno V and Pujana MA (2008). **Genetic and genomic analysis modeling of germline c-MYC overexpression and cancer susceptibility.** *BMC Genomics*

Hernández P, Huerta-Cepas J, Montaner D, Al-Shahrour F, Valls J, **Gómez L**, Capellá G, Dopazo J, Pujana MA. (2007). **Evidence for systems-level molecular mechanisms of tumorigenesis**. *BMC Genomics*.; 8:185.